

# Role of the Adenovirus Type 5 L4-100K Protein During Lytic Infection

**Dissertation**

Zur Erlangung des akademischen  
Grades eines Doktors der  
Naturwissenschaften (Dr. rer. nat.)

am Department Biologie  
der Fakultät für Mathematik, Informatik und Naturwissenschaften  
an der Universität Hamburg

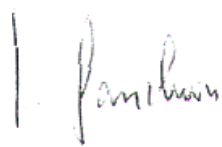
Vorgelegt von  
**Orkide Özge Koyuncu**  
Aus Ankara

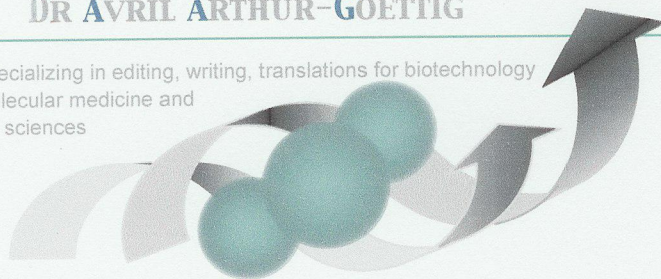
March, 2009

Genehmigt vom Department Biologie  
der Fakultät für Mathematik, Informatik und Naturwissenschaften  
an der Universität Hamburg  
auf Antrag von Professor Dr. T. DOBNER  
Weiterer Gutachter der Dissertation:  
Herr Professor Dr. J. HAUBER  
Tag der Disputation: 20. März 2009

Hamburg, den 04. März 2009



  
Professor Dr. Jörg Ganzhorn  
Leiter des Departments Biologie



**09.02.09**

**RE: the thesis submitted to the University of Hamburg  
for the degree of DOCTOR OF PHILOSOPHY  
by Orkide Ö. Koyuncu**

I hereby declare as a native English speaker and professional scientific writer that I have checked this thesis for grammatically correct English and the scientific quality of the language.

Signed,

A handwritten signature in black ink, appearing to read 'A. Goettig', with a stylized, flowing script.

Dr. Avril Arthur-Goettig

Bitte an folgenden Konto – Please use the account below:

**Bankverbindung:**

Stadtsparkasse München

Konto Nr. 909189961

Dr. Avril Arthur-Goettig

BLZ: 701 500 00

*The truth is rarely pure and never simple.*

Oscar Wilde, Irish dramatist, novelist, & poet (1854 - 1900)



# Table of Contents

---

<b>TABLE OF CONTENTS</b>	<b>I</b>
<b>ABBREVIATIONS</b>	<b>VI</b>
<b>1 ABSTRACT</b>	<b>1</b>
<b>2 INTRODUCTION</b>	<b>4</b>
<b>2.1 Adenoviruses</b>	<b>4</b>
2.1.1 Classification	4
2.1.2 Structure and Genome Organization	5
2.1.3 Productive Infection Cycle	7
2.1.4 Oncogenic Potential of Human Adenoviruses	8
<b>2.2 Regulatory Proteins of Adenovirus</b>	<b>10</b>
2.2.1 Early Proteins E1B-55K and E4orf6	10
2.2.2 Late Protein L4-100K	12
<b>2.3 Cellular Factors Mediating L4-100K Functions</b>	<b>18</b>
2.3.1 Protein Arginine Methylation	18
2.3.2 CRM1-Mediated Nuclear Export	20
<b>2.4 Aims and Objectives</b>	<b>24</b>
<b>3 MATERIALS</b>	<b>25</b>
<b>3.1 Cells</b>	<b>25</b>
3.1.1 Bacteria Strains	25
3.1.2 Mammalian Cell Lines	25
<b>3.2 Adenoviruses</b>	<b>26</b>
<b>3.3 Nucleic Acids</b>	<b>27</b>

## TABLE of CONTENTS

3.3.1	Oligonucleotides	27
3.3.2	Vectors	29
3.3.3	Recombinant Plasmids	30
<b>3.4</b>	<b>Antibodies</b>	<b>32</b>
3.4.1	Primary Antibodies	32
3.4.2	Secondary Antibodies	33
<b>3.5</b>	<b>Commercial Systems</b>	<b>34</b>
<b>3.6</b>	<b>Chemicals, Reagents and Equipment</b>	<b>34</b>
<b>3.7</b>	<b>Standards and Markers</b>	<b>35</b>
<b>3.8</b>	<b>Software and Databases</b>	<b>35</b>
<b>4</b>	<b>METHODS</b>	<b>36</b>
<b>4.1</b>	<b>Bacteria</b>	<b>36</b>
4.1.1	Culture and Storage	36
4.1.2	Transformation of <i>E. coli</i>	37
<b>4.2</b>	<b>Mammalian Cells</b>	<b>39</b>
4.2.1	Maintenance and Passage of Cell Lines	39
4.2.2	Storage of Mammalian Cells	39
4.2.3	Determination of Total Cell Number	40
4.2.4	Transfection of Mammalian Cells	40
4.2.5	Harvest of Mammalian Cells	42
<b>4.3</b>	<b>Adenovirus</b>	<b>42</b>
4.3.1	Generating Virus from DNA	42
4.3.2	Propagation and Storage of High-Titer Virus Stocks	43
4.3.3	Titration of Virus Stocks	43
4.3.4	Infection with Adenovirus	45
4.3.5	Determination of Virus Yield	45
<b>4.4</b>	<b>DNA Techniques</b>	<b>46</b>
4.4.1	Preparation of Plasmid DNA from <i>E. coli</i>	46
4.4.2	Determining DNA Concentration	47
4.4.3	Agarose Gel Electrophoresis	47

## TABLE of CONTENTS

4.4.4	Isolation of DNA Fragments from Agarose Gels	48
4.4.5	Polymerase Chain Reaction (PCR)	48
4.4.6	Viral DNA isolation	50
4.4.7	Cloning of DNA Fragments	51
<b>4.5</b>	<b>RNA Techniques</b>	<b>52</b>
4.5.1	Isolation of RNA from Mammalian Cells	52
4.5.2	Immunoprecipitation of RNA (RNA-IP)	52
4.5.3	Reverse Transcriptase Polymerase Chain Reaction (RT-PCR)	53
4.5.4	Real-Time PCR (qPCR)	54
<b>4.6</b>	<b>Protein Techniques</b>	<b>54</b>
4.6.1	Preparation of Total Cell Lysates	54
4.6.2	Quantitative Determination of Protein Concentrations	56
4.6.3	SDS-Polyacrylamide Gel Electrophoresis (SDS-PAGE)	56
4.6.4	Western Blots	57
4.6.5	Immunoprecipitation (IP)	58
4.6.6	Immunofluorescence Staining (IF)	59
4.6.7	GST Pull-down Assays from Cell Lysates	60
4.6.8	Purification of His-Tagged Sumo Conjugates	61
4.6.9	Production and Detection of Radiolabeled Proteins	63
<b>5</b>	<b>RESULTS</b>	<b>64</b>
<b>5.1</b>	<b>Cloning and Generation of Ad5 L4-100K Virus Mutants</b>	<b>64</b>
<b>5.2</b>	<b>General Characterization of Virus Mutants H5pm4151, H5pm4152 and H5pm4153</b>	<b>66</b>
5.2.1	Effects of Inserted Mutations on the Stability and Subcellular Localization of L4-100K	67
5.2.2	Inserted Mutations in the L4-100K Gene Do Not Affect Viral DNA Replication	74
5.2.3	Effects of Inserted Mutations in the L4-100K Gene on Structural Protein Synthesis and Virus Yield	75
5.2.4	Effects of Inserted Mutations in the L4-100K Gene on its Interaction with Hexon and PRMT1	78
<b>5.3</b>	<b>L4-100K Binds to E1B-55K During Lytic Infection</b>	<b>80</b>
5.3.1	Mapping the E1B-55K, Hexon and PRMT1 Binding Sites in L4-100K	81
5.3.2	Mapping the L4-100K Interacting Region in E1B-55K	84
5.3.3	E1B-55K may Mediate the Association of L4-100K with eIF4G	86

## TABLE of CONTENTS

5.3.4	E1B-Associated-Potein 5 (AP5) Relocalizes to the Replication Centers During Adenovirus Infection	87
<b>5.4</b>	<b>Analysis of the Sumo Conjugation and Sulfation Motifs in L4-100K</b>	<b>89</b>
5.4.1	Is L4-100K Sumoylated During Lytic Adenovirus Infection?	89
5.4.2	L4-100K is not Sulfated in Lytic Adenovirus Infection	92
<b>5.5</b>	<b>Arginine Methylation of Human Adenovirus Type 5 L4-100K Protein is Required for Efficient Virus Production</b>	<b>95</b>
5.5.1	Construction of C-terminal L4-100K Mutant Viruses	95
5.5.2	Amino Acid Substitutions in the RGG Boxes Reduce Arginine Methylation of L4-100K During Infection	96
5.5.3	Arginine Methylation of RGG Motifs in L4-100K is Required for Maximal Virus Growth	98
5.5.4	Effect of Amino Acid Substitutions in the RGG Motifs on the Subcellular Distribution of L4-100K During Infection	100
5.5.5	Mutations in the RGG Boxes of L4-100K Reduce Interactions with Tripartite Leader RNAs	105
5.5.6	Arginine Methylation of L4-100K may Regulate Hexon Biogenesis	108
5.5.7	Mutations in the RGG Boxes of L4-100K Alters its Proteolytic Cleavage Late in the Infection	110
<b>5.6</b>	<b>Nuclear Export of Adenovirus Type 5 L4-100K is Mediated by CRM1 and is Crucial for Efficient Virus Infection</b>	<b>112</b>
5.6.1	Construction of L4-100K Mutant Virus H5 <sub>pm4165</sub>	112
5.6.2	Nuclear Export of L4-100K During Adenovirus Infection is Mediated by CRM1	114
5.6.3	Effect of L4-100K-NES Mutation on Virus Replication	116
5.6.4	Inhibition of CRM1 by LMB in the Late Phase of Adenovirus Infection Results in Reduced Late Protein Synthesis and Virus Yield	118
5.6.5	Inactivation of NES in L4-100K does not Block its Binding to Hexon, E1B-55K and PRMT1 but Reduces eIF4G Interaction	122
<b>6</b>	<b>DISCUSSION</b>	<b>124</b>
<b>6.1</b>	<b>L4-100K plays major roles during the late phase of adenovirus infection</b>	<b>124</b>
6.1.1	L4-100K Interacts with eIF4G, hexon, PRMT1, and E1B-55K During Infection	125
6.1.2	The Association of L4-100K with E1B-55K may Contribute to Virus-Specific mRNA Transport and Translation Mechanisms	128
6.1.3	Posttranslational Modifications Regulate L4-100K's Multiple Functions	131

## TABLE of CONTENTS

6.2	Arginine methylation of L4-100K is Critical for Efficient Lytic Infection	134
6.3	The Nuclear Export of L4-100K is Mediated by CRM1 During Lytic Infection	139
7	REFERENCES	144
8	PUBLICATIONS	158
	ACKNOWLEDGEMENTS	160



# Abbreviations

---

Ad	Adenovirus
APS	Ammonium persulfate
aa	Amino acid
bp	Base pairs
BSA	Bovine serum albumin
DEPC	Diethylpyrocarbonate
dd.	Double distilled
DMSO	Dimethylsulfoxide
DTT	Dithiothreitol
EDTA	Ethylenediamine-tetraacetate
FFU	Fluorescence forming units
fw	<i>forward</i>
g	gravitational force
h p.i.	hours post infection
Ig	Immunoglobulin
kb	Kilo base
kbp	Kilo base pair
K/ kDa	Kilo dalton
min	minute
moi	multiplicity of infection
MOPS	Morpholinopropansulfonic acid
nt	Nucleotide
OD	optical density
orf	open reading frame
PBS	phosphate buffered saline
rev	<i>reverse</i>
rpm	round per minute
RT	room temperature
s	second
SDS	sodium dodecyl sulfate
TEMED	N, N, N', N'-Tetramethyl-ethylenediamine
Tris	Tris-(hydroxymethyl)-aminomethane
U	unit
vol	volume
v/v	volume per volume
w/v	weight per volume
wt	wild type

# 1      **Abstract**

---

With the onset of the late phase, one of the first adenovirus type 5 (Ad5) late proteins translated, L4-100K (100K), starts to perform a number of functions that are essential for efficient completion of lytic virus infection. This adenovirus non-structural late protein alters the cellular machinery in favor of translating large amounts of virus products, leading to their subsequent nuclear accumulation for capsid assembly. L4-100K achieves this by contributing to the transport and selective translation of late viral mRNAs, acting as a chaperone for hexon trimerization and being involved in its transport. L4-100K also plays a role in preventing apoptosis of the infected cell by interacting with granzyme-B (GrB) and inhibiting its activity. However, most of the mechanisms underlying these processes, and how 100K is regulated to accomplish these, remain unclear.

In this work the nucleocytoplasmic shuttling properties of L4-100K required to efficiently accomplish cytoplasmic and nuclear tasks and the posttranslational modifications related to this process, as well as its interaction with viral and cellular factors were investigated by generating mutant viruses. These recombinant viruses carry amino acid exchanges at the following locations: (1) C-terminal arginine-glycine-glycine (RGG) boxes; (2) Nuclear export motif; (3) Sumo conjugation motif and (4) N-terminal tyrosine residue of the L4-100K coding sequence. These mutant viruses were not only tested for DNA replication, late protein synthesis and virus yield properties, but also their L4-100K proteins were analyzed for subcellular distribution and protein-protein/RNA interaction patterns.

Arginine to glycine exchanges in the RGG boxes significantly diminished 100K methylation in the course of infection, and substantially reduced virus growth. This

demonstrates that 100K methylation in RGG motifs is an important host-cell function required for efficient Ad replication. Further investigation of this mutant virus indicated that PRMT1-catalyzed arginine methylation in the RGG boxes regulates the binding of 100K to hexon and promotes the nuclear localization and capsid assembly of the structural protein, as well as modulating 100K's tripartite leader-containing mRNA (TL-mRNA) interaction. Furthermore, substitutions in the following glycine-arginine-rich domain (GAR), but not RGG regions, affected 100K nuclear import, implying that the nuclear localization signal of 100K is located within the GAR sequence.

Significantly, phenotypic analyses in different human tumor cell lines revealed that the L4-100K-NES mutant virus is severely defective in both late viral gene expression and virus production compared to wild-type virus, suggesting that nuclear export of 100K is required for maximal virus growth. Consistent with a previous publication, localization of the 100K NES mutant was restricted to the nuclei of infected cells. A similar result was obtained when CRM1 was inactivated by leptomycin B (LMB), showing that CRM1 is the major export receptor for 100K in Ad5 infection. These results demonstrate that CRM1 plays a critical role in the late phase of lytic Ad5 infection, particularly in L4-100K shuttling.

Interestingly, the sumoylation of L4-100K could not be confirmed in the tested human tumor cell lines, although this motif is highly conserved among different Ad serotypes and shows great sequence similarity to the defined Sumo consensus motif. Consistently, the Sumo mutant virus was as efficient as the wt virus in the late phase, yielding high amounts of infectious virus particles. In contrast, the N-terminal tyrosine mutant was found to be defective in late protein synthesis and virus yield. Nonetheless, the function of this tyrosine residue in the highly conserved motif hypothesized to be modified by sulfation still remains to be clarified, since such a modification could not be detected in L4-100K.

## ABSTRACT

---

Furthermore, in this study the interaction of the late non-structural L4-100K protein with early regulator E1B-55K was determined for the first time by immunoprecipitation assays. This interaction was preserved in all of the tested L4-100K and E1B-55K mutant viruses. Interaction sites in both proteins were investigated by GST-pull-down assays using GST-fused-protein-fragments. According to the results, the interaction between these two multifunctional regulatory proteins apparently plays a critical role in the virus-specific translation mechanism, which requires further investigation.

## 2 Introduction

---

### 2.1 Adenoviruses

#### 2.1.1 Classification

Adenoviruses (Ads) were first discovered and isolated in the early 1950s from adenoid tissues and secretions from patients in studies aimed to identify the infectious agent causing the common cold (Hilleman and Werner, 1954; Rowe et al., 1953). Subsequent investigations revealed that although adenoviruses do not cause the common cold, they generally result in infections of the lower respiratory tract (Dingle and Langmuir, 1968; Ginsberg et al., 1955), the eye (Jawetz, 1959) or the gastrointestinal tract (Yolken et al., 1982). Adenoviruses are widely spread around the world infecting approximately 80% of children reaching the age of 5, and mostly causing diarrhea.

*Adenoviridae* family consists of over 100 serologically different virus types classified in four large genera (Horwitz, 1996):

- *Aviadenovirus* infecting birds,
- *Atadenovirus* infecting reptiles,
- *Siadenovirus* infecting amphibians,
- *Mastadenovirus* infecting mammals.

In addition to these four genera, a novel class of Ads were isolated recently from fish and classified as *Ichtadenovirus* (Benkö et al., 2002).

In *Mastadenovirus*, more than 50 different human adenovirus serotypes have been identified to date. They are divided in 6 subgroups (A to F) based on their sequence homology, and ability to agglutinate red blood cells as well as transform primary rodent cells (Berk, 2007). Serotypes 2 and 5 (Ad2 and Ad5) are the most widely



studied serotypes, and belong to subgroup C (Shenk, 2001).

### 2.1.2 Structure and Genome Organization

Adenoviruses are non-enveloped viruses with an icosahedral protein capsid of 80 – 110 nm in diameter. This protein shell is made up of 252 structural units called capsomeres, including 240 hexons (protein II), and 12 pentons (protein III). The adenovirus capsid not only protects the core genome but also mediates virus entry into the cell. Fibers (protein IV), which are protruding (*spikes*) from penton bases, play a major role in receptor-mediated cell adsorption together with penton base protein (Mathias et al., 1994; Wickham et al., 1994; Wickham et al., 1993). The cellular receptor mediating subgroup C adenovirus entry is the same one used by Coxsackie B virus. Hence this receptor is called Coxsackie/Adenovirus Receptor (CAR) (Bergelson et al., 1997). Minor structural components of the capsid include proteins IIIa, VI, VIII and IX (Fig. 1).

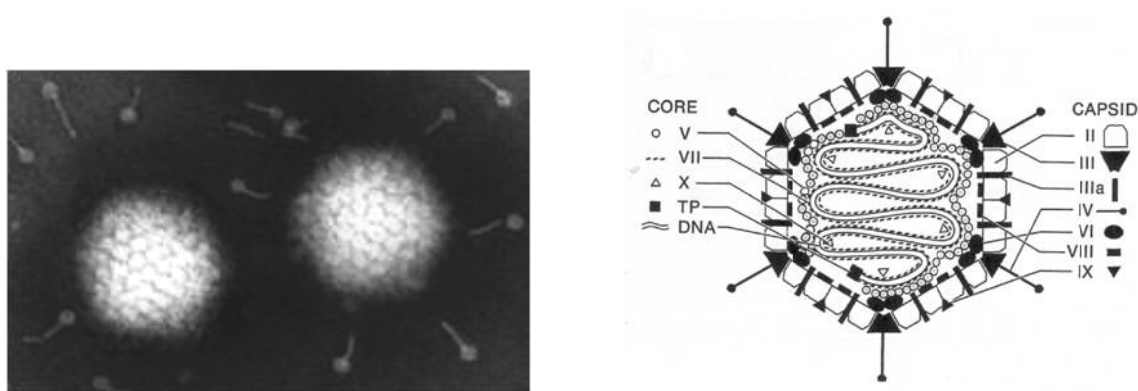


**Figure 1. Electron microscopic image and schematic representation of adenovirus**

The image on the left shows the electron microscopic appearance of 2 adenovirus particles. The icosahedral structure of the capsid and the fiber spikes can be seen. On the right, virion organization of an adenoviral particle is presented schematically, including core and capsid proteins (from Stewart and Burnett, 1993).

The adenovirus genome consists of 34 – 44 kbp long double stranded linear DNA. The genome is typically divided into 100 map units and is organized into a DNA strand oriented to the right, called the r-strand, as well as a strand oriented to the left called

the 1-strand. The genome of the most studied serotypes 2 and 5 comprises 9 transcription units encoding approximately 40 regulatory and structural proteins as well as 2 non-coding RNAs (*virus-associated RNAs*, VA-RNAs). The transcription units are composed of five early (E1A, E1B, E2, E3, E4), two delayed (IX and IVA2), and one major late unit (MLTU), generating five families of RNAs, L1 to L5, upon processing. All of these transcription units are transcribed by RNA polymerase II, whereas VA-RNAs are transcribed by RNA polymerase III (Shenk, 2001).

Each 5' end of the genome contains a characteristic inverted terminal repeat (ITR) that is covalently bound to the terminal protein (TP), and serves as a primer for viral DNA replication (Davison et al., 2003). Three other proteins are packed with the viral genome: proteins V, VII and  $\mu$ p (protein X). These arginine-rich proteins protect the viral DNA and assist in its folding.

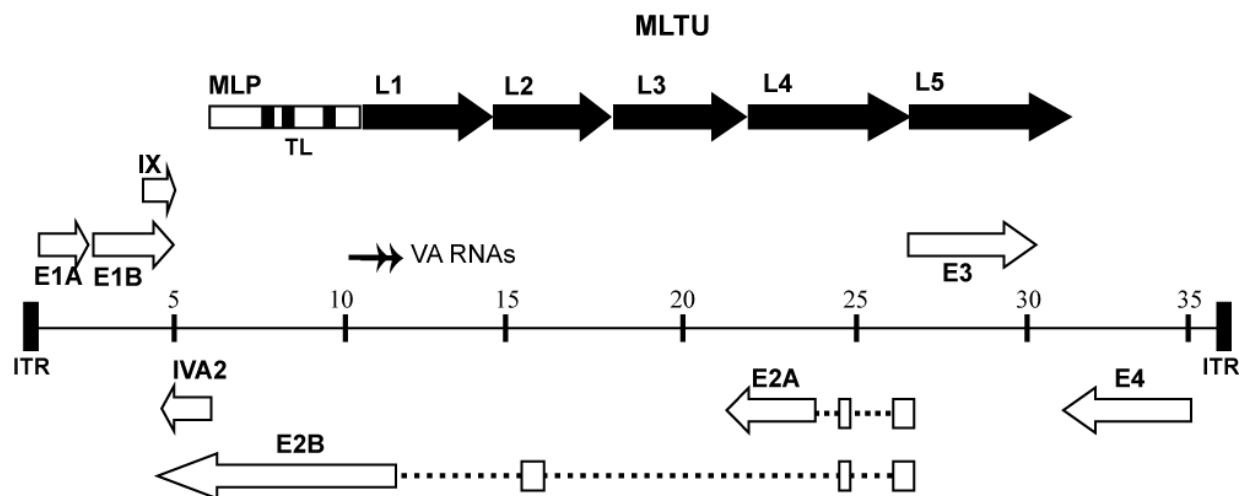


**Figure 2. Genome organization of adenovirus type 5**

The organization of early (E1A, E1B, E2A/B, E3, E4, IX und IVA2) and late (MLTU) transcription units on both DNA strands of the viral genome is demonstrated by arrows. Early proteins are responsible for DNA replication (E2), immune system modulation (E3), transcription and RNA processing (E1, E4), and cell cycle control (E1A, E1B and E4). Late units (L1-L5) mainly encode for structural proteins with a few exceptions. MLTU: *major late transcription unit*; MLP: *major late promoter*; TPL: *tripartite leader*; VA-RNAs: *virus-associated RNAs*; ITR: *inverted terminal repeat*.

### 2.1.3 Productive Infection Cycle

Human adenoviruses can infect a wide range of cell types *in vivo*, generally resting post-mitotic cells and differentiated epithelial cells of respiratory and gastrointestinal tracts. Recently, it was shown that the central nervous system also represents a common site for adenovirus infection (Kosulin et al., 2007). In tissue culture several tumor cell lines and primary cells can be infected by adenoviruses. While adenovirus causes lytic infection in human cells, infection of rodent cells results in abortive infection (Modrow, 1997; Shenk, 2001).

Lytic adenovirus infection can be divided into two phases, early and late. Upon receptor-mediated internalization of an adenovirus particle, viral DNA is imported into the cell nucleus and the early phase of infection begins with the transcription of the “immediate early” gene E1A. This leads to the transcription of E1B- to E4-RNAs that are alternatively spliced to produce early regulatory proteins, which prepare the optimal environment and conditions for viral DNA replication and further encapsidation. These early adenoviral proteins are also responsible for the induction of cell cycle progression (E1 and E4), inhibition of apoptosis and growth arrest (E1A and E1B), modulation of the immune response, and maintenance of cell viability (E3). The proteins encoded by the E2 region are responsible for viral DNA replication. E2A encodes the DNA binding protein (DBP) whereas E2B encodes the DNA polymerase and the precursor of the terminal protein (pTP) (Shenk, 2001). The E4 region encodes at least six different products transcribed from different open reading frames (orf), namely E4orf1, E4orf2, E4orf3, E4orf4, E4orf6 and E4orf6/7. Another putative product of this region, E4orf3/4, remains to be identified. These E4 proteins play critical roles in efficient viral replication (Tauber and Dobner, 2001b).

With the onset of the DNA replication, late phase begins with the activation of the major late promoter (MLP), and the late RNAs are produced from the 29 kb long major late transcription unit (MLTU) by differential splicing (Fig. 2). All of the late mRNAs (L1-L5) contain a common 5'-non-coding sequence of 201 nucleotides, called

the tripartite leader (TL). Most of the proteins encoded by these late families are structural ones involved in DNA packaging and capsid formation. In the late phase of infection, while host cell mRNA transport and translation pathways are shut-off and DNA repair processes are modulated, viral late proteins are efficiently synthesized and transported to the nucleus. DNA packaging and encapsidation take place in the nucleus. Host cell viability is maintained until the virus particles are assembled. A few known regulatory proteins (L4-100K, -33K and -22K) of the late phase orchestrate these events together with the early ones (E1B-55K, E4orf6, and E2A-72K). At the end of a productive replication cycle, approximately 24 hours post infection, up to 10,000 viral particles are released upon lysis of the cell.

### 2.1.4 **Oncogenic Potential of Human Adenoviruses**

The oncogenic potential of human adenoviruses was first discovered in 1962 by Trentin and coworkers upon subcutaneous injection of serotype 12 (Ad12) into new born hamsters (Trentin et al., 1962). Since then, the transformation potentials of these viruses, particularly of their early regulatory proteins, have been under investigation. Studies exploring the transformation capacity of other Ad serotypes in different rodent types revealed that not every serotype is capable of inducing tumorigenesis. According to these studies, subgroup A adenoviruses are highly oncogenic causing tumor formation in a short time, whereas subgroup B adenoviruses are weakly oncogenic causing inefficient tumor formation after a long incubation time. Serotypes from subgroup C to F do not cause tumor formation at all when injected into rodents (Tab. 1). Serotypes 9 and 10 from subgroup D induce mammary carcinoma in female rats (Ankerst and Jonsson, 1989; Javier et al., 1991; Thomas et al., 2001).

**Table 1. Oncogenic potentials of adenovirus serotypes**

ONCOGENICITY IN RODENTS	SUBGROUP	SEROTYPE	TUMOR TYPE
Highly oncogenic	A	12, 18, 31	undifferentiated sarcomas
	D	9, 10	Fibroadenomas
Weakly oncogenic	B	3, 7, 11, 14, 16, 21, 34, 35	undifferentiated sarcomas
Non-oncogenic	C - F	C (1, 2, 5, 6); D (8, 13, 15, 17, 19, 20, 22-30, 32, 33, 36-39, 42-49, 51); E (4); F (40, 41)	none

Interestingly, all human adenovirus serotypes can transform primary rodent cells in culture (Nevins, 1996). The transformed cells lose contact inhibition and form multilayer colonies, which are called foci. However, not all of these transformed cells can induce tumorigenesis upon inoculation into rodents. Their tumorigenicity is dependent of the adenovirus serotype or immunity of the animal (Endter and Dobner, 2004; Graham, 1984; Graham et al., 1984; Shenk, 2001; Williams et al., 1995). For instance, subgroup A adenovirus transformed cells can cause tumor development in immunocompetent rodents, whereas subgroup C transformed cells can only cause tumorigenesis in immunosuppressed (thymus deficient) rats. This shows that the tumorigenicity of Ad-transformed cells is mainly affected by the thymus-dependent CTL-components of the animal's immune system (Bernards et al., 1983; Cook and Lewis, 1987; Raska and Gallimore, 1982).

Although the molecular mechanism of this transformation in rodents is still unclear, the presence of the E1 oncoproteins in all Ad or plasmid transformed cells suggests that integration of the E1 region into the host cell genome is required to initiate cell transformation (Hutton et al., 2000; Shenk, 2001). Moreover, it was shown that E4 gene products further contribute to adenovirus-mediated cell transformation by novel mechanisms (Endter and Dobner, 2004; Tauber and Dobner, 2001a). Until recently no significant correlation between adenovirus infection and cancer was detected in humans (Chauvin et al., 1990; Mackey et al., 1979; Mackey et al., 1976; Wold et al.,



1979). However in 2007, two separate studies pointed to adenovirus infections possibly being related to tumorigenesis in brain tissue (Kosulin et al., 2007) and might correlate with childhood acute lymphoblastic leukemia (ALL) (Gustafsson et al., 2007). The possible relationship between supposed long-term, non-harmful adenovirus infection and human malignancies remains to be established.

## **2.2 Regulatory Proteins of Adenovirus**

### **2.2.1 Early Proteins E1B-55K and E4orf6**

One of the most important early regulatory proteins of Ad5 is E1B-55K, which is a 496 amino acid long multifunctional phosphoprotein. The expression of E1B-55K begins early in the infection, and it contributes to transcriptional, posttranscriptional, translational, and posttranslational regulation throughout the infection cycle. E1B-55K protein binds to tumor suppressor p53 and blocks its transactivation activity (Kao et al., 1990; Sarnow et al., 1982a; Shen et al., 2001; Yew and Berk, 1992; Yew et al., 1990). E1B-55K not only counteracts the transcriptional functions of this tumor suppressor, but further promotes its proteasomal degradation by forming a Cullin 5 based ubiquitin ligase complex together with E4orf6 (Blanchette et al., 2004; Querido et al., 2001), a small 34 kDa protein encoded by the E4 region (Fig. 3). This inhibits p53 induced apoptosis of the host cell. The ubiquitin ligase complex is similar to previously characterized E3 ligase SCF complexes (Zheng et al., 2002) and VBC (Kamura et al., 2001) and functions in targeting proteins for degradation. E1B-55K is thought to recognize target substrates for degradation, while E4orf6 appears to be important for the formation and assembly of the complex (Blanchette et al., 2004; Querido et al., 2001). This ubiquitin ligase complex targets further DNA repair pathway elements such as Mre11 of the MRN DNA double-strand break repair complex (Stracker et al., 2002) and DNA ligase 4 (Baker et al., 2007). Many possible targets are still under investigation.

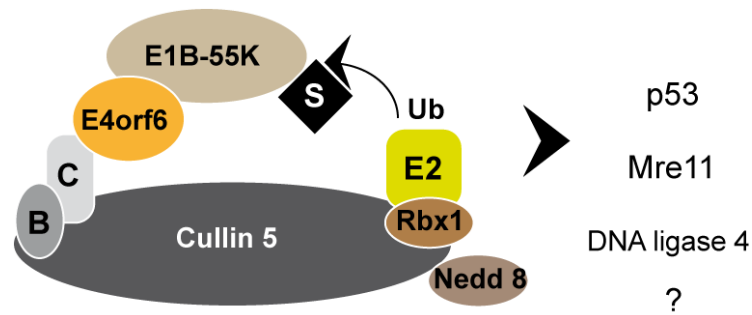


**Figure 3. Schematic representation of the E1B-55K/E4orf6 ubiquitin ligase complex**

E1B-55K and E4orf6 interact with each other. E4orf6 associates with Cullin 5 via Elongin C (C) and Elongin B (B). Cullin 5 is modified by the addition of Nedd 8, Rbx1 and an E2 ligase, which will ubiquitinate (Ub) substrates (S) such as p53, Mre11, DNA ligase 4, and maybe many more (?). E1B-55K introduces the substrate to the complex and may interact with one or more members of the Elongin-Cullin 5 complex (Blanchette et al., 2004).

Interestingly, the ubiquitin ligase activity of the E1B-55K/E4orf6 complex has also been shown to be essential for viral late mRNA transport and host shut-off (Blanchette et al., 2008; Woo and Berk, 2007). Although the mechanism is still unknown, it is now clear that E1B-55K/E4orf6 complexes promote the nuclear export of virus specific TL-mRNAs while blocking export of cellular mRNAs (Dobner and Kzhyshkowska, 2001; Flint and Gonzalez, 2003). The first evidence for such a regulation came from virus mutants unable to express E1B-55K or E4orf6 (*dl1520* and *H5dl355*, respectively). These mutants are defective in cytoplasmic accumulation of viral transcripts compared to the wt virus (Babiss et al., 1985; Bridge and Ketner, 1989). Since the double-mutant virus ( $\Delta$ E1B-55K/E4orf6) exhibited the same defect as the single mutants (Bridge and Ketner, 1990; Cutt et al., 1987), it was suggested that an active complex of E1B-55K and E4orf6 is responsible for the selective nucleocytoplasmic transport of viral late mRNAs (Babich et al., 1983; Babiss and Ginsberg, 1984; Babiss et al., 1985; Pilder et al., 1986; Williams et al., 1986). This idea was further supported when nuclear export signals (NES) that mediate nucleocytoplasmic shuttling were found in both proteins. However, neither of these nuclear export signals have been shown to mediate mRNA transport, nor has specific TL-mRNA binding activity of this complex been detected, although E1B-55K was reported to bind non-specifically to

RNA (Horridge and Leppard, 1998a). Since the tripartite leader sequence was claimed to enhance the transport of these mRNAs (Huang and Flint, 1998a), it is plausible to predict the presence of another adaptor protein in the adenoviral ubiquitin ligase complex, or an export receptor mediating this specific translocation.

Another hypothesis supports the idea that this complex (or one of its components) binds to a cellular RNA export factor and augments its activity at viral replication centers (Ornelles and Shenk, 1991). This would not only ensure the selectivity for viral mRNAs but would also deprive the cellular transcripts of this factor. Indeed, an heterogeneous ribonucleoprotein (hnRNP) that assists mRNA processing and transport was found to interact with E1B-55K, subsequently called E1B-AP5 (E1B-55K associated Protein 5) (Gabler *et al.*, 1998). Further investigations showed that E1B-AP5 might assist the transport of mRNA via TAP (Tip associated protein/NXF1), which is the major cellular mRNA transport receptor (Bachi *et al.*, 2000; Izaurralde and Mattaj, 1995). Moreover, we demonstrated the accumulation of E1B-AP5 at the periphery of replication centers during the early phase of adenovirus infection (Blackford *et al.*, 2008), supporting this hypothesis. The molecular mechanisms underlying this selective viral mRNA transport still remain to be established and are under investigation.

### 2.2.2 Late Protein L4-100K

One of the rare regulatory proteins transcribed from the adenovirus major late transcription unit is 100K from the late region 4 (L4). L4-100K is a large, dumb-bell shaped phosphoprotein with 806 amino acids and migrates at 100 kDa on an SDS gel (Fig. 4B). This late region also encodes 33K, which plays a critical role in the early- to late-phase switch together with 100K (Farley *et al.*, 2004); 22K, which was recently identified as a factor assisting the packaging of viral genome (Ostapchuk *et al.*, 2006); and pVIII, which is one of the minor capsid components (Fig. 1). L4-33K and L4-22K share the last 95 nucleotides of the L4-100K sequence, but using a different reading

frame (Fig. 4A). With the onset of the late phase, L4-100K starts to perform a number of functions that are essential for efficient completion of lytic virus infection. This adenoviral non-structural late protein is synthesized in large quantities, and alters the cellular machinery in favor of translating large amounts of virus products, leading to their subsequent nuclear accumulation for capsid assembly. L4-100K achieves this by contributing to the transport and selective translation of late viral mRNAs, acting as a chaperone for hexon trimerization as well as being involved in its transport. L4-100K also plays a role in preventing apoptosis of the infected cell by interacting with granzyme-B and inhibiting its activity. Interaction sites and modification motifs identified so far in L4-100K are depicted in Figure 4C.

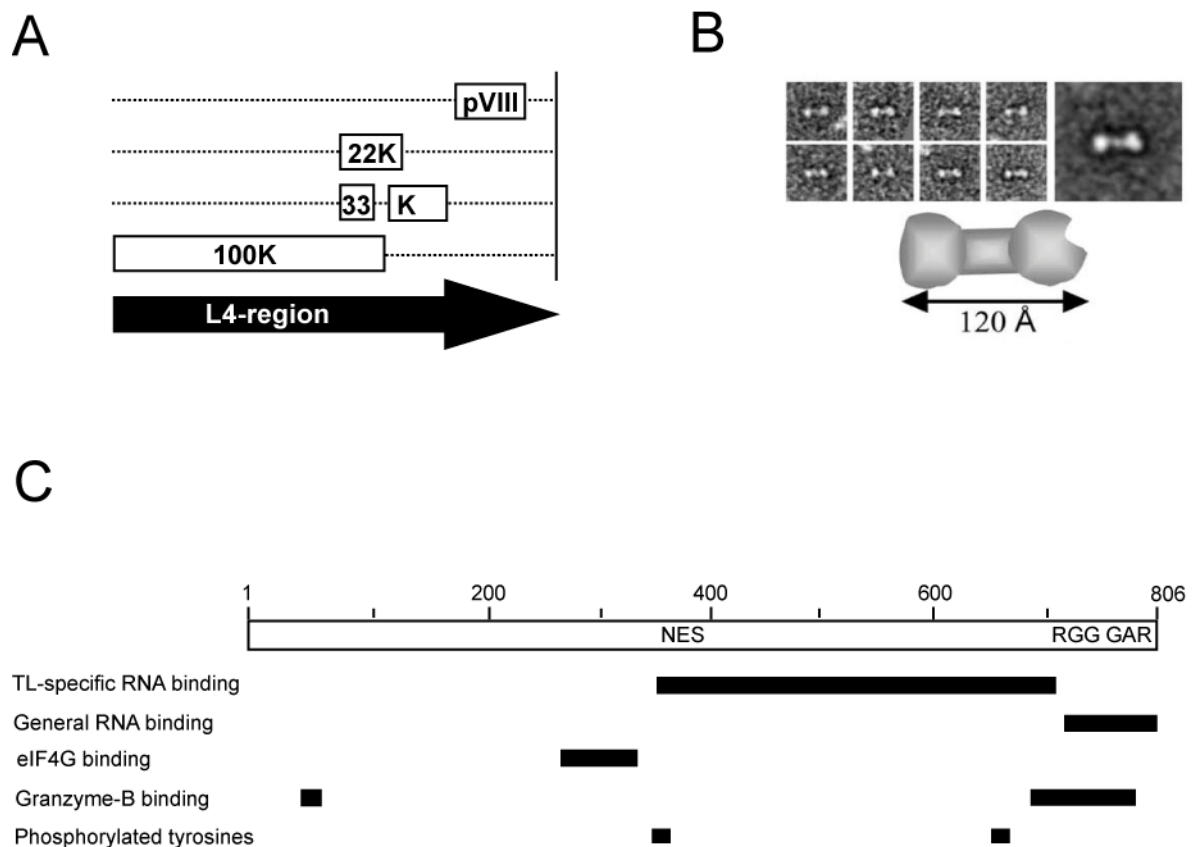


**Figure 4. The structure, domains and motifs of L4-100K protein**

(A) L4-region and the proteins (100K, 33K, 22K, and pVII) encoded by this transcription unit are represented. (B) EM analysis of Ad2 100K. The averaged image is illustrated as two globular domains connected in the middle with a rod (Hong et al., 2005). (C) Diagram of L4-100K protein. The leucine-rich nuclear export signal (NES), the RGG boxes and GAR region are shown in the protein box. The location of the TL-specific and general RNA-binding domains, eIF4G binding region, the granzyme-B

binding domains and phosphorylated tyrosine residues are indicated below. Numbers refer to amino acid positions (Assembled from several publications cited in the text).

The first insights about the functions of this late protein came from investigating hexon trimerization. Early studies demonstrated that in certain temperature-sensitive (*Ts*) adenovirus mutant infections, accumulation of hexon proteins in the cytoplasm was impaired. Further complementation analysis showed that these mutations were located in the L4-100K gene (Kauffman and Ginsberg, 1976; Oosterom-Dragon and Ginsberg, 1981). Subsequent research revealed the indispensable role of 100K in hexon biogenesis. Briefly, L4-100K acts as a chaperone for the formation of hexon trimers, which are otherwise unstable (Cepko and Sharp, 1982; Cepko and Sharp, 1983; Hong et al., 2005). In addition, it was suggested that 100K contributes to the transport of these trimers and subsequent capsid assembly (Morin and Boulanger, 1986). However, neither the binding sites on each protein nor the mechanism of this process has been elucidated so far.

Another striking role of 100K was shown in the translation of late viral transcripts. Upon determining a translation initiation defect in an L4-100K-*Ts* mutant virus infection (Hayes et al., 1990a), the role of this protein in late viral mRNA translation pathway was eagerly explored. Shortly after, L4-100K was shown to specifically bind to TL-transcripts and promote their translation (Riley and Flint, 1993). Subsequent reports revealed that L4-100K achieves this selective translation of viral transcripts via a ribosome shunting mechanism (Xi et al., 2004; Xi et al., 2005). This process involves the interaction of 100K with both the TL sequence possessed by all the late viral transcripts and the scaffolding element of the cap-dependent translation initiation complex, eIF4G (Fig. 5). Upon the latter binding to 100K, phosphorylation of the cap-binding protein eIF4E is competitively inhibited since Mnk1 (MAP kinase activating kinase/p38) and 100K bind to the same domain in eIF4G (Cuesta et al., 2000; Cuesta et al., 2004). This results in blocking the linear cap-dependent translation machinery, impairing the host cell protein synthesis (*host shut-off*), and viral transcripts are translated by a ribosome shunting mechanism. Ribosome shunting was first described

for the cauliflower mosaic virus (CaMV) 35S mRNA (Futterer et al., 1993; Ryabova and Hohn, 2000). Later it was also described for adenoviral late mRNAs, the Sendai virus Y mRNA, papillomavirus E1 mRNA, and for several mammalian mRNAs (reviewed in Xi et al., 2004). The general shunting mechanism involves loading 40S ribosome subunits onto the 5'-end of the capped mRNA followed by direct translocation of 40S subunits to the downward initiation codon, which is directed by cis-acting RNA shunting elements. In adenovirus these shunting elements were identified in the TL sequence (Dolph et al., 1990; Dolph et al., 1988; Zhang and Schneider, 1993). Although not clearly understood, the complementary nature of TL structures to 18S rRNA was suggested to drive ribosome shunting on TL-transcripts by capturing 40S ribosomes or providing a conformation that is critical for shunting initiation (Xi et al., 2004). Recently, it was shown that 100K is posttranslationally modified to confer selective binding to virus specific mRNAs, although it also has a general RNA binding motif, and this modification was reported to be tyrosine phosphorylation (Xi et al., 2005). Tyrosine phosphorylation of 100K is considered essential for efficient ribosome shunting and late protein synthesis, but not to be involved in eIF4G binding.

Another interesting but not well understood issue in adenovirus induced eIF4E dephosphorylation and inhibition of host cell protein synthesis is the possible contribution of E1B-55K protein. Previously it had been shown that in a certain E1B-55K mutant virus infection (*dl338*) eIF4E remained phosphorylated (Zhang et al., 1994). The authors suggested that inhibition of the cap-dependent translation machinery relies on a late factor and the mRNA export of this late protein was thought to be impaired in the *dl338* mutant (Zhang et al., 1994). Indeed, this late factor was then revealed to be L4-100K (Cuesta et al., 2000). Nonetheless, E1B-55K might play a more direct role in the inhibition of eIF4F complexes by interacting with L4-100K. Likewise, elaborate experiments showed that at non-permissive temperatures (32 °C) E1B-55K deleted virus (*dl1520*) could support mRNA export in H1299 cells but not late viral protein synthesis (Harada and Berk, 1999), meaning that inefficient

mRNA export cannot account for the eIF4E dephosphorylation defect observed in *dl338* infection. Concomitant with that, at elevated temperatures (39 °C) *dl1520* was observed to restore late viral protein synthesis to nearly wt levels (Harada and Berk, 1999). This can be explained by the under-phosphorylation of eIF4E in the case of a heat shock, a cellular regulation mechanism that aims to eliminate casual protein translation under such conditions (Lamphear and Panniers, 1991).

In summary, adenovirus infection induces inhibition of eIF4E phosphorylation, which is required for *host shut-off*, and late viral proteins are translated via a ribosome shunting pathway where L4-100K and TL-sequences play major roles with possible assistance from E1B-55K.

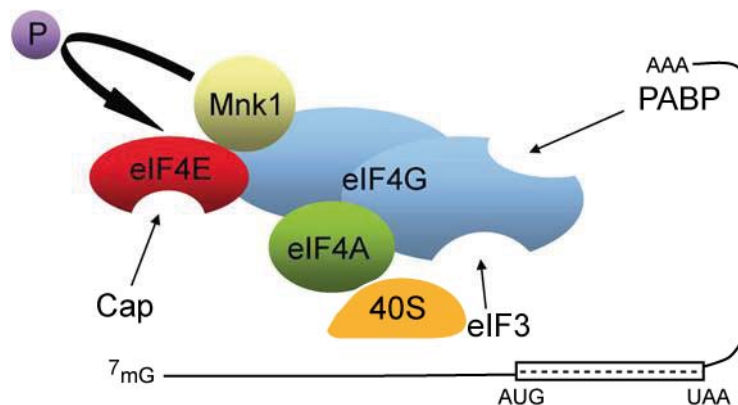


**Figure 5. Diagram of eukaryotic translation initiation complex, eIF4F**

eIF4F comprises a core group of three proteins: a 24 kDa cap-binding protein (eIF4E), a 45 kDa ATP-dependent RNA helicase (eIF4A), and a large scaffold protein that assembles the complex (eIF4G).. Mnk1 phosphorylates (P) eIF4E when both are bound to eIF4G. Also bound to eIF4G are Poly-A-binding protein (PABP), which interacts with the poly-A tail (AAA), and eIF3, which associates with the 40S ribosome. This machinery promotes a 5'-to-3' linear search for the initiation codon (AUG) through a process known as ribosome scanning when eIF4E is phosphorylated. During adenovirus infection L4-100K binds to eIF4G and inhibits Mnk1-eIF4G interactions (Cuesta et al., 2000; Cuesta et al., 2004; Xi et al., 2004).

In the last decade, another very important function of L4-100K was identified that contributes to inhibiting untimely apoptosis of the host cell in the late phase of infection. Cytotoxic lymphocytes represent the primary defense against virus-infected

cells. The cytotoxic effector cell induces target cell death through pathways initiated by Fas receptor or through granule exocytosis (Spaeny-Dekking et al., 1998). Granules secreted by cytotoxic lymphocytes mediate targeted cell death through the unique activities of granule components. Serine proteases granzyme A (GrA) and granzyme B (GrB) are the most abundant enzymes in these granules (Andrade et al., 2001; Spaeny-Dekking et al., 1998). While GrA induces single-strand DNA breaks and cleavage of PHAP II and histone H1 in a caspase-independent manner, GrB catalyzes the cleavage and activation of several downstream caspases, inducing apoptosis of the target cell (Salvesen and Dixit, 1997). GrB can also induce caspase-independent cell death mechanisms (Sarin et al., 1997). L4-100K was identified as a specific substrate for GrB (Andrade et al., 2001). Interestingly, L4-100K was shown to inhibit GrB activity, although cleaved by this protease (Andrade et al., 2001). Two distinct regions in L4-100K were identified as GrB interaction domains (Fig. 4B). One was shown to be Asp48-Pro49, which interacts with the active site of the enzyme. The other was suggested to be located between amino acids 688 to 781, which interacts with an exosite (Andrade et al., 2003). Both sites were shown to be critical for 100K and GrB interaction, which results in the cleavage of 100K at Asp48 and the inhibition of GrB activity (Andrade et al., 2003). Recently another granzyme with unknown functions, granzyme-H (GrH), was reported to directly cleave adenovirus DNA-binding protein (DBP) and L4-100K (Andrade et al., 2007). Interestingly, GrH-mediated cleavage of 100K was shown to allow gradual GrB recovery. Apparently like other viruses, adenoviruses evolved distinct mechanisms to overcome host cell immune and inflammatory responses. Early in infection E1A is blocking interferon-induced gene expression, VA-RNA is inhibiting interferon induced PKR activity (Burgert et al., 2002), the E1B-55K/E4orf6 complex is degrading p53 (Dobner et al., 1996), Mre11 (Stracker et al., 2002) and DNA ligase 4 (Baker et al., 2007), as well as several E3 proteins are preventing cytotoxic cell killing (Lichtenstein et al., 2004a; Lichtenstein et al., 2004b), while late in infection L4-100K participates in this task and inhibits GrB action.



## **2.3 Cellular Factors Mediating L4-100K Functions**

### **2.3.1 Protein Arginine Methylation**

Arginine methylation of proteins is a posttranslational modification mediated by ubiquitously expressed protein arginine methyl transferases (PRMTs), which utilize S-adenosylmethionine (AdoMet) to yield mono or dimethylated arginine residues. This modification affects major processes in the cell such as protein-protein interactions, regulation of transcription, RNA processing, DNA repair, nucleocytoplasmic shuttling of proteins, and protein stability (reviewed in (Bedford, 2007; Bedford and Richard, 2005). In addition, arginine methylation was suggested to protect this arginine residue against attack by endogenous reactive dicarbonyl agents (Fackelmayer, 2005). Following the discovery of protein arginine methylation, many proteins were found to be modified by these enzymes, including fibrillarin, nucleolin, GTPase P, MBPs, myosin, heat shock proteins and H3 histones (Chen et al., 1999; Li et al., 2004). Recent findings indicated the significance of methylation not only for cellular proteins, but also for viral transcripts. The HIV transactivator (TAT) protein was identified as the first HIV protein to contain methylated arginines (Boulanger et al., 2005). Inhibition of methylation was reported to increase HIV gene expression and the authors suggested that increasing this modification might provide protection against HIV infection. Conversely, blocking methylation was proposed as protection against hepatitis delta, since inhibition of this modification prevented hepatitis delta replication (Li et al., 2004). Also Herpes simplex virus RNA binding protein ICP27 was reported to be methylated in its RNA binding domain (Mears and Rice, 1996).

PRMTs mediate the transfer of a methyl group from AdoMet to a guanidino nitrogen of arginine, resulting in S-adenosylhomocysteine (AdoHyc) and methylarginine. Methylated arginine residues exist as monomethylarginines (MMA), asymmetric dimethylarginines (aDMA), or symmetric dimethylarginines (sDMA) (Bedford and Richard, 2005). PRMTs are classified in two groups as type I and type II according to the resulting methylarginine type. Type I PRMTs (PRMT1, PRMT3, PRMT4, and

PRMT6) asymmetrically dimethylate arginine residues yielding an aDMA residue, whereas type II PRMTs (PRMT5 and PRMT7) catalyze the formation of symmetrically methylated arginines (sDMA). Both types catalyze the formation of MMA as an intermediate. Histones were shown to have only MMA *in vivo* (Strahl et al., 2001). To date, no methylation activity has been identified for PRMT2 and PRMT8. Interestingly, all substrates of type I PRMTs, PRMT1, PRMT3, and PRMT6 were found to be methylated at a common Arg-Gly-Gly (RGG) motif and/or in a Gly-Arg-rich (GAR) sequence, whereas PRMT4 (CARM1) does not methylate GAR motifs (Bedford and Richard, 2005).

In 2004, cell type-dependent arginine methylation of L4-100K during adenovirus infection was reported by our group (Kzhyshkowska et al., 2004), meaning L4-100K was the first adenoviral protein reported to be methylated. However, the consequences of this modification on L4-100K functions remained unknown. PRMT1, which was shown to mediate 100K methylation, is the predominant methyl transferase in human cells and responsible for at least 85% of all methylation reactions (Tang et al., 2000). This enzyme was previously thought to be located predominantly in the nucleus but recent reports indicated a major localization in the cytoplasm, implicating the possibility of constant shuttling between nucleus and cytoplasm (Araya et al., 2005; Herrmann et al., 2005). PRMT1 methylates its substrates co-translationally or shortly after translation while they are still cytoplasmic (Herrmann et al., 2005). PRMT1-mediated methylation of a protein may have various consequences. For example, methylation of Mre11 in a C-terminal GAR domain by PRMT1 was recently shown to be necessary for its nuclear compartmentalization and exonuclease activity (Boisvert et al., 2005a; Boisvert et al., 2005b). In Ewing's sarcoma (EWS) gene product, RGG boxes 2 and 3, shown to be responsible for nuclear localization of this protein, were detectably methylated by PRMT1 (Araya et al., 2005). Protein arginine methylation has also been shown to regulate nuclear import of hnRNPA2 (Nichols et al., 2000), sam68, and RHA in mammals (Lukong and Richard, 2004). In addition to regulating subcellular localization, protein arginine methylation

has been implicated in modulating protein-protein/nucleic acid interactions, as shown for Mre11 (Boisvert et al., 2005a; Dery et al., 2008), hnRNP K (Ostareck-Lederer et al., 2006), and 53BP1 (Boisvert et al., 2005c). Arginine methylation of proteins may facilitate protein-protein binding, or may block certain interactions (Bedford, 2007).

In general, RNA binding proteins (RBPs) represent the major targets for PRMTs. Several RBPs were identified as being arginine methylated (Herrmann et al., 2004; Liu and Dreyfuss, 1995). One of the most important characteristics of RBPs (such as hnRNPs) is arginine methylation in GAR-RNA binding domains (Kzhyshkowska et al., 2001; Liu and Dreyfuss, 1995). Several examples demonstrated that arginine methylation acts as a direct signal for RNA interaction either in a positive or negative way (Bedford and Richard, 2005; Liu and Dreyfuss, 1995; Mears and Rice, 1996). Methylation of an RBP may prevent hydrogen bonding by sterical hindrance, or positively affect RNA interactions by providing more hydrophobicity with methyl groups, hence facilitating interactions with RNA bases (Bedford and Richard, 2005).

Until recently, arginine methylation was considered a rather static, irreversible modification since no arginine demethylase was known. Peptidyl arginine deiminases (PADs) were known to block methylation on an arginine residue by converting it to citrulline, but this reaction is not demethylation since PADs do not catalyze the deimination of MMA or DMA. The first arginine demethylase, JMJD6 (Jumonji-domain-containing protein) was reported in 2007 (Chang et al., 2007). JMJD6 was proposed to function in the nucleus as a histone arginine demethylase. Nevertheless, it remains unknown whether this enzyme has other substrates.

### 2.3.2 CRM1-Mediated Nuclear Export

CRM1 (Chromosome region maintenance 1/exportin1), one of the nuclear export receptors belonging to the importin  $\beta$  superfamily, functions as a protein and RNA transporter from the nucleus to the cytoplasm and plays critical roles during mitosis

(Hutten and Kehlenbach, 2007). CRM1 was first identified in *Schizosaccharomyces pombe* (Adachi and Yanagida, 1989), and later well established as a major nuclear export factor for proteins, rRNA and several other less abundant RNA species. Since CRM1 itself is not an RNA binding protein, certain adaptor proteins are required for RNA export. Nucleocytoplasmic transport mediated by CRM1 requires a specific nuclear export signal (NES) in the cargo molecule (Hutten and Kehlenbach, 2007). The receptor-cargo interaction and the directionality of the transport are regulated by a small GTPase called Ran (Görlich and Kutay, 1999). Ran is concentrated in the nucleus as RanGTP, whereas in the cytoplasm it is present as RanGDP (Engelsma et al., 2004). Binding of Ran binding protein 3 (RanBP3) to CRM1 further enhances the cargo interaction by acting as a cofactor (Englmeier et al., 2001; Lindsay et al., 2001). During transport, a quaternary complex containing CRM1, RanGTP, RanBP3, and the NES cargo interacts with nucleoporins. CRM1 can interact with several nucleoporins including Nup358 (RanBP2) and Nup214. In the cytoplasm, the transport complex is disassembled by hydrolysis of RanGTP, releasing NES cargo, CRM1 and GDP. CRM1 is then re-imported into the nucleus, possibly by interacting with Nup358 or other nucleoporins (Engelsma et al., 2004; Hutten and Kehlenbach, 2007) (Fig. 6A).

CRM1 has a broad substrate range and requires a leucine/hydrophobic residue-rich motif in the cargo, like the NES first identified in HIV rev (Fischer et al., 1995) and protein kinase inhibitor (PKI) (Wen et al., 1995). Today, a wide spectrum of NES sequences with varying CRM1 affinities have been identified from several cargo proteins, including viral HIV rev and MVM NS2, cellular PKI, MAPKK, NMD3, An3, I $\kappa$ B $\alpha$ , Cyclin B1, and TFIIIA (Hutten and Kehlenbach, 2007). According to the identified NES sequences, a consensus NES motif was suggested as:  $\Phi$ -X<sub>2-3</sub>- $\Phi$ X<sub>2-3</sub>- $\Phi$ -X- $\Phi$  where  $\Phi$  is L, I, V, F, or M, and X is any amino acid (Fornerod et al., 1997; Kutay and Guttinger, 2005). Under physiological conditions most NES sequences bind to CRM1 with relatively low affinity to allow efficient release of the cargo molecule in the cytoplasm (Kutay and Guttinger, 2005).

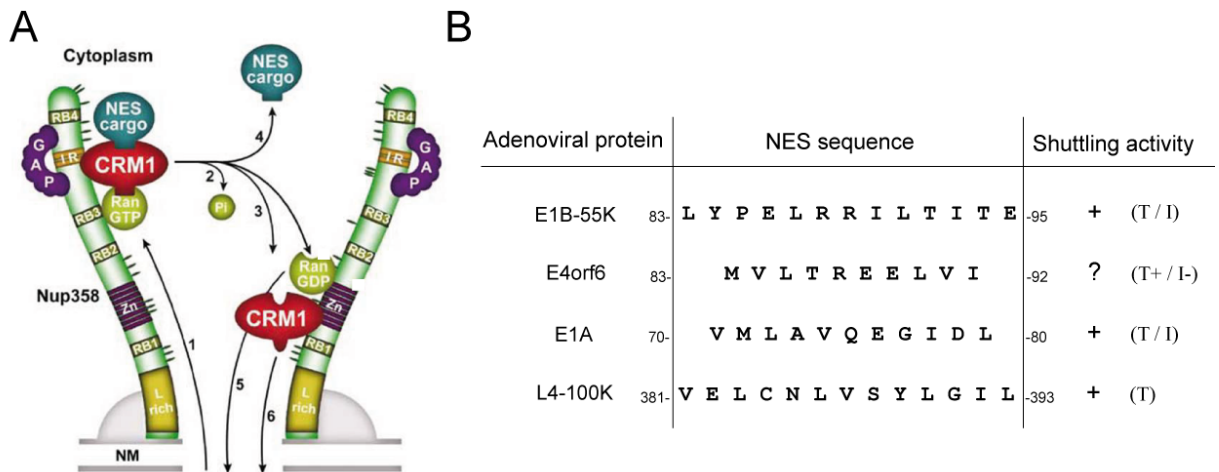


**Figure 6. A model of CRM1 export complex and identified NESs in adenoviral proteins**

(A) NES-cargo/CRM1/RanGTP complexes are translocated through the nuclear pore complex and bind to a cargo-dependent CRM1-binding site on cytoplasmic Nup358. With the hydrolysis of GTP, complex is dissociated and the cargo molecule is released into the cytoplasm, whereas CRM1/GDP is imported back to the nucleus (Engelsma et al., 2004). (B) Comparison of hitherto identified leucine-rich NES sequences in adenoviral proteins. Numbers refer to amino acid positions. Activity of this motif has been shown in either transfection (T), infection (I), or both (T/I). (Assembled from several publications cited in the text)

In the last decade, the leucine-rich NES containing adenoviral proteins identified include E4orf6 (Dobbelstein et al., 1997a), E1B-55K (Dobbelstein et al., 1997a; Krätzer et al., 2000), E1A (Jiang et al., 2006), and L4-100K (Cuesta et al., 2004) (Fig. 6B). Among these, particularly E1B-55K and E4orf6 NES sequences were intensively investigated for their ability to support protein export. Experiments *in vivo* and *in vitro* were carried out to understand the shuttling activity of the E1B-55K/E4orf6 complex with regard to its mRNA transport function. However controversial data have been reported, especially about E4orf6 NES (Carter et al., 2003; Dobbelstein, 2000; Dobbelstein et al., 1997a; Dosch et al., 2001; Rabino et al., 2000a), leaving its necessity in adenovirus infection as an open question. In the case of E1B-55K, a leucine-rich NES sequence was shown to mediate nucleocytoplasmic shuttling of the protein via a CRM1 pathway both in transfected and infected cells, and also verified by *in vitro* assays (Dobbelstein et al., 1997a; Flint et al., 2005; Kindsmuller et al., 2007; Krätzer et al., 2000). Nonetheless, inactivation of this signal had no significant effect on either E1B-55K functions or virus infection efficiency in tested human tumor cell lines (Carter et al., 2003; Flint et al., 2005; Kindsmuller et al., 2007) hinting at the

involvement of another, CRM1-independent shuttling pathway in E1B-55K's functional repertoire (Kindsmuller et al., 2007). On the other hand, NES of E1A protein was shown to be highly critical for its functions and efficient virus infection, and apparently regulated by phosphorylation of a nearby serine residue (Jiang et al., 2006). These controversial observations also put a question mark on the role of CRM1 in adenovirus infection. Recently, a putative NES was identified in the L4-100K amino acid sequence and substitution of the hydrophobic residues in this motif impaired the cytoplasmic export of transiently transfected 100K protein (Cuesta et al., 2004). However, neither the use of this signal during adenovirus infection nor the dependence of 100K export on CRM1 had been elucidated until this present study. (L4-100K is the first late adenoviral protein containing a leucine-rich NES that is interesting to investigate in the light of previous publications).

## **2.4 Aims and Objectives**

During the late phase of adenovirus infection, large amounts of viral late transcripts are produced, transported to the cytoplasm and translated in a virus-specific fashion, while host cell protein synthesis is shut-off. In this phase non-structural late protein L4-100K plays a pivotal role in promoting translation of viral messages, as well as the maturation of hexon monomers, which are the major components of the adenovirus capsid. L4-100K further prevents the untimely apoptosis of infected cells during the late phase of infection. To manage all these tasks, 100K must shuttle efficiently between the cytoplasm and nucleus, a process that is not clearly understood at present. Therefore, identifying the nuclear localization and export signals in L4-100K and a better understanding of how these processes are regulated were the specific aims and objectives of this study.

Previous studies of our group indicated that L4-100K is highly methylated during adenovirus infection. In order to identify the target motif and the effect of this modification, particularly on the subcellular localization of L4-100K, I generated RGG-box virus mutant using a direct cloning strategy. At the same time, the previously suggested nuclear export signal was inactivated by site-directed mutagenesis in the viral context, as well as the neighboring Sumo conjugation motif and a highly conserved tyrosine residue being a putative sulfation site to detect possible effects on subcellular localization and further functions. These virus mutants were tested for L4-100K subcellular localization and protein-protein/RNA interactions, as well as for viral DNA replication, late mRNA translation and virus growth properties.

The results of this study should contribute to elucidating L4-100K nucleocytoplasmic shuttling, which is highly critical for its functions, and also to identifying cellular factors mediating this process. Better understanding of the role of L4-100K in adenovirus infection, such as virus-specific translation mechanisms in human tumor cell lines and the identification of its cellular interaction partners, will further contribute to the development of oncolytic adenoviral vectors.

## 3 Materials

---

### 3.1 Cells

#### 3.1.1 Bacteria Strains

In this study, DH5 $\alpha$  and GM2163 were used to amplify recombinant plasmids. For L4-Box transformation, XL1-Blue (Invitrogen), for bacmid transformation XL2-Blue (Invitrogen), and for GST-protein expression TOP10 or DH5 $\alpha$  were used.

STRAIN	CHARACTERISTICS
TOP10	F <sup>-</sup> , <i>mcrA</i> , $\Delta$ ( <i>mrr-hsdRMS-mcrBC</i> ), $\phi$ 80 <i>lacZ</i> $\Delta$ M15, $\Delta$ <i>lacX74</i> , <i>recA1</i> , <i>araD139</i> , $\Delta$ ( <i>ara-leu</i> )7697, <i>galU</i> , <i>galK</i> , <i>rpsL</i> (Str <sup>R</sup> ), <i>endA1</i> , <i>nupG</i> (Invitrogen).
XL1-Blue	<i>recA1</i> , <i>endA1</i> , <i>gyrA96</i> , <i>thi1</i> , <i>hsdR17</i> , <i>supE44</i> , <i>relA1</i> , <i>lac</i> , [F' <i>proAB</i> , <i>lacI</i> <sup>q</sup> <i>Z</i> $\Delta$ M15, <i>Tn10</i> (Tet <sup>r</sup> )] (Bullock, 1987).
XL2-Blue	<i>recA1</i> , <i>endA1</i> , <i>gyrA96</i> , <i>thi-1</i> , <i>hsdR17</i> , <i>supE44</i> , <i>relA1</i> , <i>lac</i> , [F' <i>proAB</i> , <i>lacI</i> <sup>q</sup> <i>Z</i> $\Delta$ M15, <i>Tn10</i> (Tet <sup>r</sup> ), <i>Amy</i> , <i>Cam<sup>r</sup></i> ] (Bullock, 1987).
GM2163	F- <i>dam-13::Tn9</i> , <i>dcm6</i> , <i>hsdR2</i> , <i>leuB6</i> , <i>his4</i> , <i>thi1</i> , <i>ara14</i> , <i>lacY1</i> , <i>galK2</i> , <i>galT22</i> , <i>xyl5</i> , <i>mtl1</i> , <i>rpsL136</i> , <i>tonA31</i> , <i>tsc78</i> , <i>supE44</i> , <i>mcrA</i> <sup>-</sup> , <i>mcrB</i> <sup>-</sup> (Deutsche Sammlung für Mikroorganismen, Göttingen).
DH5 $\alpha$	<i>supE44</i> , $\Delta$ <i>lacU169</i> , ( $\phi$ 80 <i>dlacZ</i> $\Delta$ M15), <i>hsdR17</i> , <i>recA1</i> , <i>endA1</i> , <i>gyrA96</i> , <i>thi-1</i> , <i>relA1</i> (Hanahan, 1983).

#### 3.1.2 Mammalian Cell Lines

HEK-293, 911 and K16 cells were used for the generation, propagation and titration of virus mutants. H1299 cells were preferred for transfection experiments, and general virus characterization was carried out using A549, H1299 and HepaRG cells. Primary human hepatocytes (PHH), kindly provided by Thomas Weiss (University of Regensburg Hospital, Regensburg, Germany), were cultured in growth medium containing 125 mU/ml insulin, 60 ng/ml hydrocortizone and 10 ng/ml glucagon.



## MATERIALS

CELL LINE	CHARACTERISTICS
<b>HEK-293</b>	Ad5-transformed, human embryonic kidney cell line; the E1 region is integrated into the genome and the adenoviral E1A and E1B gene products are stably expressed (Graham et al., 1977). Helper cell line.
<b>911</b>	Ad5-transformed, human embryonic retinoblastoma cell line; the E1 region is integrated into the genome and the adenoviral E1A and E1B gene products are stably expressed (Fallaux et al., 1996). Helper cell line.
<b>2E2</b>	HEK-293 derived inducible helper cell line. Ad5 ITR, all E2 region, and E4orf6 protein are under the control of a tetracycline-dependent promoter (Catalucci et al., 2005).
<b>K16</b>	Ad5-L4-100K expressing, HEK-293 derived helper cell line. (Hodges et al., 2005).
<b>HeLa</b>	Human cervix carcinoma cell line (Adam <i>et al.</i> , 1986; Gey et al., 1952).
<b>A549</b>	Human lung carcinoma cell line, wild type p53 (Giard et al., 1973).
<b>H1299</b>	Human lung carcinoma cell line, p53 negative (Mitsudomi et al., 1992).
<b>HepaRG</b>	Human hepatocellular carcinoma cell line (Guillouzo et al., 2007).

### 3.2 Adenoviruses

In this work, Ad5 L4-100K virus mutants were generated and characterized. Wild type virus (H5dl309 and H5pg4100) and other mutant viruses were propagated from virus stocks established as referred in the table below.

ADENOVIRUS	CHARACTERISTICS
<b>H5dl309</b>	Wild type Ad5 with a deletion (nt 30005 to nt 30750) in the E3 region (Jones and Shenk, 1979).
<b>dl1520</b>	Ad2/Ad5-chimeric virus, a stop codon at aa position 3 and a 827 bp deletion (nt 2496-3323) were inserted in E1B-55K gene (Barker and Berk, 1987).
<b>H5dl355</b>	E4orf6 deletion mutant, a 14 bp deletion is inserted in E4-orf6 gene (Halbert et al., 1985).
<b>H5pg4100</b>	Wild type Ad5 carrying a 1863 bp deletion (nt 28602-30465) in the E3 reading frame (Kindsmuller et al., 2007).

## MATERIALS

---

<b>H5pm4101</b>	E1B-55K mutant carrying 3 aa exchanges in NES (L83A, L87A and L91A) in a H5pg4100 backbone (Kindsmüller, 2002).
<b>H5pm4102</b>	E1B-55K mutant carrying a single aa exchange in SCM (K104R) in a H5pg4100 backbone (Kindsmüller, 2002).
<b>H5pm4103</b>	E1B-55K mutant carrying aa exchanges in NES (L83A, L87A and L91A) and in SCM (K104R) in a H5pg4100 backbone (Kindsmüller, 2002).
<b>H5pm4149</b>	E1B-55K deletion mutant carrying 4 stop codons in a H5pg4100 backbone (Kindsmüller, 2002).
<b>H5pm4151</b>	L4-100K mutant carrying 3 aa exchanges in RGG-boxes (R727G, R736G, R741G) in a H5pg4100 backbone (this work).
<b>H5pm4152</b>	L4-100K mutant carrying 1 aa exchange in the Sumo motif (K408R) in a H5pg4100 backbone (this work).
<b>H5pm4153</b>	L4-100K mutant carrying 1 aa exchange (Y90A) in a H5pg4100 backbone (this work).
<b>H5pm4165</b>	L4-100K mutant carrying 4 aa exchanges in NES (L383A, L386A, L390A, I392A) in a H5pg4100 backbone (this work).

---

### 3.3 Nucleic Acids

#### 3.3.1 Oligonucleotides

The following oligonucleotides were used as primers for sequencing, PCR amplification, restriction site insertion, and site-directed mutagenesis reactions. Oligonucleotides used in this study were ordered from Metabion, and numbered according to the *Filemaker Pro* data bank of the group.

# MATERIALS

#	NAME	SEQUENCE	PURPOSE
64	E1B bp2043 fwd	5'-CGCGGGATCCATGGAGCGAAGAAACCCATC TGAGC-3'	viral DNA replication
110	E1B 361-389 rev	5'-CGGTGTCTGGTCATTAAGCTAAAA-3'	viral DNA replication
635	pcDNA3-forw	5'-ATGTCGTACAACCTCCGC-3'	sequencing
823	Abra. seq fwd	5'-GGAGTCAGTCGAGAAGAAGG-3'	sequencing
824	Abra. seq fwd	5'-GCAAGATACCCCTATCCTGC-3'	sequencing
825	Abra. seq fwd	5'-GCACTACACCTTTCGACAGG-3'	sequencing
826	Abra. seq fwd	5'-GCGGTGACGGTCTACTGG-3'	sequencing
827	Abra. seq fwd	5'-GGACATGATGGAAGACTGGG-3'	sequencing
1161	fiberlcFO	5'-AAGCTAGCCCTGCAAAACATCA-3'	RT-PCR
1162	fiberlcRE	5'-CCCAAGCTACCAGTGGCAGTA-3'	RT-PCR
1183	L4 -100K-K408R fw	5'-CTTCATTCCACGCTCAGGGGCGAGGCGC-3'	mutagenesis
1184	L4 -100K-K408R rev	5'-GCGCCTCGCCCCCTGAGCGTGGAATGAAG-3'	mutagenesis
1204	gapdhFO3	5'-CATCCTGGGCTACACTGA-3'	RT-PCR
1205	gapdhRE3	5'-TTGACAAAGTGGTCGTTG-3'	RT-PCR
1222	L4-100K-NES(f)	5'-CCAACGTGGAGGCCTGCAACGCGGTCT- CCTACGCTGGAGCTTGCACGAAAACCGC-3'	mutagenesis
1223	L4-100K-NES(r)	5'-GCGGTTTTCTGTGCAAAGCTCCAGCGTAGG- AGACCGCGTTGCAGGCCTCCACGTTGG-3'	mutagenesis
1266	L4-100K-RGG(f)	5'-GCCACCCACGGAGGAGGAATACTGG- GACAGTCAGGCGGAGGAGGTTTTGGAGGAGG- AGGAGGAGGACATGATGG-3'	mutagenesis
1267	L4-100K-RGG(r)	5'-CCATCATGTCCTCCTCCTCCTCCTCCAAAACC- TCTCCGCTGACTGTCCAGTATCCTCCTCCTC- CGTGGGTGGC-3'	mutagenesis
1268	L4box100Kdelfw	5'-GGCAGAAAAAGATCAGGAGTCAGTCGAGA- AGAAGG-3'	mutagenesis
1269	L4box100Kdelrev	5'-CCTTCTTCTCGACTGACTGACTCCTGATCTTT- TCTGCC-3'	mutagenesis
1295	L4-100K-AAA(fw)	5'-GCTTGCCGACTTGGAGGAGGCAGCCGCACT- AATGATGGCCGC-3'	mutagenesis
1296	L4-100K-AAA(rev)	5'-GCGGCCATCATTAGTGC GGCTGCCTCCTCC- AAGTCGGCAGGC-3'	mutagenesis

## MATERIALS

1328	<b>L4-100K-Y90A(fw)</b>	5'-AAAGGCATGGCGACGCCCTAGATGTGGGAG-3'	mutagenesis
1329	<b>L4-100K-Y90A(rev)</b>	5'-TTTCCGTACCGCTGCGGGATCTACACCCTC-3'	mutagenesis
1330	<b>L4-100K-RGGfullII(fw)</b>	5'-GGACATGATGGAGGACTGGGAGAGCCTGGA- GGAGGAAGCTTCGGAGGTCGAAGAGG-3'	mutagenesis
1331	<b>L4-100K-RGGfullII(rev)</b>	5'-CCTCTTCGACCTCCGAAGCTTCCTCCTCCAG- GCTCTCCAGTCCTCCATCATGTCC-3'	mutagenesis
1332	<b>L4-100K-RGGfullIII(fw)</b>	5'-GCTTCGGAGGTGGAGGAGGTGTCGGAGGA- AACACCGTCACCCTCGGTGGCATTCCCCTCGC-3'	mutagenesis
1333	<b>L4-100K-RGGfullIII(rev)</b>	5'-GCGAGGGGAATGCCACCGAGGGTGACGGTG- TTTCCTCCGACACCTCCTCCACCTCCGAAGC-3'	mutagenesis
1336	<b>Ad2100K 146 rev</b>	5'-CTGAGCGATCCTCGTCG-3'	sequencing
1369	<b>TL fw</b>	5'-ACTCTCTTCCGCATCGCTGTC-3'	RT-PCR
1370	<b>TL rev</b>	5'-GCGACTGTGACTGGTTAGACG-3'	RT-PCR
1373	<b>100K-BamHI-fw</b>	5'- CGGGATCCATGGAGTCAGTCGAGAAGAAGG -3'	cloning
1374	<b>100K-BamHI-rev</b>	5'- CGGAATTCCTACGGTTGGGTCGGCGAACGGGC -3'	cloning
1398	<b>L4-100K req rev</b>	5'- GCCATGCTGGAACCGGTTGCC -3'	sequencing
1472	<b>RGG-Box3 fw</b>	5'- GGAGGTTTTGGAGGGGAGGAGG -3'	mutagenesis
1473	<b>RGG-Box3 rev</b>	5'- CCTCCTCCTCTCCAAAACCTCC -3'	mutagenesis
1478	<b>100KGST 1-220 rev</b>	5'- CGGAATTCGCGTCCAAGACCCTCAAAGAT- TTTTGG -3'	cloning
1479	<b>100KGST 200-420 fw</b>	5'- CGGGATCCTCTTTGAGGGTCTTGGACGCGACG -3'	cloning
1480	<b>100KGST 200-420 rev</b>	5'- CGGAATTC AACGCAGTCGCGGACGTAGTCGCG -3'	cloning
1481	<b>100KGST 400-620 fw</b>	5'- CGGGATCCACTACGTCCGCGACTGCGTTTAC -3'	cloning
1482	<b>100KGST 400-620 rev</b>	5'- CGGAATTCAGCCGACGTCCACAGCCCCGG -3'	cloning
1483	<b>100KGST 600-806 fw</b>	5'- CGGGATCCCGGGGCTGTGGACGTCGGCTTACC -3'	cloning

### 3.3.2 Vectors

The following vector plasmids were used for cloning and transfection experiments. They were numbered according to the *Filemaker Pro* data bank of the group.

## MATERIALS

#	NAME	CHARACTERISTICS	REFERENCE
88	<b>pGEX5X-1</b>	Bacterial expression vector, GST-tag	PL-Pharmacia
101	<b>pGEX4T-1</b>	Bacterial expression vector, GST-tag	PL-Pharmacia
136	<b>pcDNA3</b>	Expression vector for mammalian cells, CMV promoter	Invitrogen
204	<b>pPG-S4</b>	L4-region subcloning vector	Stock of the group
210	<b>pRevTRE</b>	Tet-off inducible system vector	Clontech

### 3.3.3 Recombinant Plasmids

The following recombinant plasmids were cloned in this work, unless stated otherwise in the table, and numbered according to the *Filemaker Pro* data bank of the group.

#	NAME	VECTOR	INSERT	REFERENCE
1138	<b>GST-E1B-C-terminus</b>	pGEX-2T	348-496 E1B	Stock of the group
1154	<b>Ad5pTG-S2 (Noah)</b>	pTG	Ad5 genome	Stock of the group
1319	<b>pcDNA-E1B-55K</b>	pcDNA3	Ad5 E1B-55K	Stock of the group
1418	<b>GST-E1B-central</b>	pGEX-2T	83-188 E1B	Stock of the group
1513	<b>L4-Box-S4</b>	pPG-S4	Ad5 L4 region	Stock of the group
1520	<b>GST-E1B-156R</b>	pGEX-2T	Ad5 E1B-156R	Stock of the group
1568	<b>pTL-flag-100K</b>	pCMV/neo	TL-Ad2-100K	R. Schneider
1586	<b>pTL-flag-100K-Ts</b>	pCMV/neo	TL-Ad2-100K	this work
1587	<b>pTL-flag-100K-RGG</b>	pCMV/neo	TL-Ad2-100K	this work
1599	<b>L4-Box 100K RGG</b>	pPG-S4	Ad5 L4 region	this work
1600	<b>L4-Box 100K del</b>	pPG-S4	Ad5 L4 region	this work
1611	<b>Ad5pPG-S2 L4100K-RGG</b>	pPG-S2	Ad5 genome	this work
1612	<b>Ad5pPG-S2 L4100K-del</b>	pPG-S2	Ad5 genome	this work

## MATERIALS

1624	<b>GST-E1B-N-terminus</b>	pGEX-2T	1-79 E1B	Stock of the group
1643	<b>pTL-flag-100K-NES</b>	pCMV/neo	TL-Ad2-100K	this work
1644	<b>pTL-flag-100K-Sumo</b>	pCMV/neo	TL-Ad2-100K	this work
1645	<b>pTL-flag-100K-AAA</b>	pCMV/neo	TL-Ad2-100K	this work
1646	<b>L4-Box 100K AAA</b>	pPG-S4	Ad5 L4 region	this work
1684	<b>L4-Box 100K RGG-full-I</b>	pPG-S4	Ad5 L4 region	this work
1685	<b>L4-Box 100K RGG-full-II</b>	pPG-S4	Ad5 L4 region	this work
1686	<b>Ad5pPG-S2 L4100K-RGG-full-II</b>	pPG-S2	Ad5 genome	this work
1687	<b>L4-Box 100K Y90A</b>	pPG-S4	Ad5 L4 region	this work
1688	<b>pTL-flag-100K-Y90A</b>	pCMV/neo	TL-Ad2-100K	this work
1689	<b>Ad5pPG-S2 L4100K-Y90A</b>	pPG-S2	Ad5 genome	this work
1726	<b>wt100K/TL-pRevTRE</b>	pRevTRE	TL-Ad2-100K	this work
1727	<b>Ts100K/TL-pRevTRE</b>	pRevTRE	TL-Ad2-100K	this work
1734	<b>pTL-flag-100K-RGG full-I</b>	pCMV/neo	TL-Ad2-100K	this work
1735	<b>pTL-flag-100K-RGG full-II</b>	pCMV/neo	TL-Ad2-100K	this work
1745	<b>pHis-sumo-1-GG</b>	pSG5	Sumo-1-GG	S. Müller
1824	<b>GST-L4-100K</b>	pGEX-4T1	Ad5 L4-100K	this work
1852	<b>L4-Box GAR-I</b>	pPG-S4	Ad5 L4 region	this work
1856	<b>L4-Box GAR-II</b>	pPG-S4	Ad5 L4 region	this work
1857	<b>pTL-flag-100K-RGG GAR</b>	pCMV/neo	TL-Ad2-100K	this work
1865	<b>Ad5pPG-S2 L4100K-GAR</b>	pPG-S2	Ad5 genome	this work
1930	<b>pTL-flag-100K-RGG3</b>	pCMV/neo	TL-Ad2-100K	this work
1931	<b>L4-Box 100K NES/Sumo</b>	pPG-S4	Ad5 L4 region	this work
1935	<b>pTL-flag-100K- NES/Sumo</b>	pCMV/neo	TL-Ad2-100K	this work
1945	<b>GST-100K-F1</b>	pGEX4T-1	1-220 Ad5-L4-100K	this work
1946	<b>GST-100K-F3</b>	pGEX4T-1	404-620 Ad5-L4-100K	this work

## MATERIALS

1947	<b>GST-100K-F4</b>	pGEX4T-1	614-806 Ad5-L4-100K	this work
1951	<b>GST-100K-F2</b>	pGEX5X-1	215-420 Ad5-L4-100K	this work
1965	<b>pcDNA4/TO-100K</b>	pcDNA4/TO	Ad5 L4-100K	this work

### 3.4 Antibodies

#### 3.4.1 Primary Antibodies

NAME	PROPERTIES
<b>6B10</b>	Monoclonal rat antibody raised against Ad5-L4-100K protein, N-terminal (Kzhyshkowska et al., 2004).
<b>2A6</b>	Monoclonal mouse antibody raised against Ad5-E1B-55K protein, N-terminal (Sarnow et al., 1982b).
<b>6A11</b>	Monoclonal rat antibody raised against Ad5-E4orf3 protein (Nevels et al., 1999).
<b>B6-8</b>	Monoclonal mouse antibody raised against Ad5-E2A-72K protein (Reich et al., 1983).
<b>7C11</b>	Monoclonal rat antibody raised against Ad5-E1B-55K protein, C-terminal (Kindsmuller et al., 2007).
<b>RSA3</b>	Monoclonal mouse antibody raised against the N-terminus of E4orf6 and E4orf6/7 proteins of Ad5 (Marton et al., 1990).
<b>6C5</b>	Monoclonal rat antibody raised against E1B-AP5 protein (Kzhyshkowska et al., 2001).
<b><math>\alpha</math>-late (L133)</b>	Polyclonal rabbit antiserum raised against Ad5 late structural proteins (Kindsmuller et al., 2007).
<b>Ad5 Hexon</b>	Polyclonal rabbit antiserum raised against Ad5 Hexon protein (Abcam).
<b><math>\alpha</math>-SUMO1 (21C7)</b>	Monoclonal mouse antibody raised against SUMO1 protein (Zymed).
<b><math>\alpha</math>-SAF-A</b>	Polyclonal rabbit antibody raised against SAF-A protein (Herrmann et al., 2005).
<b><math>\alpha</math>-PRMT1</b>	Polyclonal rabbit antiserum raised against PRMT1 (Upstate).

## MATERIALS

<b><math>\alpha</math>-eIF4G</b>	Polyclonal rabbit antiserum raised against eIF4G (Byrd et al., 2005).
<b><math>\beta</math>-actin (AC-15)</b>	Monoclonal mouse antibody against $\beta$ -Actin (Sigma).
<b>Ab412</b>	Monoclonal mouse antibody recognizing methylated/asymmetrically dimethylated arginines (Abcam).
<b>ASYM-24</b>	Polyclonal rabbit antibody recognizing asymmetrically dimethylated arginines (Upstate).

### 3.4.2 Secondary Antibodies

The following secondary antibodies were used for *Western blot* analysis:

NAME	PROPERTIES
HRP-Anti-Mouse IgG	HRP ( <i>horseradish peroxidase</i> ) coupled antibody raised against mouse IgGs in sheep (Amersham Life Science).
HRP-Anti-Rat IgG	HRP ( <i>horseradish peroxidase</i> ) coupled antibody raised against rat IgGs in goat (Amersham Life Science).
HRP-Anti-Rabbit IgG	HRP ( <i>horseradish peroxidase</i> ) coupled antibody raised against rabbit IgGs in donkey (Amersham Life Science).

The following secondary antibodies were used for immunofluorescence analysis:

NAME	PROPERTIES
FITC-Anti-Rat IgG	Fluorescein-isothiocyanat (FITC)-coupled antibody raised against rat IgGs in donkey; (H + L; Dianova).
FITC-Anti-Mouse IgG	Fluorescein-isothiocyanat (FITC)-coupled antibody raised against mouse IgGs in donkey; (H + L; Dianova) (H + L; Dianova).
FITC-Anti-Rabbit IgG	Fluorescein-isothiocyanat (FITC)-coupled antibody raised against rabbit IgGs in donkey; (H + L; Dianova) (H + L; Dianova).
<i>Texas Red</i> -Anti-Rat IgG	<i>Texas Red</i> (TR)-coupled antibody raised against rat IgGs in donkey; (H + L; Dianova).
<i>Texas Red</i> -Anti-Mouse IgG	<i>Texas Red</i> (TR)-coupled antibody raised against mouse IgGs in donkey;



## MATERIALS

(H + L; Dianova).

Alexa™ 488 Anti-Mouse IgG    Alexa™ 488 antibody raised against mouse IgGs in goat (H + L; F(ab')<sub>2</sub> Fragment; Molecular Probes).

### 3.5 Commercial Systems

The following commercial systems were purchased from the indicated companies:

NAME	COMPANY
CellLytic™NuCLEAR™ Extraction Kit	Sigma
QIAquick Gel Extraction Kit	Qiagen
QuikChange™ Site-Directed Mutagenesis Kit	Stratagene
Plasmid Purification Mini, Midi und Maxi Kit	Qiagen
Protein Assay	BioRad
SuperScript™III First Strand	Invitrogen
SuperSignal® West Pico Chemiluminescent Substrate	Pierce
RNeasy Mini Kit	Qiagen
Vivapure® AdenoPack 20	Sartorius

### 3.6 Chemicals, Reagents and Equipment

The chemicals and reagents used in this study were purchased from Sigma, Merck, Biomol, AppliChem, Roche and New England Biolabs. Cell culture materials were obtained from Falcon, Gibco BRL and Pan, other plastic materials and equipment were purchased from Falcon, Sarstedt, VWR, Whatman, Nunc, Biorad, Eppendorf GmbH, Brand, Protean, Schleicher & Schuell, Engelbrecht, Biozym, Hellma, and Greiner.

### 3.7 Standards and Markers

Size determination of DNA fragments on agarose gels was based on a 1 kb and 100 bp DNA ladder (Gibco BRL), and Precision Protein Standard (BioRad) was used to determine the molecular weight of proteins on SDS-gels.

### 3.8 Software and Databases

The following software and databases were used in the preparation of this work:

SOFTWARE	PURPOSE	SOURCE
Acrobat 9.0	Reading and writing PDF data	Adobe
Bio Edit 7.0.5.2	Sequence data processing	<a href="http://www.mbio.ncsu.edu/BioEdit/page2.html">http://www.mbio.ncsu.edu/BioEdit/page2.html</a>
EndNote 9.0	Reference organization	Thomson
File Maker Pro 8.0	Database of the group	FileMaker, Inc.
GeneRunner	Sequence data processing	Hastings Software Inc.
Gene Tools	Quantification of DNA and protein bands	SynGene
Illustrator CS4	Figure preparation	Adobe
Microsoft Office XP 2007	Preparation of text and tables	Microsoft
Photoshop CS4	Image processing	Adobe
PubMed	Literature database (National Library of Medicine)	<a href="http://www.ncbi.nlm.nih.gov/PubMed">http://www.ncbi.nlm.nih.gov/PubMed</a>
Vector NTI	Sequence analysis/alignment	Invitrogen

## 4 Methods

---

### 4.1 Bacteria

#### 4.1.1 Culture and Storage

For the liquid culture of *E. coli*, single colonies were picked from plates containing successful transformants and inoculated in sterile Luria Bertoni Medium (LB medium) containing 100 µg/ml ampicillin or 50 µg/ml kanamycin. Cultures were incubated at 37 °C with shaking at 220 rpm (New Brunswick). After 16-20 h incubation, bacteria concentrations were determined by measuring the optical density (OD) of the cultures at 600 nm wavelength (SmartSpec™ 3000, BioRad) against plain medium (1 OD<sub>600</sub> = 8 × 10<sup>8</sup> cells/ml).

For plate cultures, LB-agar was made by adding 15 g/l agar to LB. This medium was sterilized by autoclaving and appropriate antibiotics were added after cooling. Aliquots of LB-agar were poured onto plates and left to cool in a fume hood. LB-agar plates were stored at 4°C until used for bacteria spreading. Transformed bacteria or aliquots from glycerol stocks were spread on LB-agar plates and incubated overnight at 37 °C in an incubator. After picking single colonies, plate cultures were sealed with parafilm (Pechiney Plastic Packaging) and kept at 4 °C.

For the long-term storage of bacteria, single colonies were picked and inoculated in liquid LB-medium and incubated at 37 °C with shaking at 220 rpm (New Brunswick). Before the culture reached stationary phase, bacteria were pelleted by centrifugation at 4000 rpm for 10 min (Multifuge 3 S-R, Heraeus). Bacteria pellets were resuspended in 0.5 ml sterile glycerol-LB (1:1) and transferred into *CryoTubes*™ (Nunc). These glycerol stocks were stored at -80 °C.

LB-Medium		
	Trypton	10 g/l
	Yeast extract	5 g/l
	NaCl	5 g/l
	• autoclaving	

<b>Antibiotic Solutions</b>	Ampicillin (500 x)	50 mg/ml in H <sub>2</sub> O <sub>dd</sub>
	Kanamycin (200 x)	10 mg/ml in H <sub>2</sub> O <sub>dd</sub>
	• filter sterilization	
	• storage at -20 °C	

#### 4.1.2 Transformation of *E. coli*

##### 4.1.2.1 Electroporation

Electrocompetent *E. coli* cells were prepared as described (Sharma and Schimke, 1996). 1 l YENB medium was inoculated with 10 ml fresh overnight culture of bacteria and incubated in a 37 °C shaker incubator (New Brunswick) until OD<sub>600</sub> reached 0.5 – 0.9. Cells were cooled on ice for 5 min and centrifuged at 6000 rpm at 4°C (Centrikon T-124, Kontron Instruments). The bacteria pellet was washed two times with 100 ml ice cold H<sub>2</sub>O<sub>dd</sub> and once with 20 ml 10% glycerol. Finally, bacteria were resuspended in 3 ml 10% glycerol and stored at -80 °C as 50 µl aliquots.

<b>YENB</b>	Bacto Yeast Extract	7.5 g/l
	Bacto Nutrient Broth	8 g/l
	• autoclaving	
<b>SOC medium</b>	Trypton	20 g/l
	Yeast extract	5 g/l
	NaCl	10 mM
	KCl	2.5 mM
	MgCl <sub>2</sub>	10 mM
	MgSO <sub>4</sub>	10 mM
	Glucose	20 mM
	• autoclaving	

For transformation, a 50 µl aliquot of electrocompetent cells was thawed on ice. Ligation mixture or 20-50 ng plasmid DNA diluted in H<sub>2</sub>O<sub>dd</sub> was added to the cells. This mixture was transferred into an electroporation cuvette (BioRad). *Gene Pulser*

(BioRad) was used for electroporation (1.25 kV, 25  $\mu$ F 200  $\Omega$ ). Immediately after 5 m exposure, cells were transferred into a 1.5 ml reaction tube (Eppendorf), rinsed with 1 ml SOC medium, and incubated at 37 °C in a shaker incubator for 1 h. After centrifuging the bacteria, the pellet was resuspended in approximately 50  $\mu$ l LB and spread on an LB-plate containing the appropriate antibiotic and incubated at 37 °C overnight.

#### 4.1.2.2 Chemical Transformation of *E. coli*

XL1-Blue, XL2-Blue and DH5 $\alpha$  cells were used for L4-Box plasmid, adenoviral bacmid and recombinant plasmid transformation, respectively. Aliquots of 50 – 100  $\mu$ l bacteria were transferred into a 15 ml Falcon 2059 tube after thawing. Two  $\mu$ l of  $\beta$ -Mercaptoethanol (1.2 M) and 1 - 10  $\mu$ l of plasmid DNA dilution were gently mixed with the cells and incubated on ice for 30 min. This mixture was kept at 42 °C for 45 s and subsequently transferred to ice for 2 min. After this heat shock, 1 ml of NZCYM or SOC medium, which was preheated at 42 °C, was added to the cells and this mixture was further incubated for 1 h at 37 °C at 220 rpm in a shaker incubator (New Brunswick). After centrifuging the transformed bacteria, the pellet was resuspended in 50  $\mu$ l LB containing appropriate antibiotics. This bacteria suspension was spread on a LB-agar plate as described in Section 4.1.1.

#### NZCYM

NZ amine	10 g/l
NaCl	0.5 g/l
Yeast extract	0.2 g/l
MgSO <sub>4</sub> x 6 H <sub>2</sub> O	0.2 g/l
Casamino acids	1 g/l
• pH 7.5	
• autoclaving	

## 4.2 Mammalian Cells

### 4.2.1 Maintenance and Passage of Cell Lines

Adherent cells were maintained as monolayers in cell culture flasks or dishes (Falcon). The growth medium used was *Dulbecco's Modified Eagles Medium* (DMEM; Gibco BRL; Dulbecco and Freeman, 1959) with 0.11 g/l sodium pyruvate, which was supplemented with 5-10% fetal calf serum (FCS; Pan) and a 1% penicillin/streptomycin solution (1000 U/ml penicillin and 10 mg/ml streptomycin in 0.9% NaCl; Pan). Cultured cells were incubated at 37 °C in a CO<sub>2</sub> incubator (Heraeus) with 5% CO<sub>2</sub>. Depending on their confluency, cells were split (1:3 to 1:10) every 3-5 days. To split the cells, medium was removed and cells were washed once with PBS. Then they were trypsinized using an appropriate volume of trypsin/EDTA solution (Pan). When all the cells had been efficiently detached from the culture dish, protease activity was neutralized by adding 1 volume of medium. Cells were collected and transferred into a 15 ml or 50 ml reaction tube (Falcon) and pelleted by centrifugation at 2000 rpm (Multifuge 3 S-R, Heraeus) for 3 min. Cell pellets were resuspended in an appropriate volume of growth medium. If required, the cell number was determined and cells were seeded in a suitable sized cell culture dish.

PBS (pH 7.0 – 7.7)	NaCl	140 mM
	KCl	3 mM
	Na <sub>2</sub> HPO <sub>4</sub>	4 mM
	KH <sub>2</sub> PO <sub>4</sub>	1.5 mM
	• autoclaving	

### 4.2.2 Storage of Mammalian Cells

For long-term storage of mammalian cells, subconfluent cultures were trypsinized and cell pellets were obtained as described above (4.2.1). These pellets were then resuspended in 1 ml FCS (Pan), supplemented with 10% DMSO (Sigma) and

transferred into *CryoTubes*<sup>™</sup> (Nunc). Cells were slowly cooled down with the help of “Mr. Frosty” (Zefa Laborservice) and either transferred to liquid nitrogen storage tanks or stored at -80 °C. To reculture the frozen cells, the cryo tube was rapidly unfrozen at 37 °C and the cells were immediately seeded in an appropriate cell culture dish (Falcon) containing pre-warmed growth medium. When cells were attached to the bottom of the culture dish, DMSO-containing medium was exchanged with fresh 10% FCS-containing growth medium and further cultured as described in the previous section.

#### 4.2.3 Determination of Total Cell Number

Cells were counted using a Neubauer cell counter. Trypsinized cells were centrifuged and resuspended in DMEM as described (4.2.1). A 50 µl aliquot of cell suspension was mixed with 50 µl trypan blue in a 1.5 ml reaction tube (Eppendorf). After resuspending, a small volume was put on to the cell counter. Cells spread within a 16-square area were counted under a light microscope (Leica DM IL). The number of cells was multiplied by the dilution factor and factor 10<sup>4</sup> to obtain the cell number in 1 ml of suspension.

Trypan blue solution	Trypan blue	0.15%
	NaCl	0.85%

#### 4.2.4 Transfection of Mammalian Cells

##### 4.2.4.1 Calcium Phosphate Method

Adherent mammalian cells were seeded in a 6-well or a 100 mm dish (Falcon) 6-24 h before transfection. Transfection was performed when cells attached to the culture dish and reached a confluency of 50-70%. In this procedure, plasmid or linear DNA molecules were covered with calcium phosphate crystals, which would be adsorbed by the cells and internalized by endocytosis. For this procedure 30 µg of DNA was

## METHODS

---

diluted in sterile  $\text{H}_2\text{O}_{\text{dd}}$  and mixed with 300  $\mu\text{l}$  of  $1/10$  dilution of 250 mM  $\text{CaCl}_2$  in a polystyrene reaction tube (Falcon). While gently vortexing (Vortex, 1000 rpm) 300  $\mu\text{l}$  of 2 x BBS was added drop by drop to this solution. Tubes were kept for 15 min at RT to allow complex formation. This mixture was resuspended once and added to the cells drop by drop, and transfected cells were placed in the cell culture incubator. Medium was replaced with fresh 10% medium approximately 16 h after transfection. Cells were harvested 24-48 h post transfection using a cell scraper, and collected in a 15 or 50 ml Falcon tube. After centrifugation at 2000 rpm, for 3 min, the cell pellet was washed once with PBS and stored at  $-20^\circ\text{C}$  until used for experiments.

<b>2 x BBS</b> ( <i>BES buffered saline</i> )		BES	50 mM
		NaCl	280 mM
		$\text{Na}_2\text{HPO}_4$	1.5 mM
		• pH 7.02 exact	
		• filter sterilized	
<b>2.5 M <math>\text{CaCl}_2</math></b>		$\text{CaCl}_2$	2.5 M
		• filter sterilized	

### 4.2.4.2 Polyethyleneimine (PEI) Method

H1299 ( $2.5 \times 10^6$ ) or HEK-293 cells ( $5 \times 10^6$ ) seeded in 10 cm dishes were transfected with 10  $\mu\text{g}$  of plasmid DNA by the polyethylenimine (PEI, 25 kDa, linear-Polysciences) transfection method. PEI was dissolved in  $\text{H}_2\text{O}_{\text{dd}}$  to give a concentration of 1 mg/ml. The solution was neutralized (pH 7.2) with 0.1N HCl, filter sterilized (0.2  $\mu\text{m}$ ), aliquoted and stored at  $-80^\circ\text{C}$ . The working solution is stable at  $4^\circ\text{C}$  for 1 - 2 months. For transfection, 50  $\mu\text{g}$  PEI was added to the DNA dissolved in 600  $\mu\text{l}$  of DMEM and kept at RT for 10 min. The DNA-PEI mixture was added to the cells seeded in DMEM without FCS and antibiotics. Six hours post transfection medium was replaced with normal growth medium. Transfected cells were harvested 24 or 48 h post transfection as described in Section 4.2.5.



### 4.2.4.3 Polysome Method

To reach maximal transfection efficiency, mammalian cells were transfected with plasmid or linearized bacmid DNA using *Lipofectamine*<sup>TM</sup>2000 reagent (Invitrogen). In this method, cationic lipid vesicles or liposomes interact with negatively charged DNA molecules. These lipid-DNA complexes fuse with cell membranes and mediate the internalization of DNA molecules. Adherent cells were seeded 6-12 h before transfection in appropriate culture dishes (6-well or 10 cm dish, Falcon) to reach a confluency of 70-90% at the time of transfection. Cells were washed once with PBS before adding DMEM without FCS or antibiotics. DNA-liposome complexes, prepared according to the manufacturer's instructions, were added to the cells. This transfection medium was changed with 10% FCS containing growth medium 6-12 h post transfection. Cells were harvested 24-72 h after transfection as described in Section 4.2.5.

### 4.2.5 Harvest of Mammalian Cells

Transfected or infected adherent mammalian cells were harvested using cell scrapers (Sarstedt). Collected cells were transferred into 15 or 50 ml Falcon tubes and centrifuged at 2000 rpm for 3 min at RT (Multifuge 3 S-R, Heraeus). After removing the supernatant, the cell pellet was washed once with PBS and stored at -80 °C for following experiments.

## 4.3 Adenovirus

### 4.3.1 Generating Virus from DNA

To generate mutant viruses, first the viral genome was released from the recombinant bacmid by *PacI* digestion. This linearized DNA was precipitated with  $1/10$  vol 3 M NaOAc and 1 vol of isopropanol and washed with 75% ethanol. Five micrograms of

purified viral DNA were used to transfect  $3 \times 10^5$  complementing K16 cells seeded in a 10 mm dish (Falcon) by the calcium phosphate procedure (Graham and van der Eb, 1973). The transfection medium was changed to normal growth medium 16 h post transfection. After 5 days, cells were harvested (4.2.5), centrifuged at 2000 rpm for 5 min (Multifuge 3 S-R, Heraeus) and the cell pellet was resuspended in 1 ml of DMEM. Viruses were released from these cells by three cycles of freezing in liquid nitrogen and thawing at 37 °C in a water bath. Virus particles released into the medium were separated from the cell debris by centrifugation at 4500 rpm for 5 min (Multifuge 3 S-R, Heraeus). The virus-containing supernatant was used to infect  $1 \times 10^6$  K16 cells seeded onto a 60 mm dish and infectious viral particles were collected 3-5 days after infection by freezing/thawing as described above. This re-infection procedure was repeated 2 to 5 times until a cytopathic effect was observed in 90% of the cells. The preliminary virus solution obtained was used to yield a high-titer virus stock after confirming the inserted mutations by DNA sequencing and testing the integrity and identity of the viral genome by *HindIII* digestion.

#### 4.3.2 Propagation and Storage of High-Titer Virus Stocks

In order to establish a high titer virus stock, several 150 mm dishes were infected with the virus obtained as described in 4.3.1. After 3-5 days of incubation, cells were harvested and centrifuged at 2000 rpm for 5 min (Multifuge 3 S-R, Heraeus). The virus-containing cell pellet was washed once with PBS and resuspended in DMEM without FCS and antibiotics. After releasing the viral particles from the cells by freezing/thawing as described above (4.3.1), virus-containing supernatant was mixed with 87% glycerol (sterile, 10% final concentration) for preservation at -80 °C.

#### 4.3.3 Titration of Virus Stocks

The titer of the virus stocks was determined in terms of fluorescent forming units (FFU) by immunofluorescence staining of the infected cells with an antibody (B6-8) against the E2A-72K DNA binding protein (DBP) of adenovirus. To do this,  $3 \times 10^5$  K16

## METHODS

cells were seeded in the wells of a 6-well dish (Falcon) and infected with 1 ml of virus dilution ( $10^{-2}$  to  $10^{-6}$  in infection medium) 12 to 24 h after seeding. After incubation at 37 °C in an incubator (Heraeus) with gentle shaking every 15 min for efficient and homogenous virus adsorption, infection medium was replaced with 2 ml of 10% FCS-containing growth medium per well. Infected cells were fixed 20 h p.i. with 1 ml of ice-cold methanol and further incubated at -20 °C for 15 min. After removing the alcohol, 6 wells were air-dried at RT and washed once with TBS-BG buffer before immunostaining. Cells were incubated with 2 ml of TBS-BG for 30 min at RT. Primary antibody B6-8 was diluted in TBS-BG (1:10) and 1 ml of antibody dilution was added to each well after removal of TBS-BG. Cells were incubated with the primary antibody for 2 h at RT or overnight at 4 °C with gentle agitation. After removing the primary antibody solution, cells were washed 3 times with 1 ml of TBS-BG for 5 min. For the fluorescence reaction, FITC-coupled secondary mouse antibody was diluted 1:100 in TBS-BG and 1 ml of this dilution was added to each well. This step was carried out in the dark to prevent bleaching of the fluorescent signal. The cells were incubated with the secondary antibody for 2 h at RT or overnight at 4 °C with gentle agitation. Infected cells were counted using a fluorescence microscope after washing the samples 3 times with TBS-BG. The total infectious particle number of a virus stock was calculated according to the counted infected cell number and virus dilutions.

<b>Infection medium</b>	CaCl <sub>2</sub>	2 mM
	MgCl <sub>2</sub>	2 mM
	FCS	0.2%
	Penicillin/Streptomycin	1%
	• in PBS	
<b>TBS-BG</b>	Tris/HCl, pH 7.6	20 mM
	NaCl	137 mM
	HCl	3 mM
	MgCl <sub>2</sub>	1.5 mM
	Tween 20	0.05%
	Sodium azide	0.05%
	Glycine	5 mg/ml
	BSA	5 mg/ml

#### 4.3.4 Infection with Adenovirus

Mammalian cells were seeded in appropriate dishes 6-16 h before infection, resulting in a confluency of 60-80%. Growth medium was removed and cells were washed once with PBS. According to the size of the dish, virus dilutions (1-50 FFU/cell) were prepared in an appropriate volume of DMEM without antibiotics and FCS. Cells were incubated with this infection medium 1 – 2 h at 37 °C. During incubation, the dish was gently shaken every 15 min to achieve efficient and homogenous adsorption of virus particles. Finally, infection medium was replaced with DMEM containing 10% FCS and 1% penicillin/streptomycin. Infected cells were harvested or fixed according to the experiment at indicated time points after infection.

#### 4.3.5 Determination of Virus Yield

To determine the progeny virion production efficiency of an adenovirus stock,  $1 \times 10^6$  HeLa or A549,  $5 \times 10^5$  H1299, or  $2.5 \times 10^5$  HepaRG cells were seeded into the wells of a 6-well plate, infected with adenovirus (1-10 FFU/cell) as described in 4.3.4. The infected cells were harvested 24, 48, or 72 h post infection using a cell scraper (Sarstedt). Collected cells were transferred into a 15 ml reaction tube (Falcon) and centrifuged at 2000 rpm for 5 min (Multifuge 3 S-R, Heraeus). After removing the supernatant, the cell pellet was washed once with PBS and resuspended in 1 ml of DMEM without antibiotics or FCS. To release the virus particles from the cells, the cell suspension was subjected to 3 sequential freeze and thaw cycles as described in 4.3.1, and further centrifuged at 4500 rpm for 10 min (Multifuge 3 S-R, Heraeus). Supernatant containing the released virus particles was transferred into a 1.5 ml reaction tube (Eppendorf) and stored at 4 °C. To determine the particle number in this virus solution titration was carried out as described in 4.3.3, and the particle number produced per cell was calculated.

## 4.4 DNA Techniques

### 4.4.1 Preparation of Plasmid DNA from *E. coli*

For large-scale plasmid preparation, 100-500 ml liquid cultures of bacteria were prepared in LB medium containing appropriate antibiotics. After inoculation, the culture was incubated for 16-20 h at 37 °C with shaking at 200 rpm (New Brunswick). The bacteria pellets were collected by centrifuging the cultures at 4500 rpm (Multifuge 3 S-R, Heraeus) for 10 min at RT. Plasmid DNA was isolated from bacteria pellets using a Qiagen DNA extraction kit (midi or maxi) according to the manufacturer's instructions.

For analytic approaches, small volumes (5-20 ml) of liquid cultures were inoculated and plasmid DNA was isolated as follows. After centrifuging the bacteria culture at 8,000 rpm for 5 min at RT (Eppendorf table-top centrifuge 5417, Eppendorf), the cell pellet was resuspended in 300-450 µl of Buffer A. This bacteria suspension was gently mixed with 300-450 µl of Buffer B to lyse the cells. After incubating for 5 min at RT, 300-450 µl of Buffer C was added to the lysate and this mixture was further incubated for 5 min on ice for neutralization. Finally, bacteria lysate was centrifuged at 14,000 rpm for 10 min at 4 °C (Eppendorf table-top centrifuge 5417, Eppendorf). Plasmid-containing supernatant was transferred into a new 1.5 ml reaction tube (Eppendorf) and subjected to isopropanol-ethanol precipitation. First 630 µl of isopropanol and  $1/10$  vol of 3 M NaOAc were added to the DNA solution, and upon centrifugation at 14,000 rpm for 30 min at RT (Eppendorf table-top centrifuge 5417, Eppendorf), the resultant supernatant was removed and the DNA pellet was washed once with 700 µl of 75% ethanol. The DNA pellet was then dissolved in an appropriate volume (20-50 µl) of H<sub>2</sub>O<sub>dd</sub> or 10 mM Tris-Cl (pH 8.0) buffer.

#### Buffer A

Tris/HCl, pH 8.0	50 mM
EDTA	10 mM
RNAse A	100 µg/ml
• storage at 4 °C	

---

---

<b>Buffer B</b>	NaOH SDS	200 mM 1% (w/v)
<b>Buffer C</b>	Ammonium acetate • storage at 4 °C	7.5 M

#### 4.4.2 Determining DNA Concentration

The concentration of DNA samples was measured using a spectrophotometer (DU®800, Beckman Coulter) at a wavelength of 260 nm . A DNA sample was diluted in H<sub>2</sub>O<sub>dd</sub> (1:20 or 1:100) and transferred into a 1 cm quartz cuvette. UV absorption of the sample was measured at a wavelength range between 230 to 300 nm against H<sub>2</sub>O<sub>dd</sub>. For a double-stranded DNA molecule, an absorption value of 1.0 at 260 nm corresponds to a concentration of 50 µg/ml. For a single-stranded DNA molecule; 1 OD<sub>260</sub> = 33 µg/ml. The purity of the isolated DNA was determined by the ratio of absorption at 260 nm to 280 nm. Optimum purity is obtained when this OD<sub>260</sub>/OD<sub>280</sub> ratio is 1.8.

#### 4.4.3 Agarose Gel Electrophoresis

Agarose gels were prepared by dissolving agarose (*Seakem® LE agarose*, FMC Bioproducts) in 1x TBE buffer to a final concentration of 0.6-1%. The resultant slurry was heated to boiling point in a microwave oven (Moulinex) in order to dissolve the agarose, and allowed to cool. Ethidium bromide was added to a final concentration of 0.5 µg/ml. This gel preparation was then poured on an agarose gel tray, and left to set. Samples were diluted with 6x loading buffer. Electrophoresis was carried out in TBE buffer at 5–10 V per cm of gel length, for approximately 1 hour. DNA was visualized with a UV transilluminator (*G:BOX*, SynGene, 312 nm). For preparative gels, to minimize the harmful effects of the UV, a wavelength of 365 nm was preferred (Bachofer), and 1 mM guanosine was dissolved in the gel, especially for large DNA molecules.

<b>5 x TBE</b>	Tris	0.45 M
	Boric acid	0.45 M
	EDTA	10 mM
	• with acetic acid pH 7.8	
<b>6x loading buffer</b>	Bromphenol blue	0.25% (w/v)
	Xylene cyanol	0.25% (w/v)
	Glycerol	50% (v/v)
	50 x TAE	2% (v/v)
<b>Ethidium bromide solution</b>	Ethidium bromide	10 mg/ml
	• storage at 4 °C, light protection	

#### 4.4.4 Isolation of DNA Fragments from Agarose Gels

The extraction of DNA fragments from agarose gels was performed using *Qiagen Gel Extraction Kit* (Qiagen) according to the instructions of the manufacturer. For bacmid-DNA fragment extraction, the DNA band was cut out of the gel using a disposable scalpel (Feather) under 365 nm UV-light, and the excised gel block was centrifuged for 2 h at 20,000 rpm in a SS34-Rotor (Centrikon T-24, Kontron Instruments). DNA-containing supernatant was mixed with  $1/10$  vol of 3 M NaOAc and 1 vol of isopropanol for precipitation. After ethanol washing, the DNA pellet was resuspended in 40  $\mu$ l of 10 mM Tris/HCl pH 8.0.

#### 4.4.5 Polymerase Chain Reaction (PCR)

##### 4.4.5.1 Standard PCR Protocol

For the standard amplification of a DNA template, a 50  $\mu$ l reaction mixture was prepared by mixing 0.01-1  $\mu$ g of DNA, 0.2  $\mu$ M forward and reverse primers, 1  $\mu$ l dATP, dTTP, dCTP and dGTP (each 1 mM), 5  $\mu$ l of 10 x PCR buffer and 0.5  $\mu$ l *Taq*-DNA polymerase (5 U/ $\mu$ l; Roche) in a 0.2 ml reaction tube (Biozym). The

thermocycler (*GeneAmp<sup>TM</sup> PCR System 9700*, Perkin Elmer) was programmed as follows:

0.5 - 1 min	95 °C	DNA denaturation
0.5 - 1 min	55 – 70 °C	Annealing of primers on target sequence
1 min/kbp	72 °C	Extension

After 20- 30 cycles, samples were further incubated for 10 min at 72 °C and stored at 4 °C. 5 µl of amplified DNA were loaded on an agarose gel (4.4.3) and examined under UV light.

### 4.4.5.2 Site-Directed Mutagenesis by PCR

Point mutations were inserted in target plasmids using a *QuikChange<sup>TM</sup> Site-Directed Mutagenesis Kit* (Stratagene) according to the manufacturer's protocol. Desired mutations were included in both forward and reverse primer sequences, which were ordered from Metabion. PCR conditions were as follows:

0.5 min	95 °C	DNA denaturation
1 min	55 °C	Annealing of primers on target sequence
2 min/kbp (18 cycles)	68 °C	Extension

### 4.4.5.3 Viral DNA Replication Assay by PCR

For the viral DNA replication assay, 5-10 µl aliquots of infected cell lysates (4.6.1) were mixed with Tween 20 (final concentration 0.5%) and Proteinase K (final concentration 100 µg/ml) and filled with H<sub>2</sub>O<sub>dd</sub> to 24.5 µl. The digestion reaction took place at 55 °C in a thermoblock (Eppendorf Thermomixer comfort) for 1 h. After 10 min incubation at 100 °C for enzyme inactivation, Standard PCR (denaturation: 30 s at 95 °C, annealing: 1 min at 55 °C and polymerization: 2 min at 72 °C, 20 cycles) reactions were performed. As primers, E1B bp2043 fwd (#64) and E1B 361-389 rev (#110) were used, which target and amplify a 389 bp long fragment of the Ad5 E1B-55K gene. PCR products were loaded on a 1% agarose gel and analyzed using *Quantity One* software from ChemiDoc (BioRad) or *Gene Tolls* software from SynGene.



#### 4.4.6 Viral DNA isolation

Infected cells were harvested and washed once with PBS. The cell pellet was resuspended in 0.5 ml 100 mM Hepes (pH 7.4) per  $10^7$  cells. The cell suspension was subjected to 3 sequential freeze/thaw cycles and the cell debris was spun down by centrifugation at 4500 rpm for 10 min (Heraeus Multifuge 3S-R). The supernatant was gently loaded onto a discontinuous CsCl gradient in an SW-28 tube (vol  $\approx$  16 ml). This mixture was centrifuged for 180 min at 28,000 rpm at 15 °C. The suspended virus band between 1.25 g/cm<sup>3</sup> and 1.4 g/cm<sup>3</sup> in the CsCl solution was carefully transferred to a cryo tube. From this concentrated virus solution, 500  $\mu$ l were injected into a *Slide-A-lyzer®Dialysis Casette* (10,000 MWCO-Pierce), and dialyzed against 1-5 l of PBS overnight. Then, the virus solution was transferred from the dialysis cassette into a 1.5 ml Eppendorf tube and digested with Proteinase K (200  $\mu$ g/ml) in a reaction mixture containing 0.5% SDS and 6  $\mu$ l RNase T1 for 3 h at 37 °C. Viral DNA was then isolated using phase-lock tubes (Eppendorf). First, 2 ml phase-lock tubes were centrifuged at 13,000 g for 30 s. Then the viral sample was added to the tube, and a sample volume of phenol-chloroform-isoamylalcohol solution (PCI, Fluka) was added. The solutions were mixed well before centrifugation at 13,000 g for 5 min at 4 °C. The clear supernatant was transferred into a new 1.5 ml reaction tube and the DNA was purified by isopropanol/ethanol precipitation (4.4.1). The DNA pellet was resuspended in 20-40  $\mu$ l of 10 mM Tris/HCl pH 8.0.

<b>HBS (Hepes buffered saline)</b>	NaCl	137 mM
	KCl	3 mM
	Hepes, pH 7.4	25 mM

<b>CsCl solutions</b>	1.25 g/cm <sup>3</sup>	36.16 g CsCl/100 ml HBS
	1.34 g/cm <sup>3</sup>	51.20 g CsCl/100 ml HBS
	1.40 g/cm <sup>3</sup>	62.00 g CsCl/100 ml HBS

#### 4.4.7 Cloning of DNA Fragments

##### 4.4.7.1 Enzymatic Restriction of DNA

Restriction endonucleases were purchased from New England Biolabs and Roche, and were supplied with their 10 x buffers. For analytic restriction digest reactions, 0.5 – 1 µg of DNA was incubated with 3 – 10 U of restriction enzyme for 1 h at 37 °C, unless indicated otherwise. For preparative restriction digest reactions, 5 - 20 µg of DNA with 50 U of the enzyme were incubated for at least 2 h at an optimal working temperature. For the cloning of adenoviral bacmid-DNA, 25 U of restriction enzyme was used for each 1 µg of DNA. The digested fragments were purified for subsequent procedures (PCR, ligation, etc.) either by isopropanol/ethanol precipitation (4.4.1) or agarose gel extraction (4.4.4).

##### 4.4.7.2 Ligation and Transformation

Enzymatically restricted DNA fragments were ligated using 5 U of *thermosensitive alkaline phosphatase* (tsAP, Roche) for 30 min at 37 °C and if required, dephosphorylated at 65 °C for 45 min. For a standard ligation reaction 20-100 ng of vector DNA was mixed with 3-5 times more insert DNA in a final volume of 20 µl, including 2 µl of 10 x ligation buffer and 1 U of T4 DNA ligase (Roche). To allow the formation of covalent phosphodiester bonds, reactions were incubated overnight at 13 °C and the ligation product was transformed into *E. coli* (4.1.2).

##### 4.4.7.3 DNA Sequencing

For DNA sequencing, 500 ng of plasmid or 2 µg of bacmid/viral DNA and 10 µM sequencing primer were mixed with H<sub>2</sub>O<sub>dd</sub> to give an end volume of 8 µl. Sequencing reactions were performed by GeneArt.

## 4.5 RNA Techniques

### 4.5.1 Isolation of RNA from Mammalian Cells

Cytoplasmic, nuclear and total RNAs were isolated from mammalian cells using *RNeasy*<sup>®</sup> Mini-Systems (Qiagen) kits. Freshly harvested cells were used for fractionation. The cell pellet, obtained as described above (4.2.5), was resuspended in 175 µl of cold RLN-buffer, transferred into a 1.5 ml reaction tube (Eppendorf) and incubated on ice for 5 min. The sample was then centrifuged at 4 °C for 2 min at 950 × g. The supernatant was carefully transferred into a new 1.5 ml reaction tube (Eppendorf). This fraction served as the cytoplasmic fraction whereas the pellet served as the nuclear fraction. RNA extraction was performed according to the manufacturer's protocol and RNAs obtained were stored at -20 °C. The RNA concentration was determined by measuring the sample in a quartz cuvette (1 cm, Hellma) using a spectrophotometer (Lambda 25, PerkinElmer) set at 260 nm. Absorption of 1.0 at this wavelength gives an RNA concentration of 40 µg/ml. DEPC-treated water was used to prepare buffers and dissolve RNA. DEPC reacts with amine, hydroxy and thiol groups of proteins (such as RNases) and inactivates them. Treatment involves adding DEPC to 0.1% (v/v) and incubating at 37 °C for 1 hour to overnight followed by autoclaving.

<b>RLN buffer</b>	Tris/HCl, pH 8.0	50 mM
	NaCl	140 mM
	MgCl <sub>2</sub>	1.5 mM
	Nonidet P40	0.5% (v/v)
	• in H <sub>2</sub> O <sub>DEPC</sub>	
	• storage at 4 °C	

### 4.5.2 Immunoprecipitation of RNA (RNA-IP)

RNAs were co-immunoprecipitated from infected and non-infected cells as described (Eystathioy et al., 2002; Xi et al., 2004) using rat 6B10 mab. A549 cells (3×10<sup>6</sup>) were collected 48 h post infection, washed with cold PBS and resuspended in two pellet

## METHODS

---

volumes of polysome lysis buffer supplemented with 1 mM DTT, 100 unit/ml Rnase OUT (Invitrogen), 0.2 mM PMSF (Fluka), 1 mg/ml pepstatin A (Biomol), 5 mg/ml aprotonin (MP Biomedicals), and 20 mg/ml leupeptin (Sigma). Resuspended cells were incubated on ice for 5 min and then centrifuged at 16,000 x g for 10 min at 4 °C. Resultant supernatants were used for the further IP procedures. Protein G-sepharose beads were swollen in NT2 buffer for 1 h at 4 °C and further incubated with 6B10 mAb for 1 h at 4 °C. Antibody-coupled beads were then washed twice with ice cold NT2 buffer and resuspended in NT2 buffer supplemented with 100 units/ml of Rnase OUT and 1 mM DTT. Half of the cell lysates containing mRNPs were incubated with the antibody-coupled beads overnight at 4 °C. Beads were then washed six times with ice cold NT2 buffer. Washed beads were resuspended in 100 µl of NT2 buffer supplemented with 0.1% SDS and 30 µg of proteinase K, and incubated for 30 min at 55 °C. The immunoprecipitated mRNAs were isolated by phenol-chloroform-isoamyl alcohol extraction and ethanol precipitation. Isolated RNAs were reverse transcribed (4.5.3) and quantified by real-time PCR as described below (4.5.4).

<b>Polysome lysis buffer</b>	KCl	100 mM
	NaCl	5 mM
	Hepes, pH 7.0	10 mM
	Nonidet P-40	0.5% (v/v)
	• in H <sub>2</sub> O <sub>DEPC</sub>	
	• storage at 4 °C	
<b>NT2 buffer</b>	Tris/HCl, pH 7.4	50 mM
	NaCl	150 mM
	MgCl <sub>2</sub>	1 mM
	Nonidet P40	0.5% (v/v)
	BSA	5% (w/v)
	• in H <sub>2</sub> O <sub>DEPC</sub>	
	• storage at 4 °C	

### 4.5.3 Reverse Transcriptase Polymerase Chain Reaction (RT-PCR)

Isolated and purified total cellular (4.5.1) or immunoprecipitated RNAs (4.5.2) were reverse transcribed using SuperScript™III First Strand (Invitrogen) DNA synthesis

kits. Aliquots of 1 µg of RNA were incubated with 1 µl of 50 µM oligo dT and 1 µl 10 mM dNTP mix (final volume 10 µl) at 65 °C for 5 min, briefly centrifuged, and put on ice. The reaction mix was made up containing the following: 4 µl MgCl<sub>2</sub> (25 mM), 2 µl 10x reaction buffer, 2 µl 0.1 M DTT, 1 µl RNase OUT (40 u/µl) and 1 µl SS III RT. This mixture was added to the RNA-dNTP-oligo-dT mix and the reaction was further incubated for 50 min at 50 °C, 5 min at 85 °C and 1 min on ice. Samples of cDNAs were treated with 1 µl of RNase H for 20 min at 37 °C before being stored at -20 °C.

#### 4.5.4 Real-Time PCR (qPCR)

Complementary DNAs (cDNAs) were diluted to 50 µl in nuclease-free water. Real-time PCR was performed with a Rotor-Gene 6000 (Corbett Life Sciences, Sydney, Australia), using Sybr®Green PCR Master Mix (Applied Biosystems). The PCR conditions were: 10 min at 95 °C, 55 cycles of 10 s at 95 °C, 30 s at 60 °C and 20 s at 72 °C. The average Ct (cycle threshold) values of triplicate reactions were determined and levels of the tripartite leader (TL) and fiber mRNAs relative to glyceraldehyde 3-phosphate dehydrogenase (GAPDH) were calculated as described (Hartl et al., 2008). For the co-immunoprecipitated mRNA quantification, Ct values of these reactions were normalized with total TL and fiber RNA. Primers #1161, #1162, #1204, #1205, #1369 and #1370 used for the quantitative real-time PCR are listed in Section 3.3.1.

## 4.6 Protein Techniques

### 4.6.1 Preparation of Total Cell Lysates

For the analysis of proteins, cell pellets were prepared from mock/Ad-infected or transfected cells at indicated times and washed two times in ice cold PBS. The cell pellets were resuspended in Radio-immunoprecipitation buffer (RIPA) or in RIPA-*light* supplemented with 1 mM DTT, 0.2 mM PMSF, 1 mg/ml pepstatin A, 5 mg/ml aprotinin, and 20 mg/ml leupeptin or with a protease inhibitor cocktail *Complete*

## METHODS

*EDTA-free* (Roche). After 1 h incubation on ice, the lysates were sonicated (30 – 45 s, *output* 0.45 - 0.6 impulse/s; Branson Sonifier 450) and the insoluble debris was pelleted at 15,000 x g at 4 °C. The supernatants were transferred to new 1.5 ml reaction tubes (Eppendorf) and protein concentrations were determined as described below (4.6.2). Protein samples were stored at -20 °C.

<b>RIPA lysis buffer</b> (high stringency)	Tris/HCl, pH 8.0	50 mM
	NaCl	150 mM
	EDTA	5 mM
	Nonidet P40	1% (v/v)
	SDS	0.1% (w/v)
	Sodium desoxycholate	0.5% (w/v)
<b>RIPA-light</b> (middle stringency)	Tris/HCl, pH 8.0	50 mM
	NaCl	150 mM
	EDTA	5 mM
	Nonidet P40	1% (v/v)
	SDS	0.1% (w/v)
	Triton X-100	0.1% (v/v)

### 4.6.1.1 Preparation of Fractionated Cell Lysates

Nucleocytoplasmic fractionation was performed using the *CellLytic™NuCLEAR™ Extraction* kit (Sigma) according to the manufacturer's protocol. Cells were collected 18-48 h after mock or virus infection and washed once with PBS. The cell pellets were incubated in hypotonic lysis buffer for 15 min on ice. Samples were then centrifuged at 450 x g (Eppendorf table-top centrifuge 5417R) and the supernatants were removed. Resuspended cells were then passed through a 27-gauge needle (Terumo neolus) 7 times using a 1 ml syringe (BD Biosciences). After centrifuging the lysates at 11,000 x g for 20 min at 4 °C, the supernatants were collected as the cytoplasmic fraction. The pellets were further incubated with extraction buffer for 30 min at 4 °C with agitation. These samples were then centrifuged at 21,000 x g for 5 min and the supernatant was collected as the nuclear fraction.

#### 4.6.2 Quantitative Determination of Protein Concentrations

Protein concentrations in samples were determined using *Protein-Assays* (BioRad) according to Bradford (Bradford, 1976) by measuring the 595 nm absorption of proteins bound to chromogenic substrates of the assay. A small volume (1-2 µl) of protein solution was mixed well with 1 ml of PBS and 200 µl of Bradford reagent and incubated at RT for 5-30 min. Bovine serum albumin (BSA, Sigma) of known concentrations ranging from 0 to 12 µg/ml were used to generate a standard curve and the protein samples were measured in a spectrometer (Biorad) at a wavelength of 595 nm against a blank of PBS plus 200 µl of Bradford reagent.

#### 4.6.3 SDS-Polyacrylamide Gel Electrophoresis (SDS-PAGE)

Proteins in a sample or cell lysates were separated by SDS-PAGE according to their molecular weights. Polyacrylamide gels were made using a 30% acrylamide/bisacrylamide solution, 37.5:1 mixture (BioRad), which was diluted with water to give the appropriate percentage. Proteins were first concentrated by a lower percentage stacking gel and run in a separating gel (Laemmli, 1970). Generally, separating gels used in this study contained 10% acrylamide. Acrylamide polymerization was initiated by addition of ammonium persulphate (APS) to a final concentration of 0.1%. Gels were assembled using apparatus from Biometra according to the supplied instructions, and run in TGS buffer. Protein samples were prepared for SDS-PAGE by the addition of Laemmli sample buffer (Sambrook, 1989), before being heated at 90 °C for 5 min in a thermoblock (Eppendorf Thermomixer comfort). Pre-stained protein molecular weight markers were used to identify desired proteins. After loading samples onto the gel, the apparatus was run 2 h at a constant current (20 mA per gel) depending on the size of the proteins of interest. Proteins separated on an SDS gel were then transferred to a nitrocellulose membrane by Western blotting (4.6.4).

<b>30% Acrylamide- Stock solution</b>		Acrylamide	37.5% (w/v)
		N, N'Methylenbisacrylamide	1% (w/v)

## METHODS

<b>Stacking gel (5%)</b>	Acrylamide stock solution	17% (v/v)
	Tris/HCl, pH 6.8	120 mM
	SDS	0.1% (w/v)
	APS	0.1% (w/v)
	TEMED	0.1% (v/v)
<b>Seperating gel (10%)</b>	Acrylamide stock solution	38% (v/v)
	Tris/HCl, pH 8.8	250 mM
	SDS	0.1% (w/v)
	APS	0.1% (w/v)
	TEMED	0.1% (v/v)
<b>TGS Buffer</b>	Tris	25 mM
	Glycine	200 mM
	SDS	0.1% (w/v)
<b>Laemmli sample buffer</b>	Tris/HCl, pH 6.8	100 mM
	SDS	4% (w/v)
	DTT	200 mM
	Bromphenol blue	0.2% (w/v)
	Glycerol	20%

### 4.6.4 Western Blots

For immunoblotting, equal amounts of proteins were separated by SDS-polyacrylamide gel electrophoresis (SDS-PAGE) and transferred to nitrocellulose membranes (Schleicher & Schüll) using *Trans-Blot<sup>®</sup> Electrophoretic Transfer Cell* (BioRad) in *Towbin* buffer. Briefly, gels and nitrocellulose membranes were soaked in *Towbin* buffer and each gel was laid onto a nitrocellulose membrane of similar size, sandwiched between two pieces of pre-soaked Whatman blotting paper, and two blotting pads within in a plastic cassette. These were then placed into the blotting tank and electro-transfer was carried out for 90-120 min at 400 mA. To test the transfer efficiency, membranes were first reversibly stained with Ponceau S (Sigma) solution and washed in PBS. Then, they were incubated at least 1 h at RT or overnight at 4 °C in PBS, 0.1% Tween 20 (PBS-T20) containing 5% nonfat dry milk and then for 2 h in PBS, 1% nonfat dry milk containing the appropriate primary antibody dilution.



Membranes were washed three times in PBS-T20, and further incubated for 2 h at RT with a dilution of (1:5000-30,000) secondary antibody linked to horseradish peroxidase (HRP, Amersham) in PBS-T20 and washed three times in PBS-T20. The bands were visualized by enhanced chemiluminescence using *SuperSignal<sup>®</sup> West Pico Chemiluminescent Substrate* (Pierce) as recommended by the manufacturer on X-ray films (CL-XPosure™, Pierce or Kodak X-Omat AR) using *GBX Developer*, Kodak. Autoradiograms were scanned and cropped using Adobe Photoshop CS4 and figures were prepared using Adobe Illustrator CS4 software.

<b>PBS-T20</b>		Tween 20 • in PBS	0.1% (v/v) 200 mM
<b>Towbin buffer</b>		Tris/HCl, pH 8.3 Glycine SDS Methanol	25 mM 200 mM 0.05% (w/v) 20% (v/v)
<b>Ponceau S</b>		Ponceau S Trichloroacetic acid Sulfosalicylic acid	0.2% (w/v) 3% (w/v) 3% (w/v)

#### 4.6.5 Immunoprecipitation (IP)

Cell lysates were prepared as described (4.6.1) using appropriate volumes of ice-cold immunoprecipitation (IP) buffer RIPA-*light*, or NP-40 supplemented with protease inhibitors. Protein concentrations of individual samples were determined (4.6.2) and lysate volumes containing equal amounts of protein (250 µg-2 mg) were precleared by addition of Protein G- or A-sepharose (Sigma-Aldrich) for 1 hour at 4 °C with rotation (GFL, Gesellschaft für Labortechnik). Simultaneously, antibodies were coupled with Protein G- or A-sepharose. After centrifugation at 6000 rpm for 5 min (Eppendorf 5417), antibody-coupled beads were added to the cleared lysates and antigen-antibody complexes were left to form overnight at 4 °C. The following day, Protein G-/A-sepharose-immune complexes were spun down and washed five times in ice-cold

IP buffer before the addition of 10 µl of Laemmli sample buffer to elute the proteins. Samples were boiled for 5 min and spun down in preparation for SDS-PAGE and Western blotting.

<b>NP-40</b> (low stringency)	Tris/HCl, pH 8.0	50 mM
	NaCl	150 mM
	EDTA	5 mM
	Nonidet P-40	0.15% (v/v)
	Protease Inhibitor Mix	1 tablet per 50 ml
	<i>Complete EDTA-free ; Roche</i>	

#### 4.6.6 Immunofluorescence Staining (IF)

Adherent mammalian cells were grown on glass coverslips (VWR), placed on cell culture dishes, and infected or transfected as described in previous sections. At indicated times, the medium was removed, and the cells were incubated with ice-cold methanol for 15 min at -20 °C. After the removal of the alcohol, coverslips were air dried at RT and kept at -20 °C until staining. Before incubating with the primary antibody dilutions, fixed cells were washed once with PBS containing 0.1% Tween 20 (PBS-T20) for 5 min with agitation, and incubated with PBS-T20 containing 5% nonfat dry milk for 1 h at RT with agitation. Appropriate dilutions of primary antibodies were prepared in PBS-T20, and 50 µl aliquots of these dilutions were put onto each coverslip. The reaction was incubated at RT in a damp chamber for 1 h. After washing the coverslips three times with PBS-T20, cells were further incubated for 1 h with fluorescence coupled secondary antibody (dilution 1:100) in PBS-T20 supplemented with 0.5 µg/ml DAPI (4',6-diamidino-2'-phenylindol dihydrochloride) at RT in a damp and dark chamber. Coverslips were then mounted in *Glow Mounting Medium* (EnerGene) after three washes with PBS-T20, and digital images were acquired using a DMRB fluorescence microscope (Leica) with a charge-coupled device camera (Leica). These images were cropped and decoded by Photoshop CS4 (Adobe Systems) and assembled with Illustrator CS4 (Adobe Systems).

## 4.6.7 GST Pull-down Assays from Cell Lysates

### 4.6.7.1 GST-Protein Expression

GST-tagged proteins were cloned using pGEX4T-1 or pGEX5X-1 (Amersham Pharmacia) vectors and transformed into *E. coli* as described (4.1.2). From glycerol stocks, 5 ml starter cultures were inoculated and incubated at 37 °C overnight. The following day 2 ml of the starter culture was inoculated into 100 ml of expression culture. When the OD<sub>600</sub> of the culture reached 0.6 (2-4 h post inoculation), bacteria were induced with 0.1-0.5 mM (final concentration) Isopropylthio-β-D-galactosid (IPTG). This expression culture was further incubated at 30 or 37 °C (according to the expressed protein) for 4 h. Bacteria were centrifuged at 4500 rpm for 10 min and the pellet was washed once with 6 ml of STE buffer. Washed pellet was either stored at -20 °C or used directly for protein purification (4.6.7.2)

STE buffer	Tris/HCl, pH 8.0	10 mM
	NaCl	150 mM
	EDTA	1 mM

### 4.6.7.2 GST-Protein Purification

Washed and pelleted expression bacteria were resuspended in 5 ml of STE buffer and a spatula tip of lysozyme was added. This lysate was incubated on ice for 15 min. DTT was added to the lysate to a final concentration of 5 mM and mixed thoroughly by vortexing. The lysate was sonicated twice for 30 s and centrifuged at 10,000 x g for 5 min at 4 °C (SS34 rotor). The supernatant was transferred into a new 15 ml Falcon tube, and 1.5 ml of Triton X-100 from a 10% stock was added and mixed by vortexing. The resulting suspension was filtered through a 0.45 µm filter (PALL Life Sciences). Then the homogenized protein solution was mixed with 100 µl of 50% GST-beads equilibrated with PBS and incubated 1 h at 4 °C, rotating. GST-protein beads were precipitated by centrifuging at 4500 rpm for 5 min and washed 6 times with ice-cold PBS. After adding 50-100 µl of PBS to the beads, 10 µl of the sample was examined by SDS-PAGE. After electrophoresis, gels were placed in a staining solution containing

0.1% Coomassie Brilliant Blue R-250 (Sigma), 10% glacial acetic acid, 20% methanol in water, and left at RT for 10 min with agitation. Gels were then placed in destaining solution containing 10% glacial acetic acid, 20% methanol in water, until proteins became clearly visible.

#### 4.6.7.3 GST Pull-Down Assays

*In vivo* GST pull-down assays were carried out as follows. Cell lysates were prepared as described (4.6.1) in RIPA-*light*. Typically, 50 µg of GST-fusion protein was mixed with 1 mg of cell lysate and incubated at 4 °C overnight. GST-fusion protein complexes were precipitated by centrifuging at 6000 rpm for 5 min at 4 °C. The beads were washed 6 times in RIPA-*light*, before releasing GST-fusion protein complexes by the addition of Laemmli loading buffer. Samples were analyzed by SDS-PAGE (4.6.3), followed by Western blotting (4.6.4).

#### 4.6.8 Purification of His-Tagged Sumo Conjugates

H1299 cells were transfected with His-sumo-1 plasmid (Muller et al., 2000) by the PEI method (4.2.4.2). 6 h post transfection, these cells were either mock or virus infected (4.3.4). 36 h post transfection, cells were washed once with PBS and harvested (4.2.5). Histidine purification was carried out as previously described (Xirodimas et al., 2001). First, the cell pellets were lysed in 6 ml of 6 M guanidinium-HCl. 75 µl of Ni<sup>2+</sup>-NTA-agarose beads (Qiagen) were then added to each lysate and the samples were rotated at RT for 4 h. The beads were sequentially washed with wash buffers WB1, WB2, WB3, and WB4 for 5 min at RT. After the last wash, His-tagged sumoylated proteins were eluted by incubating the beads in elution buffer at RT for 20 min. The eluates were analyzed by SDS-PAGE (4.6.3) and Western blotting (4.6.4).

## METHODS

<b>6 M guanidinium-HCl</b>	Guanidinium-HCl	6 M
	Na <sub>2</sub> HPO <sub>4</sub> /NaH <sub>2</sub> PO <sub>4</sub>	0.1 M
	Tris/HCl, pH 8.0	10 mM
	Imidazole	5 mM
	β-mercaptoethanol (freshly added)	10 mM
<b>WB1</b>	Guanidinium-HCl	6 M
	Na <sub>2</sub> HPO <sub>4</sub> /NaH <sub>2</sub> PO <sub>4</sub>	0.1 M
	Tris/HCl, pH 8.0	10 mM
	β-mercaptoethanol	10 mM
	(freshly added)	
<b>WB2</b>	Urea	8 M
	Na <sub>2</sub> HPO <sub>4</sub> /NaH <sub>2</sub> PO <sub>4</sub>	0.1 M
	Tris/HCl, pH 8.0	10 mM
	β-mercaptoethanol	10 mM
	(freshly added)	
<b>WB3</b>	Urea	8 M
	Na <sub>2</sub> HPO <sub>4</sub> /NaH <sub>2</sub> PO <sub>4</sub>	0.1 M
	Tris/HCl, pH 6.3	10 mM
	β-mercaptoethanol	10 mM
	(freshly added)	
<b>WB4</b>	Urea	8 M
	Na <sub>2</sub> HPO <sub>4</sub> /NaH <sub>2</sub> PO <sub>4</sub>	0.1 M
	Tris/HCl, pH 6.3	10 mM
	Triton X-100	0.1% (v/v)
	β-mercaptoethanol	10 mM
	(freshly added)	
<b>Elution buffer</b>	Imidazole	200 mM
	Tris/HCl, pH 6.7	150 mM
	Glycerol	30% (v/v)
	SDS	5% (w/v)
	β-mercaptoethanol	720 mM
	(freshly added)	

#### 4.6.9      **Production and Detection of Radiolabeled Proteins**

To analyze the sulfation of L4-100K,  $^{35}\text{SO}_4^{2-}$  (GE Healthcare) was used during adenovirus infection. To detect incorporation of the labeled sulfate molecule into the proteins, first the infected cells' medium was replaced by a sulfate-free medium (Hyclone). After incubating the cells for 1 h in the absence of sulfate, 0.5 mCi of  $^{35}\text{SO}_4^{2-}$  was added to  $2.5 \times 10^6$  cells for 3 h. Finally, the cells were harvested (4.2.5) and protein samples were prepared as described (4.6.1). Total protein lysates and immunocomplexes obtained from IP reactions (4.6.5) were separated by 10%-SDS-PAGE (4.6.3) and the gels were incubated in 1 M sodium salysilic acid for 30 min, at RT to amplify the signals. Gels were then dried (Slab Gel Dryer 2000) under vacuum at 70 °C for 2 hours. Dried gels were exposed for autoradiography at -20 °C using Amersham Hyperfilm (GE Healthcare). Radioactive signals were detected using Phosphor-Screen (Imaging Screen K, Biorad). Using Molecular Imager® FX, detected images were scanned and documented with the ChemiDoc (Biorad) system.

## 5 Results

---

### 5.1 Cloning and Generation of Ad5 L4-100K Virus Mutants

For a long time, the functions and functional regions of adenoviral proteins had been investigated by mutating the proteins in a cDNA construct that was transfected in to mammalian cells. To obtain infection conditions, these transfected cells were concomitantly infected with adenovirus. This is how one tried to analyze the effects of the inserted mutations on target proteins during adenovirus infection. However, these data were not always as accurate as could be in a natural environment, since the foreign plasmid interfered with the physiological expression of the protein. In addition, the presence of the wt gene in the viral context complicated evaluation of the results.

The most reliable way to study the functions of single proteins in adenovirus infection is to generate mutant adenoviruses. To insert point mutations into the 36 kb linear genome of adenovirus, colleagues in our group, Peter Groitl (Groitl and Dobner, 2007) and Thomas Zeller (Zeller, 2004) established a cloning strategy. This strategy involves two plasmid systems that are cloned in bacterial expression vectors by restriction site insertions, a small region-specific plasmid (E1-, E4-, or L4-Box) and a large viral bacmid. Desired mutations can easily be inserted into the small “boxes” using the *QuikChange<sup>TM</sup> Site-Directed Mutagenesis Kit* (Stratagene), and these mutated boxes are then re-cloned into the viral “backbone”. Figure 7 outlines our strategy for constructing Ad5 L4-100K mutant viruses H5pm4151, H5pm4152, H5pm4153, and H5pm4165. This involved two recombinant plasmids containing Ad5 late region 4 (L4) from nt 21438-27081 (pL4-1513) or the Ad5 wt genome lacking a portion of E3 (pH5pg4100). Plasmid pL4-1513 was used to introduce mutations into the L4-100K gene by site-directed mutagenesis, while plasmid pH5pg4100 served as the DNA backbone to recombine the mutations into the Ad5 chromosome by direct cloning. To

generate L4-100K mutant viruses, infectious viral DNAs were released from the recombinant plasmids by *PacI* digestion and transfected into the L4-100K-complementing cell line K16 (Hodges et al., 2001). Viral progenies were isolated, amplified and viral DNAs were analyzed by restriction pattern and DNA sequencing. Nevertheless, this cell line expresses very small amounts of 100K protein due to its toxicity, and this was not always enough to support virus growth in the case of deleterious mutations.

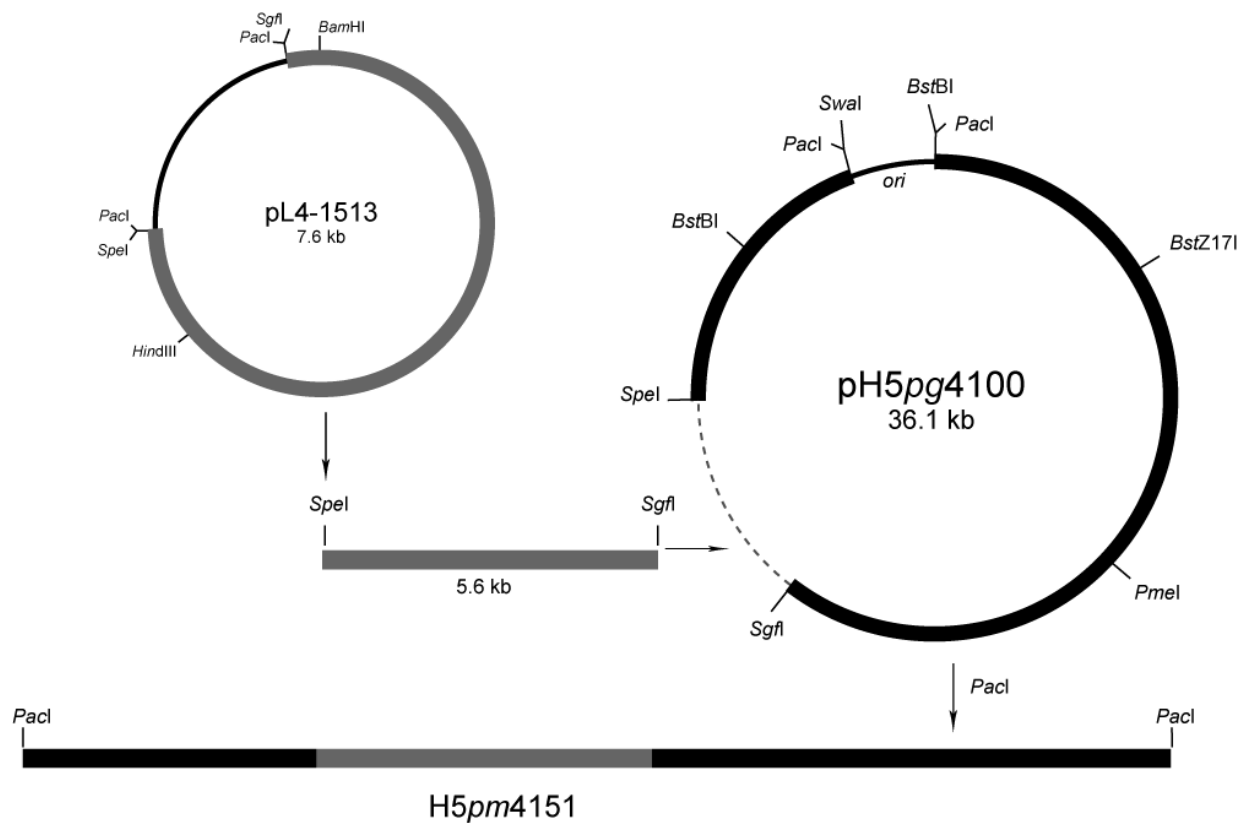


**Figure 7. Generation of L4-100K mutant viruses**

Point mutations were introduced into the L4-100K gene in pL4-1513 by site-directed mutagenesis. The L4 plasmid and bacmid pH5pg4100 were linearized with *SgfI* plus *SpeI* and the 5.6 kb *SgfI*/*SpeI* fragment from pH5pg4100 was replaced with the corresponding fragment from the mutated pL4 construct. The viral genome was released by *PacI* digestion and used for transfection of the 100K-complementing cell line K16. Viruses were then isolated and propagated using K16 cells.



## 5.2 General Characterization of Virus Mutants H5pm4151, H5pm4152 and H5pm4153

To gain a better understanding of the role of L4-100K in lytic adenovirus infection, the evolutionary conserved motifs and domains in this multifunctional protein were screened. We chose to mutate those that show high sequence similarity to previously established protein-protein interaction or posttranslational modification motifs. In the L4-100K sequence, RGG boxes were targeted as a putative methylation domain, K<sup>408</sup> as a sumo conjugation motif (SCM), Y<sup>90</sup> as a sulfation site, and a leucine-rich amino acid sequence between residues 383 and 392 was targeted as a nuclear export signal (NES). The inserted mutations are summarized in Figure 8.

The virus mutants H5pm4151, H5pm4152 and H5pm4153 were generated and propagated efficiently using K16 cells, except the NES mutant H5pm4165, RGG.GAR, and GAR mutants, which will be discussed in the following sections. H5pm4165 virus could be produced by additional wt-100K protein complementation, although only a low titer virus stock could be obtained. Therefore, characterization of this mutant is presented in Section 5.6.

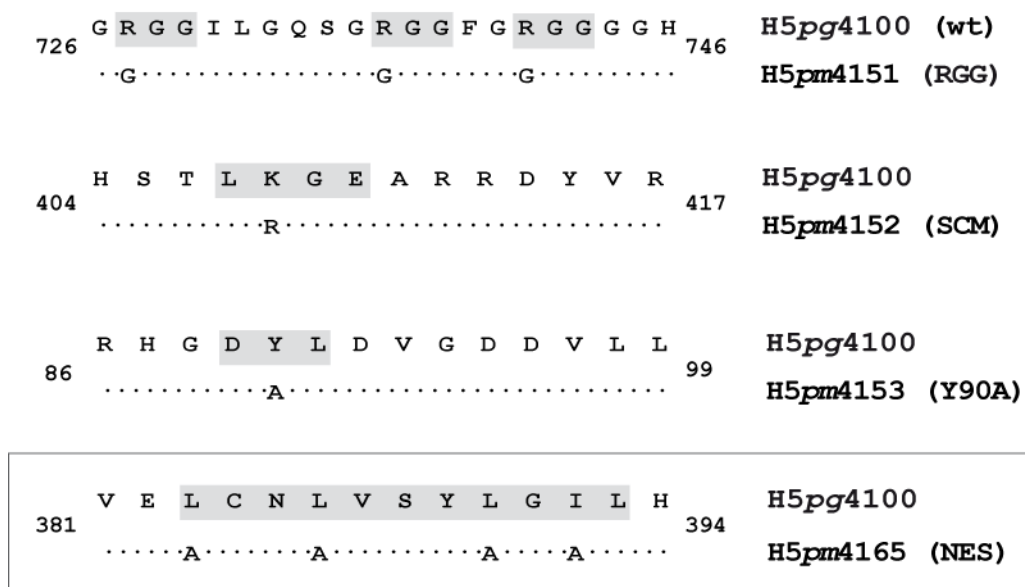


Figure 8. RGG, SCM, Y90A, and NES mutations in L4-100K gene

Introduced point mutations were shown in the L4-100K proteins of RGG (H5pm4151), Sumo conjugation motif; SCM (H5pm4152), Y90A (H5pm4153), and NES (H5pm4165) mutants. Numbers refer to amino acid residues in the L4-100K protein from H5pg4100, which is the wt virus used in this study. Regions marked with grey boxes show the targeted consensus motifs. Amino acid substitutions are indicated below the wt sequences, and dots represent the unchanged residues. NES mutant H5pm4165 is framed to highlight its incompetency.

### 5.2.1 Effects of Inserted Mutations on the Stability and Subcellular Localization of L4-100K

#### 5.2.1.1 Analysis of Protein Steady-State Levels

It has been well established that virus mutants lacking the L4-100K gene are not capable of accumulating late structural proteins or encapsidating the newly synthesized genomes, therefore can not produce infective progeny virions (Hodges et al., 2001). Indeed, this defective phenotype can provide a convenient feature for adenovirus gene therapy vectors, since neither lysis of the infected cell, nor expression of late proteins – due to their toxicity – is desired in this case. On the other hand, in the field of oncolytic adenovirus vector development, there is great demand to build an adenovirus vector fully capable of replicating in, and lysing tumor cells, while being abortive in quiescent cell infection.

First, we tested the generated mutant viruses for their ability to produce a stable L4-100K protein during infection of mammalian tumor cell lines in culture (A549, HeLa, and H1299). In Figure 9, infection of A549 cells with wt and mutant viruses in a time course is shown as an example, since the other cell lines also provided the same results. Steady-state levels of early and late viral proteins were detected by immunoblotting using appropriate antibodies as described in Section 4.6. PRMT1 was used as a control, representing a cellular protein. All of the examined viruses displayed a gradually increasing 100K expression pattern, first visualized at 16 h post infection (long exposure) and reaching high levels at 48 h post infection (Fig. 9). Only the Y90A (H5pm4153) mutant showed an obvious reduction in 100K expression, never

## RESULTS

reaching wt levels. The efficiency of the infections was verified by immunoblotting using an antibody against the E2A-72K DNA binding protein (DBP), which showed a similar pattern in all virus infections. When analyzing accumulation of the major capsid protein hexon, slightly reduced production was observed in H5pm4151 and H5pm4152 infections compared to the wt virus, whereas H5pm4153, exhibiting a poor 100K accumulation, was found to be severely defective in hexon production. However, this mutant was shown to be fully capable of expressing early protein E1B-55K, indicating that the defect observed in late protein synthesis was not due to a defect in the early phase. The other mutant viruses were also observed to express E1B-55K protein as efficiently as H5pg4100. The steady-state expression levels of cellular PRMT1 were detected to be equal in all virus infections.

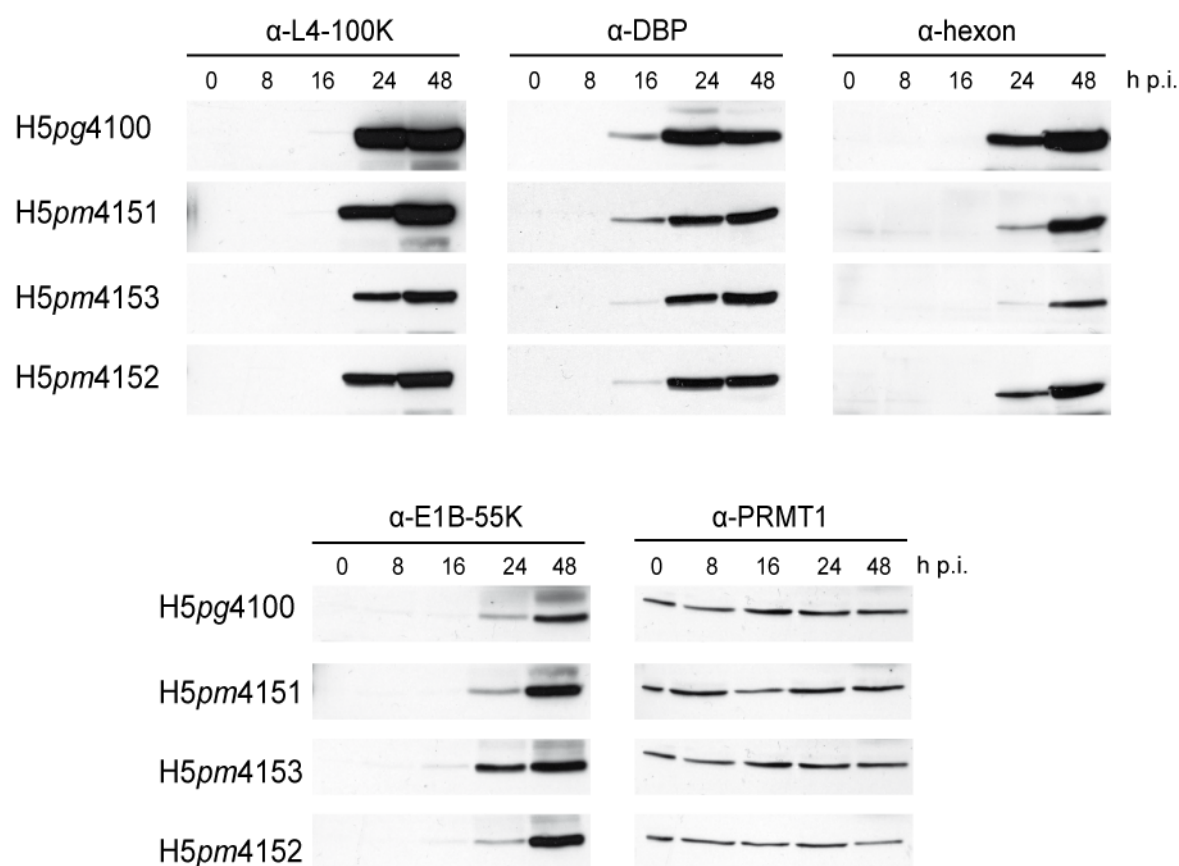


**Figure 9. Steady-state levels of early and late proteins in wt and mutant virus infections**  
A549 cells were infected with H5pg4100, H5pm4151, H5pm4153, and H5pm4152 viruses at 10 FFU/cell.

Total cell extracts were prepared from non-infected (0) and infected cells harvested at indicated hours post infection (h p.i.). Twenty-five µg aliquots of lysates were separated by SDS-10% PAGE and analyzed by immunoblotting using L4-100K rat mab 6B10, anti-hexon antibody, B6-8 mouse mab recognizing E2A-72K protein, 2A6 mouse mab recognizing E1B-55K protein, and anti-PRMT1 antibody.

### 5.2.1.2 Analysis of L4-100K Subcellular Localization

#### 5.2.1.2.1 Immunofluorescence Analysis (IF)

Subcellular localizations of the wt and mutant L4-100K proteins were analyzed during infection by immunofluorescence (IF) microscopy. First, the distribution of L4-100K in H5pg4100 infected A549 cells was determined in a time course. As can be seen in Figure 10, consistent with the previous reports (Gambke and Deppert, 1981a; Oosterom-Dragon and Ginsberg, 1980), L4-100K displayed a dominant, diffusely distributed cytoplasmic localization (panel a) early in the late phase (18 h p.i.) when the replication centers could be observed as large dots in the nucleus (panel b). As the infection progresses (24 h p.i.), when the replication centers became structured (panel e), this late protein was observed to start translocating into the nuclei of infected cells (panel d), and showed an exclusively nuclear localization (panel g) late in the infection before the lysis of the cell. At this time point (48 h p.i.), replication centers could no longer be distinguished as individual dots (panel h).

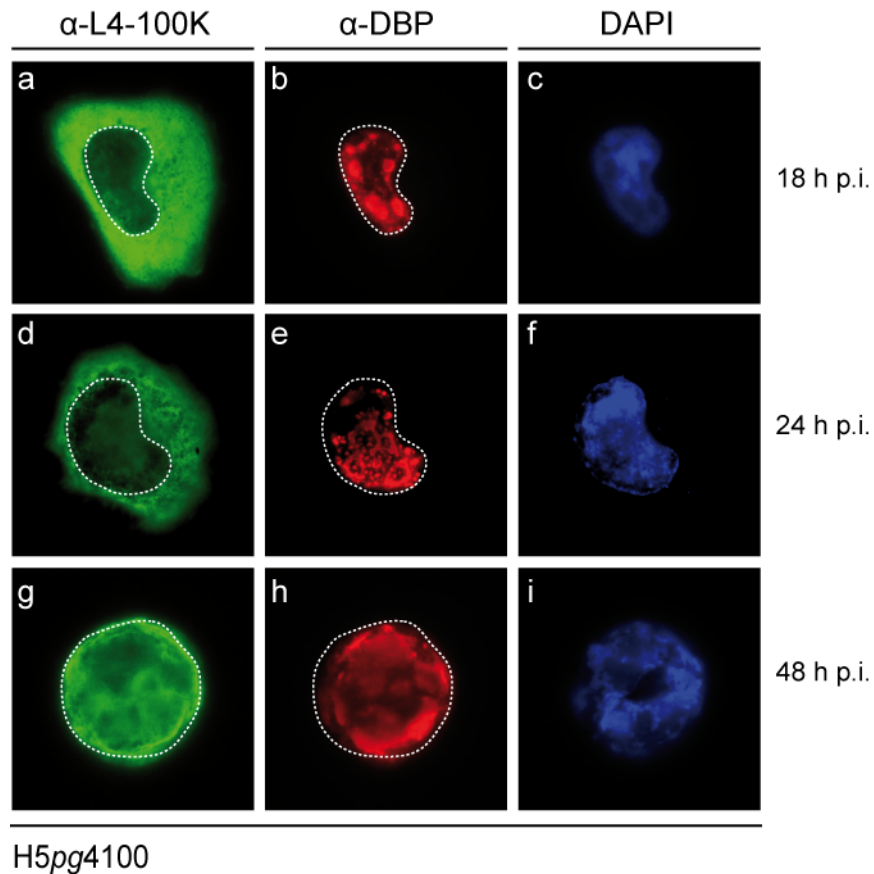


**Figure 10. Immunofluorescence analysis of L4-100K subcellular localization during wt virus infection**

A549 cells were seeded on glass cover slips and infected with H5pg4100 at 10 FFU/cell when confluency reached 60-80%. Infected cells were fixed with methanol at indicated hours post infection (h p.i.) and incubated with L4-100K rat mab 6B10 and DBP mouse mab B6-8. Signals were detected using FITC-coupled anti-rat antibody (a, d, g) and Texas red-coupled anti-mouse antibody (b, e, h). Nuclei were visualized using DAPI (c, f, i) and represented as dotted lines on the images.

Similarly, mutant L4-100K distributions were investigated in several human cell types infected with the mutant viruses. In the cell types examined none of the mutant viruses showed any obvious alteration in the localization of this late protein. Figure 11 represents infection of A549 cells (A) and primary human hepatocytes (B) with wt and mutant viruses. Dominant cytoplasmic distribution of L4-100K with minor nuclear staining can be seen in panels a to d in both cell types at 24 h post infection (Fig. 11). Interestingly, regardless of the cell type, H5pm4153 infection displayed a rather structured L4-100K staining in the cytoplasm, consisting of dot and rod shaped structures in 5-10% of all infected cells (Fig.11A/B, panel c, Fig. 23C). These cells were co-stained with either anti-E1B-55K (A) or anti-DBP (B) antibody. Distributions of these early proteins were found to be similar to that of the wt virus infection. E1B-55K,

## RESULTS

as already described (Endter et al., 2001), showed punctuated cytoplasmic, and diffuse nuclear staining in all virus infections. A proportion of this early protein localized at some structures in the nucleus (Fig. 11A, panels e-h) resembling replication centers (Ornelles and Shenk, 1991). The formation of replication centers was visualized by staining DBP in primary human hepatocytes, and showed a similar pattern among different virus infections (Fig. 11B, panels e-h).

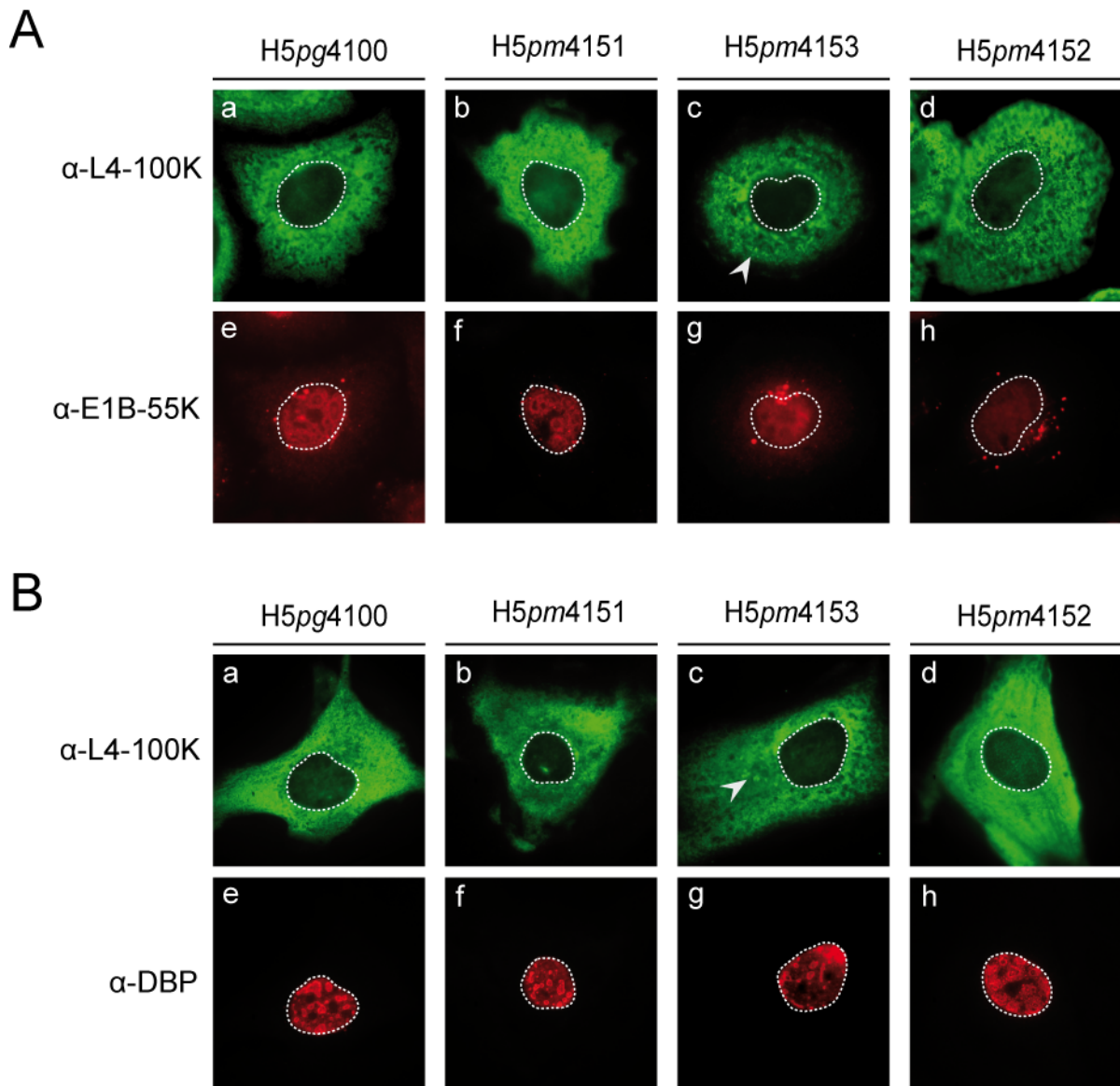


**Figure 11. Immunofluorescence analysis of L4-100K subcellular localization in A549 cells and primary human hepatocytes during wt and mutant virus infections**

A549 cells (A) and primary human hepatocytes (B) were seeded on glass cover slips and infected with H5pg4100, H5pm4151, H5pm4153, and H5pm4152 viruses at 10 and 50 FFU/cell, respectively, when confluency reached 60-80%. Infected cells were fixed with methanol at 24 h post infection, and

incubated with L4-100K rat mab 6B10 (a-d) together with E1B-55K mouse mab 2A6 (e-h) (A), or L4-100K rat mab 6B10 (a-d) together with DBP mouse mab B6-8 (e-h).. Signals were detected using FITC-coupled anti-rat and Texas red-coupled anti-mouse antibodies. Nuclei are represented by dotted lines according to DAPI staining. Arrow heads indicate different L4-100K structures.

### **5.2.1.2.2 Nucleocytoplasmic Fractionation**

To confirm the subcellular distribution of wt and mutant L4-100K proteins indicated by immunofluorescence staining, nucleocytoplasmic fractionation was performed using A549 cells infected with H5pg4100, H5pm4151, H5pm4153, and H5pm4152 viruses at 10 FFU per cell. Cytoplasmic and nuclear steady state levels of viral proteins were determined during infection. Consistent with the IF data, L4-100K was observed in both fractions at 24 h p.i. (Fig. 12A), while the majority of the protein was found in the nuclear extract (Fig. 12B) at a later time point (48 h p.i.) as observed in all virus infections. Hexon expression showed a similar pattern and gradually accumulated in the nuclear fraction during wt and mutant virus infections, although much less in the case of H5pm4153 compared to the wt virus. Interestingly, E1B-55K protein amounts were detected in higher quantities in the nuclear fractions of the studied virus infections, although this early protein was observed predominantly in the cytoplasm of infected cells by IF microscopy. These experiments lead to the conclusion that neither the arginines in the triple RGG boxes or the ninetieth tyrosine residue, nor the sumo conjugation motif (SCM) of L4-100K play a role in the subcellular localization of this protein. Nevertheless, a severe defect in the accumulation of late proteins was observed in H5pm4153 infections, highlighting the significance of this tyrosine residue. Moreover, a similar but milder effect could be seen in H5pm4151 infections, which will be discussed in more detail in Section 5.5.

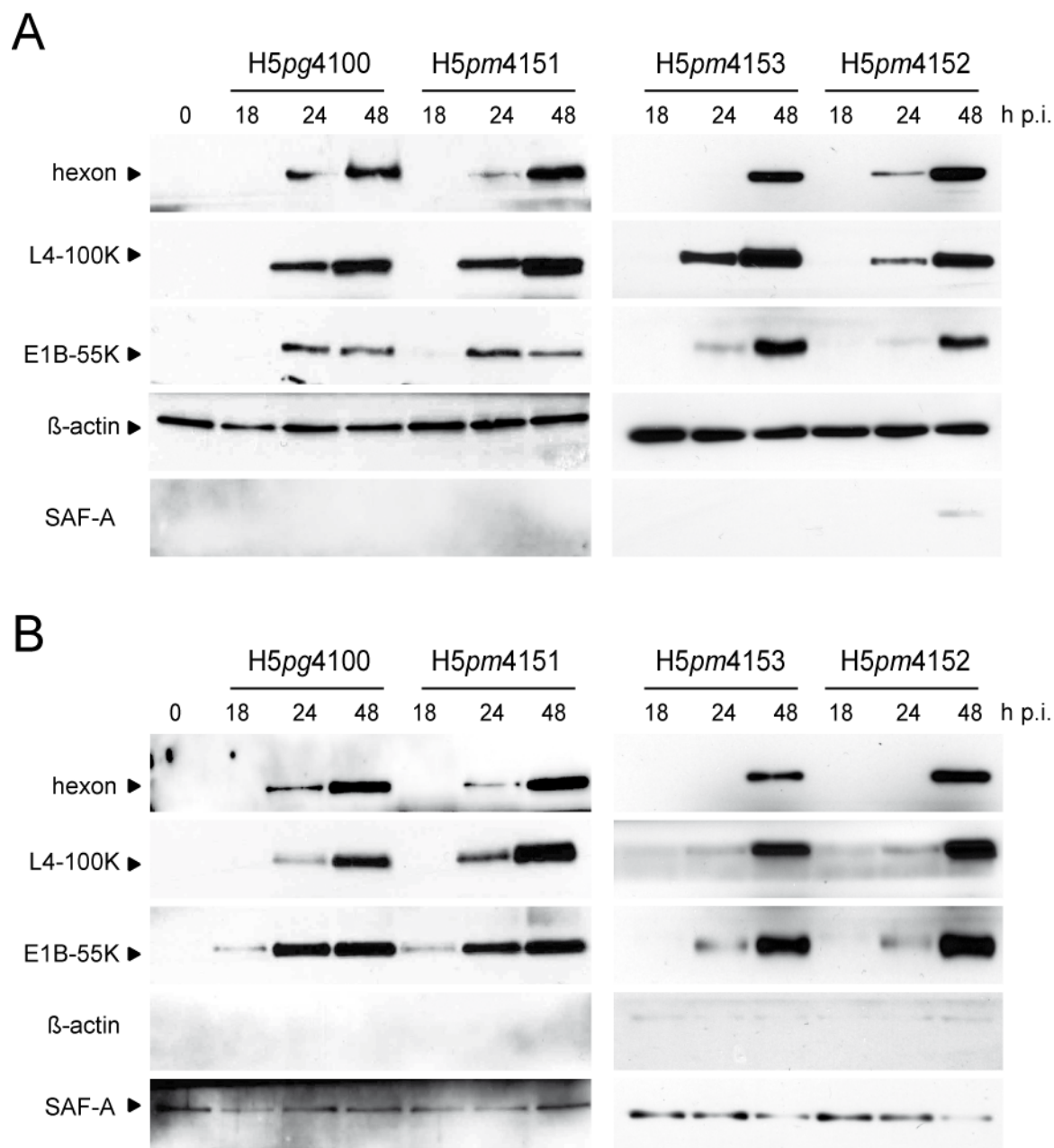


**Figure 12. Determination of the cytoplasmic and nuclear steady-state levels of viral proteins in A549 cells infected with wt and mutant viruses**

A549 cells were infected with H5pg4100, H5pm4151, H5pm4153, and H5pm4152 viruses at 10 FFU/cell. Non-infected (0) and infected cells were harvested at indicated hours post infection (h p.i.), and cytoplasmic (A) and nuclear (B) fractions were separated. Two  $\mu$ g aliquots of nuclear and 5  $\mu$ g aliquots of cytoplasmic extracts were separated by SDS-10% PAGE and analyzed by immunoblotting using L4-100K rat mab 6B10, anti-hexon antibody, and 2A6 mouse mab recognizing E1B-55K protein. Anti- $\beta$ -actin antibody was used as the marker of the cytoplasmic, and anti-SAF-A antibody as the marker of the nuclear fraction.



### 5.2.2 Inserted Mutations in the L4-100K Gene Do Not Affect Viral DNA Replication

To ensure that any defect or delay observed in late phase progression during mutant virus infections is not caused by a fault in the early phase, DNA replication efficiencies of mutant viruses were determined and compared to the wt values. This was accomplished by performing modified semi-quantitative PCR with DNA samples obtained from H5pg4100, H5pm4151, H5pm4153, and H5pm4152 infected A549 cells in a time course of infection. PCR reactions were performed as described in Section 4.4.5.3 using primers targeting a fragment of the E1B-55K gene. Amplified products were analyzed on agarose gels using the *Gene Tools* program of the SynGene system to quantify the band intensities. The mean values of three independent experiments can be seen in Figure 13.

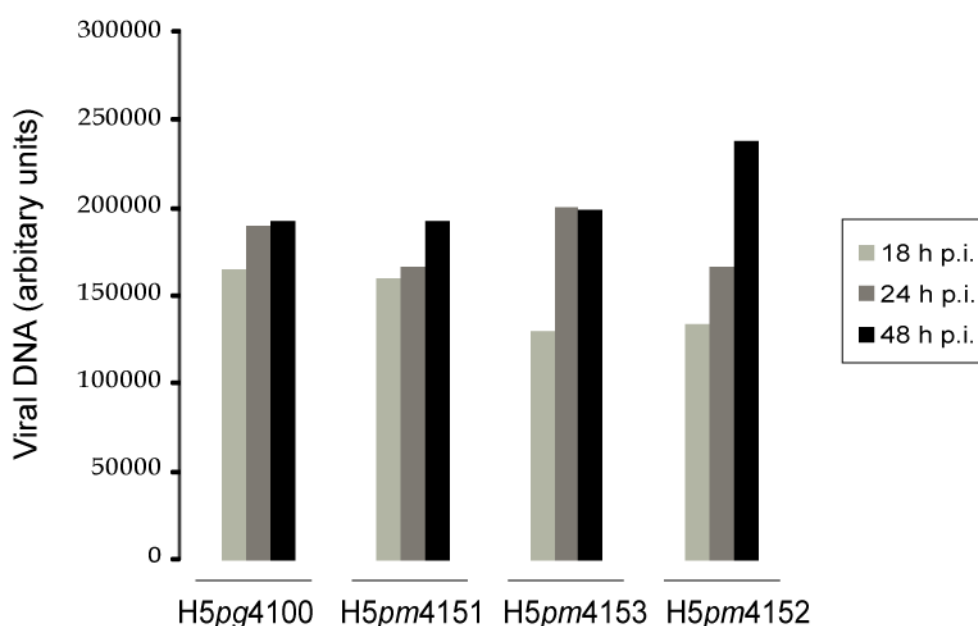


**Figure 13. Analysis of viral DNA replication**

A549 cells were infected with H5pg4100, H5pm4151, H5pm4153, and H5pm4152 viruses at 10 FFU/cell. Infected cells were harvested at indicated hours post infection (h p.i.). Viral DNA synthesis was determined as described in 4.4.5.3. Amplified E1B gene products were analyzed on an agarose gel and the band intensities were quantified using *Gene Tools* software of the SynGene system.

PCR analysis of replicating viral DNA demonstrated that the inserted mutations in the L4-100K gene have no significant effect on viral replication efficiency during infection. Viral DNA amplifications could be observed 8 hours post infection on agarose gels and reached measurable levels 18 hours post infection, followed by an increase during the late phase reaching maximum levels at 48 hours post infection. Similar amplification patterns could be detected in the mutant virus infections, indicating that early phase progression of these mutants is as efficient as the wt virus.

### **5.2.3 Effects of Inserted Mutations in the L4-100K Gene on Structural Protein Synthesis and Virus Yield**

In all L4-100K virus mutants examined in this study, infectivity, early phase progression and 100K stability properties proved to be as efficient as the wt virus. However, three of the mutant viruses (H5pm4151, H5pm4153, and H5pm4165) exhibited a delayed and/or defective late phase process. To further investigate the late phase progression efficiency of the infection, A549, HeLa, and H1299 cells were infected with H5pg4100, H5pm4151, H5pm4153, and H5pm4152 viruses at 1 to 50 FFU per cell, and harvested in a time course during infection. Structural proteins were analyzed on nitrocellulose membranes by Western blots (4.6.4). The synthesis pattern of adenoviral capsid proteins in A549 cells infected at 10 FFU per cell can be seen in Figure 14. Major capsid proteins (II, III, IV) became visible on the membranes 16 hours post infection and started to accumulate over time, as did the minor capsid proteins (VI, VII, VIII, and IX).

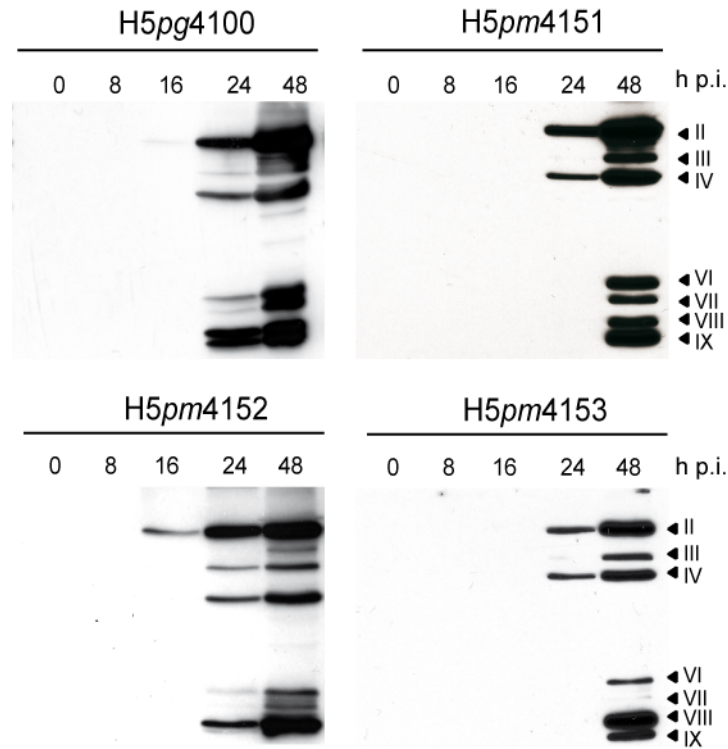


**Figure 14. Structural protein synthesis**

A549 cells were infected with H5pg4100, H5pm4151, H5pm4153, and H5pm4152 viruses at 10 FFU/cell. Total cell extracts were prepared at indicated times post infection (h p.i.). Proteins (25  $\mu$ g samples) were separated by SDS-10% PAGE, transferred to nitrocellulose membranes and probed with the anti-Ad5 rabbit polyclonal serum L133. Bands corresponding to major capsid proteins hexon (II), penton (III), fiber (IV) and minor capsid proteins (VI, VII, VIII, IX) are indicated on the right.

Consistent with the protein steady-state expression (5.2.1.1) and fractionation data (5.2.1.3), H5pm4153 displayed a severe reduction in the synthesis of late structural proteins. In the case of H5pm4151 infection, a delay was observed (compare 24 h p.i. lanes) in the accumulation of these components, especially the minor capsid proteins. In contrast, the SCM mutant H5pm4152 showed a comparable expression pattern of structural protein accumulation to that of the wt virus (Fig. 14).

## RESULTS

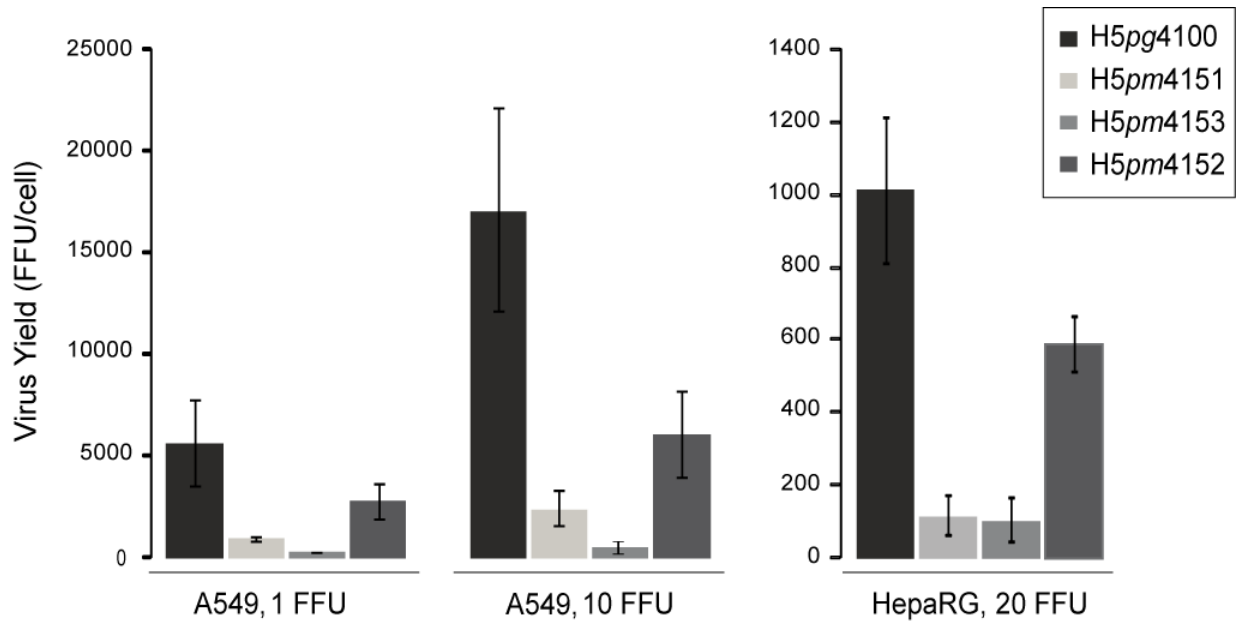


**Figure 15. Production of progeny virions**

A549 and HepaRG cells were infected with H5pg4100, H5pm4151, H5pm4153, and H5pm4152 viruses at indicated FFU per cell. Infected cells were harvested 48 h post infection and virus yields were determined as described in Section 4.3.5. The results represent the averages from three independent experiments. Error bars indicate the standard error of the mean.

As expected, the virus mutants that showed reduced late protein synthesis also exhibited decreased production of progeny as verified by virus yield experiments (Fig. 15). Different human cell lines were infected with wt and mutant viruses at varying multiplicity of infection (moi, 1-50 FFU/cell). These cells were harvested 48 hours post infection, and newly produced viruses were determined as described in Section 4.3.5. In Figure 15, virus yields of the mutant viruses are represented at low and high moi in A549 and at 20 moi in HepaRG cells. Under these conditions, H5pm4151 produced approximately 6 times less progeny than the wt virus in A549 cells, whereas H5pm4153 could only yielded 2% of the wt virus. In HepaRG cells, this reduction increased further for H5pm4151, reaching a 10-fold difference, while H5pm4153 replicated much better here than in A549 cells. H5pm4152 replicated efficiently in all of the tested cell lines, showing at most a 2-fold reduction compared to wt virus. These results not only demonstrate that arginines in the RGG boxes and the tyrosine residue at position 90 are critical for L4-100K functions promoting late protein expression and capsid assembly, but also hint at cell line-dependent growth of L4-100K mutant

viruses. The functions of these residues and the reasons for the observed defects were investigated in detail with respect to L4-100K tasks and interaction partners.

#### **5.2.4 Effects of Inserted Mutations in the L4-100K Gene on its Interaction with Hexon and PRMT1**

Possible roles of the investigated residues on L4-100K functions were assessed by examining the binding of known interaction partners to mutant L4-100K proteins. The indispensable role of L4-100K in hexon biogenesis has been demonstrated in several reports (Hong et al., 2005; Kauffman and Ginsberg, 1976; Oosterom Dragon and Ginsberg, 1981; Wodrich et al., 2003). According to these publications, 100K is responsible for correct hexon quaternary structure by acting as a chaperone to form hexon trimers. Although the mechanism of this process is still unknown, hexon monomers proved to be instable in the absence of functional 100K protein (Hong et al., 2005; Wodrich et al., 2003). Therefore, L4-100K mutant viruses were first tested in their ability to bind this major capsid component during lytic infection. In the immunoprecipitation experiments, viral protein levels were equalized by using 1.5 to 2 times more protein in the case of H5 $pm$ 4153 infections due its reduced late protein expression levels. Hexon efficiently co-precipitated L4-100K during adenovirus infection, with this gradually increasing over time in A549 cells (Fig. 16). Surprisingly, RGG mutant H5 $pm$ 4151 co-precipitated in greater amounts than the wt protein especially at 48 h post infection. This increased binding of RGG-100K to hexon was reproduced several times in different human cell lines and will be discussed in more detail in Section 5.5. Y90A (H5 $pm$ 4153) and SCM (H5 $pm$ 4152) L4-100K mutants also co-precipitated with hexon at levels comparable to wt, although an altered pattern of interaction was observed with H5 $pm$ 4153: here binding increased then decreased, unlike the gradually increasing binding pattern observed with the wt virus infection.

## RESULTS

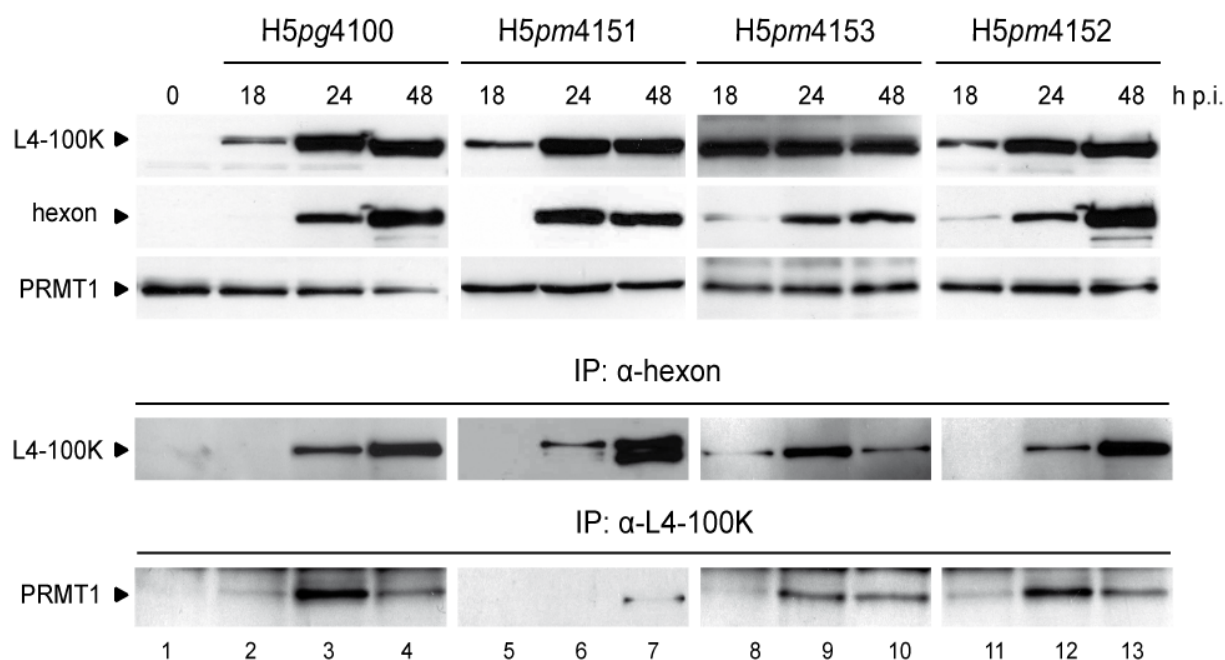


**Figure 16. Binding of mutant L4-100K proteins to hexon and PRMT1**

A549 cells were infected with H5pg4100, H5pm4151, H5pm4153, and H5pm4152 viruses at a multiplicity of 10 FFU per cell, and harvested at the indicated time points after infection (h p.i.). Total cell extracts were prepared from non-infected (0) and infected cells. 50 µg aliquots of lysates were separated by SDS-10% PAGE and analyzed by Western blotting using L4-100K rat mab 6B10, rabbit mab recognizing the hexon protein, or rabbit mab recognizing PRMT1. The same lysates were used for immunoprecipitation (IP) with anti-hexon and 6B10 mab. The immunocomplexes were separated by SDS-10% PAGE and analyzed by immunoblotting using mab 6B10, or anti-PRMT1.

Second, the PRMT1 interaction capacity of the mutant 100K proteins was also investigated by co-immunoprecipitation assays. Since our group had previously shown the arginine methylation of L4-100K, and PRMT1 was identified as the enzyme catalyzing this reaction (Kzhyshkowska et al., 2004), this study aimed to identify the target motif in the L4-100K sequence, as well as clarify the consequence of this modification during infection. Targeting conserved RGG boxes in the C-terminus of L4-100K, these arginines were substituted by glycines since PRMT1 methylates arginines in RGG or GAR motifs (Bedford and Richard, 2005). As expected, only the RGG mutant showed a severe defect in PRMT1 binding (Fig. 16). The resulting effect of this defect and the methylation profile of this mutant protein will be presented in Section 5.5.

### 5.3 L4-100K Binds to E1B-55K During Lytic Infection

E1B-55K is a multifunctional regulatory protein that plays critical roles in both the early and late phase of adenovirus infection. In the early phase, it contributes to eliminating specific cellular factors by forming a ubiquitin ligase complex together with E4orf6 (Blanchette et al., 2004; Querido et al., 2001; Querido et al., 2000). This complex further contributes to the transport of late viral transcripts in the late phase of infection (Blanchette et al., 2008). Moreover, observations suggest a role for E1B-55K in virus-specific translation pathways (Harada and Berk, 1999). To investigate whether there is any interplay between L4-100K and the E1B-55K/E4orf6 complex with regard to late mRNA transport and translation; binding of these early proteins to L4-100K was investigated using different virus infections with L4-100K, E1B-55K and E4orf6 mutants. E1B-55K deleted (H5 $pm$ 4149) and E4orf6 deleted (*dl*355) viruses were used as negative controls. Immunoprecipitation assays demonstrated that L4-100K strongly interacts with E1B-55K protein during infection when both proteins are present, regardless of the inserted mutations (Fig. 17). Interestingly, no interaction could be detected between L4-100K and E4orf6 proteins, implying that L4-100K, E1B-55K and E4orf6 do not form a trimeric complex, despite the strong interaction between E1B-55K and L4-100K. The association of these two, early and late, regulatory proteins in lytic adenovirus infection is confirmed for the first time by the immunoprecipitation assays in this study. How the possible functions of this interaction and the binding regions in both proteins were explored will be discussed in the following section.

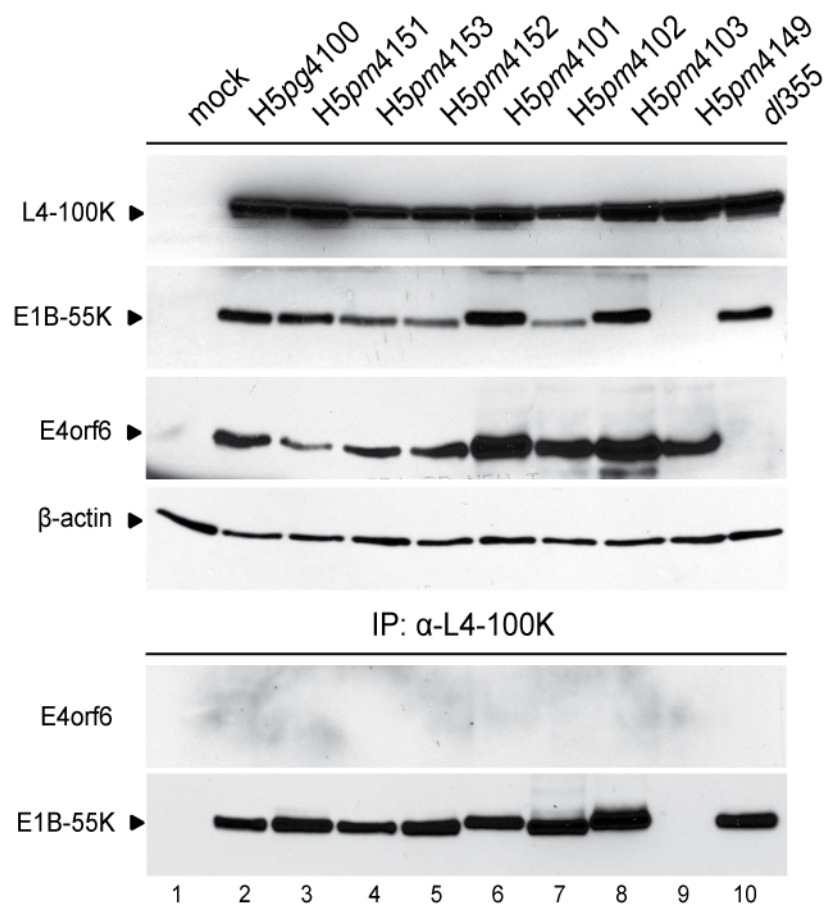


**Figure 17. Interaction of L4-100K with E1B-55K and E4orf6**

A549 cells were infected with different viruses as described in (3.2) at a multiplicity of 10 FFU per cell, and harvested at 48 h post infection (h p.i.). Total cell extracts were prepared from non-infected (mock) and infected cells. 50 µg aliquots of lysates were separated by SDS-10% PAGE and analyzed by Western blotting using L4-100K rat mab 6B10, E4orf6 mouse mab RSA3, E1B-55K mouse mab 2A6, or anti-β-actin antibody as a loading control. The same lysates were used for immunoprecipitation (IP) with 6B10. The immunocomplexes were separated by SDS-10% PAGE and analyzed by immunoblotting using RSA3, or 2A6.

### 5.3.1 Mapping the E1B-55K, Hexon and PRMT1 Binding Sites in L4-100K

A number of modified residues and protein-protein/protein-RNA interacting regions in the L4-100K sequence have been reported as summarized in Section 2.2.2 (Fig. 4C). Although a detailed analysis of the L4-100K - hexon association has been carried out, the hexon-binding domain of L4-100K remained to be identified. Therefore, to locate hexon, PRMT1 and E1B-55K binding regions in this late regulatory protein, GST



fusion constructs including full-length and different fragments of L4-100K (F1-F4) were designed as outlined in Figure 18A, and generated in *E. coli* as described in 4.6.7 (Fig. 18B). In addition, since L4-100K was reported to form dimers (Xi et al., 2005), which might be important for its functions, the dimerization site in 100K was also investigated using these constructs. H5pg4100 infected A549 cell lysates were used to provide *in vivo* trimerized hexon, E1B-55K, as well as cellular PRMT1 proteins for the GST pull-down assay. To detect L4-100K self-association and discriminate the pulled down 100K from the GST-fused protein, lysates from H1299 cells transfected with flag-tagged-100K plasmid (pTL-flag-wt-100K) were used in the pull-down assays. Despite the fact that the GST fused wt L4-100K protein appears to be unstable when expressed in bacteria (Fig. 19B, lane 6), it was also included in the experiments and successfully precipitated flag-tagged 100K, and E1B-55K (Fig. 18C). Hexon was precipitated strongly by the F2 fragment (mid-N-terminus) and to a lesser extent by F4 (C-terminus), whereas E1B-55K was efficiently pulled down by F1 (N-terminus) and F2 (mid-N-terminus) constructs (Fig. 18C). The N-terminal construct could also precipitate flag-100K, indicating that the dimerization domain is located between amino acids 1 to 220. Although not efficiently shown, PRMT1 was detected to associate with only the C-terminal fragment, which includes RGG boxes and the GAR region. These results demonstrate that the different regions or domains in L4-100K mediate different interactions or tasks of this multifunctional protein. Detailed analyses of these data will provide a basis for the overall characterization of L4-100K.

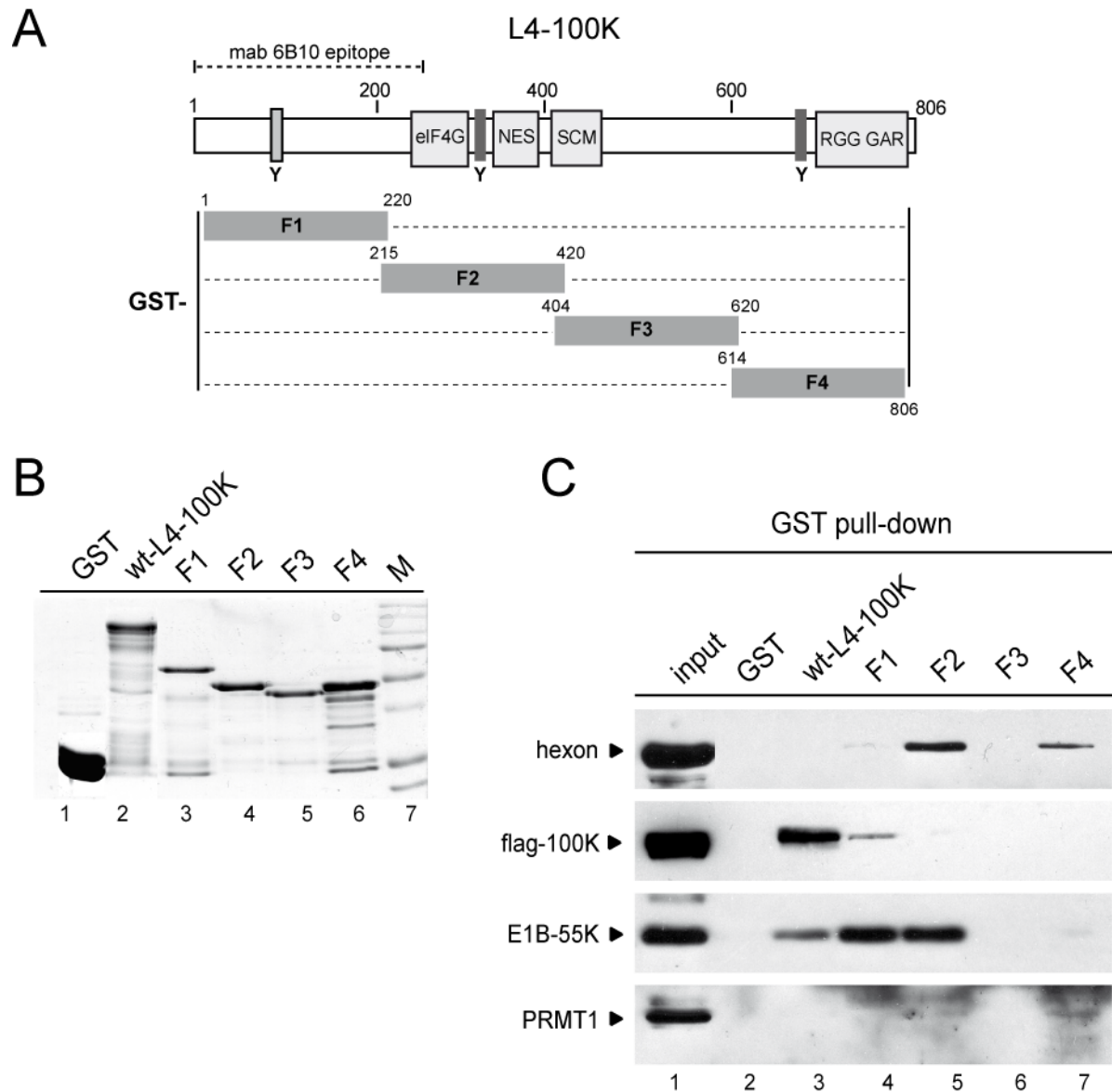


**Figure 18. Mapping hexon, E1B-55K, and PRMT1 binding regions and the dimerization site in L4-100K**

(A) Schematic diagram showing the location of Y90 (light grey), phosphorylated tyrosine residues (dark grey), nuclear export signal (NES), sumo conjugation motif (SCM), C-terminal RGG boxes and glycine-arginine-rich region (GAR) in the L4-100K protein. GST-tagged fusion fragments of L4-100K (F1-F4) are depicted below the protein map. Numbers refer to amino acid residues of Ad5-L4-100K. (B) GST and GST-100K fragments were purified from *E. coli* using glutathione-sepharose. Purified proteins were subjected to SDS-PAGE and Coomassie Brilliant Blue staining. M: molecular weight marker. (C) H5pg4100 infected A549 or pTL-flag-100K transfected H1299 cell lysates were incubated with GST or GST-fusion fragments. Aliquots of 25  $\mu$ g from the cell lysates were used as the input. GST-protein complexes were isolated with glutathione-sepharose and subjected to SDS-PAGE and Western blotting with anti-hexon antibody, anti-flag antibody, E1B-55K mouse mab 2A6, L4-100K rat mab 6B10, and anti-PRMT1 antibody.

### 5.3.2 Mapping the L4-100K Interacting Region in E1B-55K

During lytic adenovirus infection, five different gene products are produced by alternative splicing from the E1B transcription unit of Ad5. These proteins are E1B-19K (E1B-176R), the major protein E1B-55K (E1B-496R), and three smaller forms containing the same 79-residue N-terminus: E1B-156R, E1B-93R and E1B-84R (Anderson et al., 1984; Virtanen and Pettersson, 1985). Lytic functions and transformation potentials of these E1B proteins have been widely studied in our group, and several GST-fused E1B fragments have been constructed as summarized in Figure 19A. To better understand the E1B-55K and L4-100K interaction, and map the 100K binding site in this early protein, these GST-E1B constructs were used in GST pull-down assays. GST-E1B fusion proteins as well as the GST-wt-L4-100K construct generated in this study were expressed in and purified from *E. coli* as described in 4.6.7 (Fig. 19B). H5pg4100 infected A549 cell lysates were incubated with these purified proteins, and the resulting interactions were analyzed by SDS-PAGE and Western blotting.

As can be seen in Figure 19C, L4-100K was precipitated by the C-terminal (C), and to a lesser extent by the N-terminal (N) E1B fragment. Binding was detectably enhanced when both regions (N/C) were present as in the E1B-156R construct. No binding of L4-100K was observed to the middle fragment (E1B-m) or to GST alone, confirming the specificity of the detected interactions. These data indicate that L4-100K mainly interacts with the transcriptional repression domain of E1B-55K, but also less efficiently with the 79 residue N-terminal part of this protein. Most probably, during infection L4-100K also associates with E1B-N/C. In light of previous reports, this interaction was considered to play a role in virus-specific translation and host shut-off mechanisms. Thus the possible function of this association was investigated in this context and is presented in the next section.

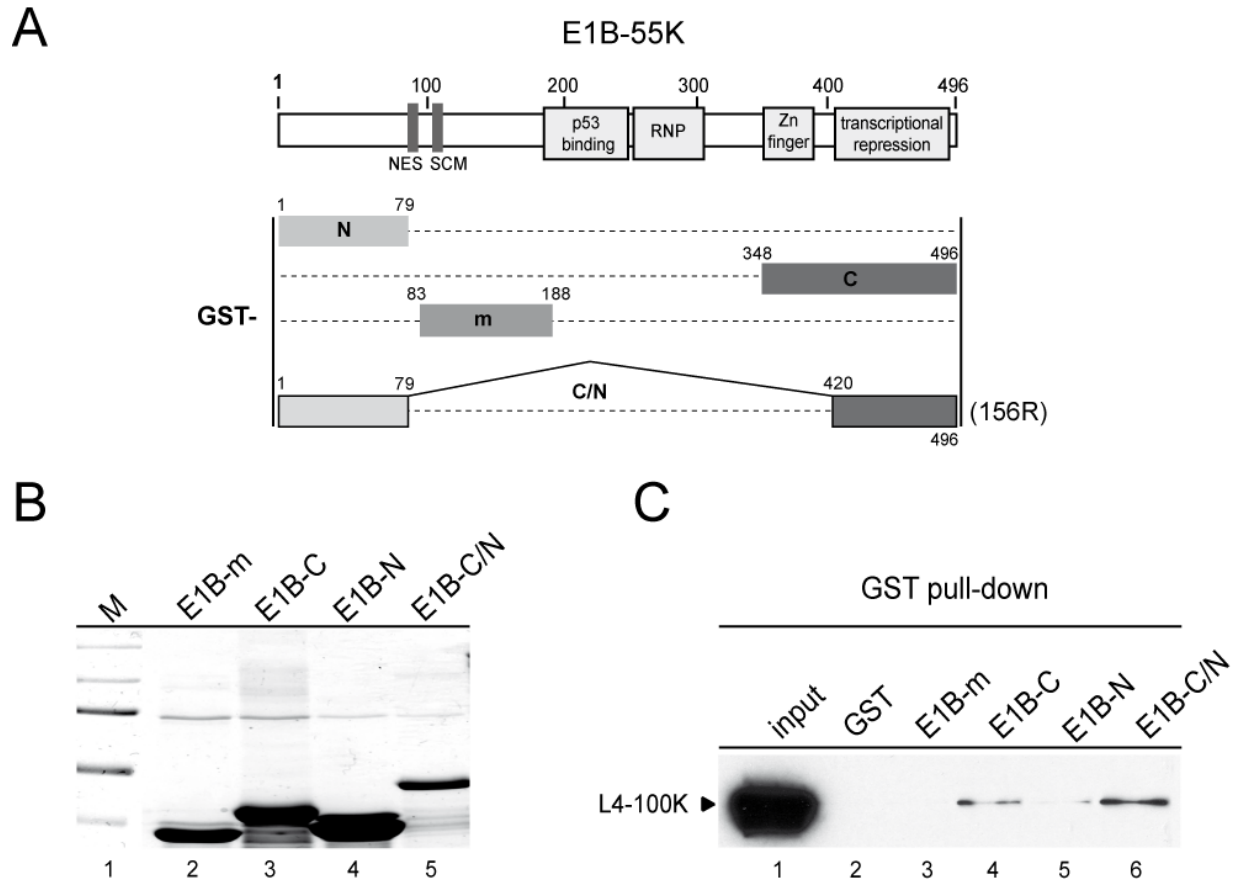


**Figure 19. Mapping the L4-100K binding region in E1B-55K protein**

(A) Schematic diagram showing the location of the nuclear export signal (NES), sumo conjugation motif (SCM), p53-binding region, and transcriptional repression domain in E1B-55K protein. GST-tagged fusion fragments of E1B-55K are depicted below the linear map. Numbers refer to amino acid residues of Ad5-E1B-55K. N: N-terminus, C: C-terminus, m: middle. C/N fragment corresponds to the E1B-156R sequence. (B) GST-E1B-fragments and wt-GST-L4-100K protein were purified from *E. coli* using glutathione-sepharose. Purified proteins were subjected to SDS-PAGE and Coomassie Brilliant Blue staining. M: molecular weight marker. (C) H5pg4100 infected A549 cell lysates were incubated with GST or GST-fusion fragments. An aliquot of 25  $\mu$ g from the cell lysate was used as the input. GST-protein complexes were isolated with glutathione sepharose and subjected to SDS-PAGE and Western blotting with L4-100K rat mab 6B10.

### 5.3.3 E1B-55K may Mediate the Association of L4-100K with eIF4G

L4-100K was shown to promote ribosome shunting on TL (what is TL?) containing late viral transcripts while inhibiting host cell translation by interacting with the scaffolding element (eIF4G) of the eukaryotic translation initiation complex, eIF4F (Cuesta et al., 2000; Xi et al., 2004; Zhang and Schneider, 1993). This association competitively inhibits phosphorylation of the cap-binding element (eIF4E) of the complex (Cuesta et al., 2004; Zhang et al., 1994). L4-100K was shown to bind eIF4G efficiently (Cuesta et al., 2000), and the binding site was located between amino acids 280 to 345 in L4-100K (Cuesta et al., 2004). Interestingly, in most of these experiments the authors used 293 or 293T cells, which stably express E1B proteins, to investigate this interaction. Surprisingly, in an E1B-55K mutant virus (*dl338*) infection (Zhang et al., 1994) dephosphorylation of eIF4E was observed to be inefficient. Since the results of this present study confirm a strong association between E1B-55K and L4-100K (Figs 17-19), a possible interplay between E1B-55K, L4-100K, and eIF4G was further investigated. HEK-293 (E1B-55K+) and H1299 (E1B-55K-) cells were used to explore the interaction of plasmid or virus encoded 100K proteins with eIF4G, as well as the binding of E1B-55K to the translation factor. Immunoprecipitation experiments showed that E1B-55K strongly associates with eIF4G in HEK-293 cells regardless of the presence of L4-100K or any other viral protein (Fig. 20, lanes 1 and 2). On the other hand, binding of plasmid encoded 100K to eIF4G could not be detected in H1299 cells. However, this interaction was successfully shown in either H1299 cells infected with wt virus H5pg4100 (Fig. 20, lane 6), or HEK-293 cells transfected with p100K plasmid (Fig. 20, lane 2). Under these conditions, E1B-55K was also efficiently precipitated by eIF4G. Taken together, L4-100K was observed to strongly interact with eIF4G when the early protein E1B-55K is present. Moreover, this is the first time that the interaction of eIF4G with E1B-55K, either in an infection environment or not, has been shown, suggesting at least an enhancing role for this early regulatory protein in L4-100K - eIF4G association.

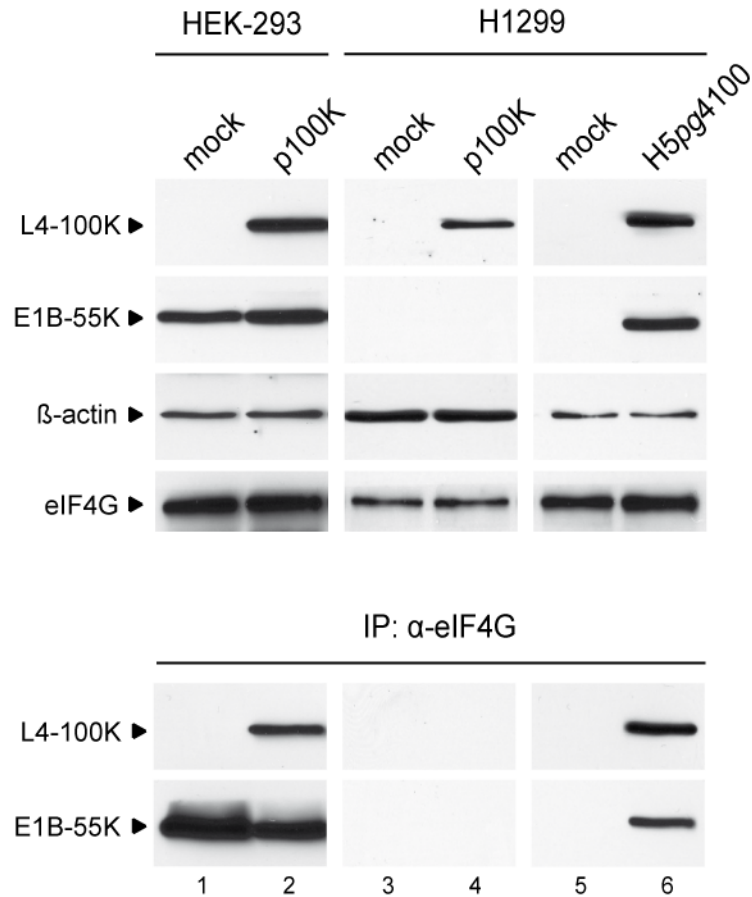


**Figure 20. Interaction of L4-100K with eIF4G in the presence or absence of E1B-55K**

HEK-293 cells were either mock transfected or transfected with pTL-flag-wt-L4-100K plasmid (p100K). H1299 cells were either transfected with p100K or infected with H5pg4100 at a multiplicity of 10 FFU per cell. These cells were harvested at 48 h post infection or transfection. Total cell extracts were prepared from mock, transfected, and infected cells, 50  $\mu$ g aliquots of lysates were separated by SDS-10% PAGE and analyzed by Western blotting using L4-100K rat mab 6B10, E1B-55K mouse mab 2A6, anti- $\beta$ -actin (as loading control), or anti-eIF4G antibody. The same lysates were used for immunoprecipitation (IP) with anti-eIF4G antibody. The immunocomplexes were separated by SDS-10% PAGE and analyzed by immunoblotting using 6B10 or 2A6.

#### 5.3.4 E1B-Associated-Protein 5 (AP5) Relocalizes to the Replication Centers During Adenovirus Infection

E1B-AP5 was first identified as an E1B-55K associated protein (AP), and found to be a novel member of the heterogeneous nuclear ribonucleoprotein family (hnRNP) (Gabler et al., 1998). These nuclear RNA binding proteins play several distinct roles in RNA biogenesis (Kzhyshkowska et al., 2000; Kzhyshkowska et al., 2001). Since overexpression of E1B-AP5 in adenovirus infected cells was found to contribute to

restoring host cell mRNA transport activity blocked by the viral ubiquitin ligase complex, this protein was suggested to play a role in adenoviral mRNA transport and host shut-off mechanisms (Gabler et al., 1998). To understand whether the interaction of E1B-55K and L4-100K contributes to adenoviral late mRNA transport through utilizing an hnRNP such as E1B-AP5, the possible interaction of these three proteins was investigated during infection. Interestingly, redistribution of E1B-AP5, which is normally diffusely distributed in the nucleus, was observed during adenovirus infection as it formed ring-like structures around the periphery of replication centers (Fig. 21). However, neither efficient co-localization of E1B-AP5 with E1B-55K nor with L4-100K could be observed in these cells. As already shown in Figure 11A, only a small portion of E1B-55K was found to locate at these replication bodies, indicating that the association of E1B-55K with these structures is highly dynamic. Being a dominant cytoplasmic protein, L4-100K could neither be detected to co-localize with E1B-55K or E1B-AP5 at the replication centers. Interestingly, immunoprecipitation assays demonstrated that L4-100K can successfully precipitate E1B-AP5 protein during adenovirus infection, but only in the presence of E1B-55K. In E1B-55K deleted virus *dl1520* infection, this binding was eliminated (Fig. 21B), indicating that the interaction of L4-100K and E1B-AP5 is indirect, probably occurring via E1B-55K, but may have a function in late viral mRNA transport and *host-shut-off*.

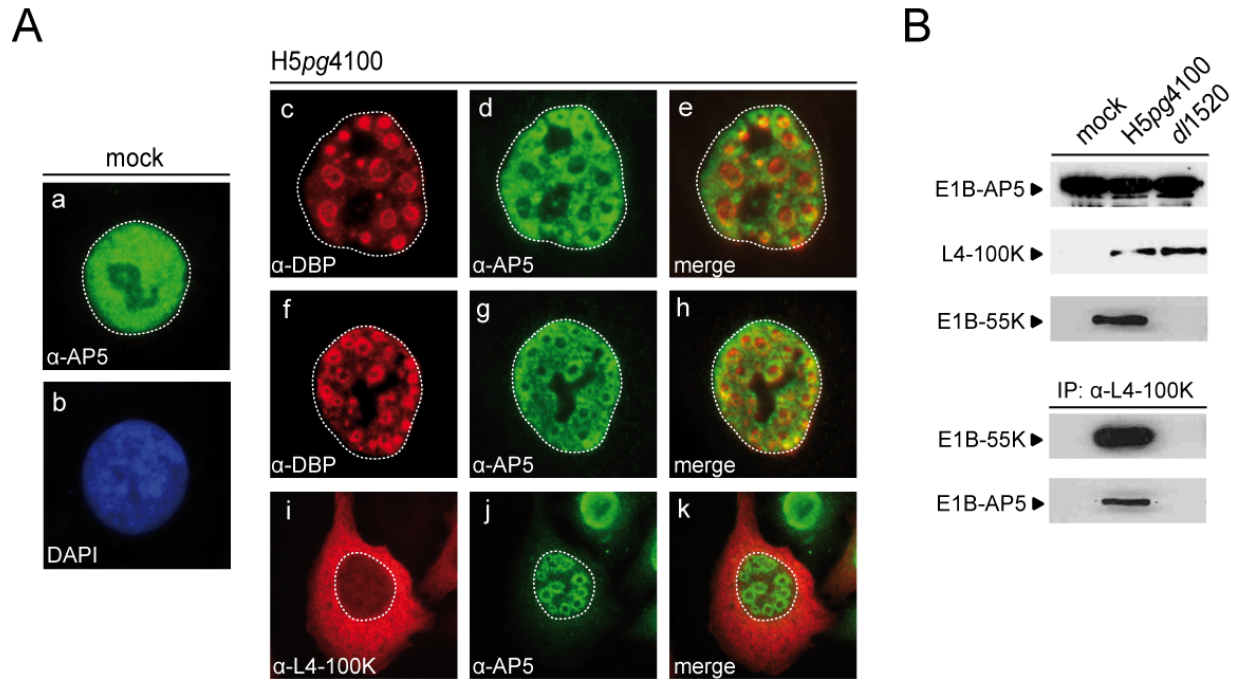


**Figure 21. Redistribution and L4-100K interaction of E1B-AP5 during adenovirus infection**

(A) A549 cells were seeded on glass cover slips and either not infected (mock), or infected with H5pg4100 at 10 FFU/cell when confluency reached 60-80%. These cells were fixed with methanol 24 h post infection, and incubated with either E1B-AP5 rat mab 6C5, and DBP mouse mab B6-8 (a-h), or E1B-AP5 rat mab 6C5 and L4-100K rat mab 6B10 (i-k). Merged images can be seen in panels e, h, and k. Signals were detected using FITC-coupled anti-mouse and Texas red-coupled anti-rat antibody. Nuclei were represented within dotted lines based on DAPI staining. (B) A549 cells were infected with H5pg4100 and dl1520 viruses at a multiplicity of 10 FFU per cell, and harvested 48 h post infection. Total cell extracts were prepared from non-infected (mock) and infected cells. 50  $\mu$ g aliquots of lysates were separated by SDS-10% PAGE and analyzed by Western blotting using L4-100K rat mab 6B10, rabbit anti-E1B-AP5 antiserum, or E1B-55K mouse mab 2A6. The same lysates were used for immunoprecipitation (IP) with 6B10. The immunocomplexes were separated by SDS-10% PAGE and analyzed by immunoblotting using 6C5, or 2A6.

## 5.4 Analysis of the Sumo Conjugation and Sulfation Motifs in L4-100K

### 5.4.1 Is L4-100K Sumoylated During Lytic Adenovirus Infection?

The covalent attachment of the small ubiquitin-like modifier (Sumo) to a lysine residue of a substrate protein has emerged as a multi-faceted posttranslational modification affecting several aspects of a protein, including stability, subcellular



distribution, or protein-protein interactions. Sumoylation is a multi-step process requiring a number of enzymes as well as a consensus sumo conjugation motif (SCM) in the substrate molecule, as reviewed in (Melchior, 2000). Since a similar SCM was also found in L4-100K amino acid sequences highly conserved among different serotypes (Fig. 21A), it was hypothesized that this protein is modified by sumoylation.

To reveal whether 100K is modified by sumo-1, A549 cells were infected with a panel of viruses including L4-100K, E1B-55K and E4orf6 mutants (Fig. 22C). The E1B-55K-NES mutant (H5pm4101) and E4orf6 deleted virus (*dl355*) were used as positive controls since these mutant viruses exhibit highly elevated levels of sumoylated E1B-55K (Kindsmüller, 2002). First, immunocomplexes from an immunoprecipitation (IP) assay using L4-100K rat mab 6B10 were analyzed for sumo conjugation by Western blotting with a mouse mab against sumo-1. Surprisingly, immunoblotting revealed a protein band at 100 kDa that was detected in all virus mutants except H5pm4152 (Fig. 22C). However, the size of the observed protein band precluded it as a sumoylated L4-100K form, because in general, covalent sumo attachment to a protein results in a 20 (Palacios et al., 2005) to 40 (Zhao et al., 2004) kDa increase in the protein's molecular weight. For instance, the sumoylated form of E1B-55K runs a little above the 75 kDa marker band meaning more than a 20 kDa increase in its molecular weight (Endter et al., 2001; Kindsmüller et al., 2007). To verify the identity of this protein band, the IP reaction was performed the other way around, using the anti-sumo-1 antibody to precipitate all conjugated proteins, and L4-100K and E1B-55K specific antibodies as immunoblotting probes. Consistent with the previous IP, L4-100K protein was detected on the immunoblot at 100 kDa in all examined viruses except H5pm4152. Interestingly, in both IP reactions H5pm4153 infection showed an increase in the precipitated protein amount compared to the wt virus, indicating enhanced sumo-1 association. When the same membrane was probed with an anti-E1B-55K mouse mab, sumoylated E1B-55K bands were efficiently detected above 75 kDa from the lysates of H5pm4101 and *dl355* infected cells, as indicated by arrow heads (Fig. 22B, bottom panel). In accordance with previous reports (Endter et al., 2001;

## RESULTS

Kindsmuller et al., 2007), only a minor proportion of wt-E1B-55K was observed as conjugated to sumo-1, whereas no sumoylated E1B-55K could be detected in E1B-SCM (H5pm4102) and E1B-SCM/NES (H5pm4103) virus infections.

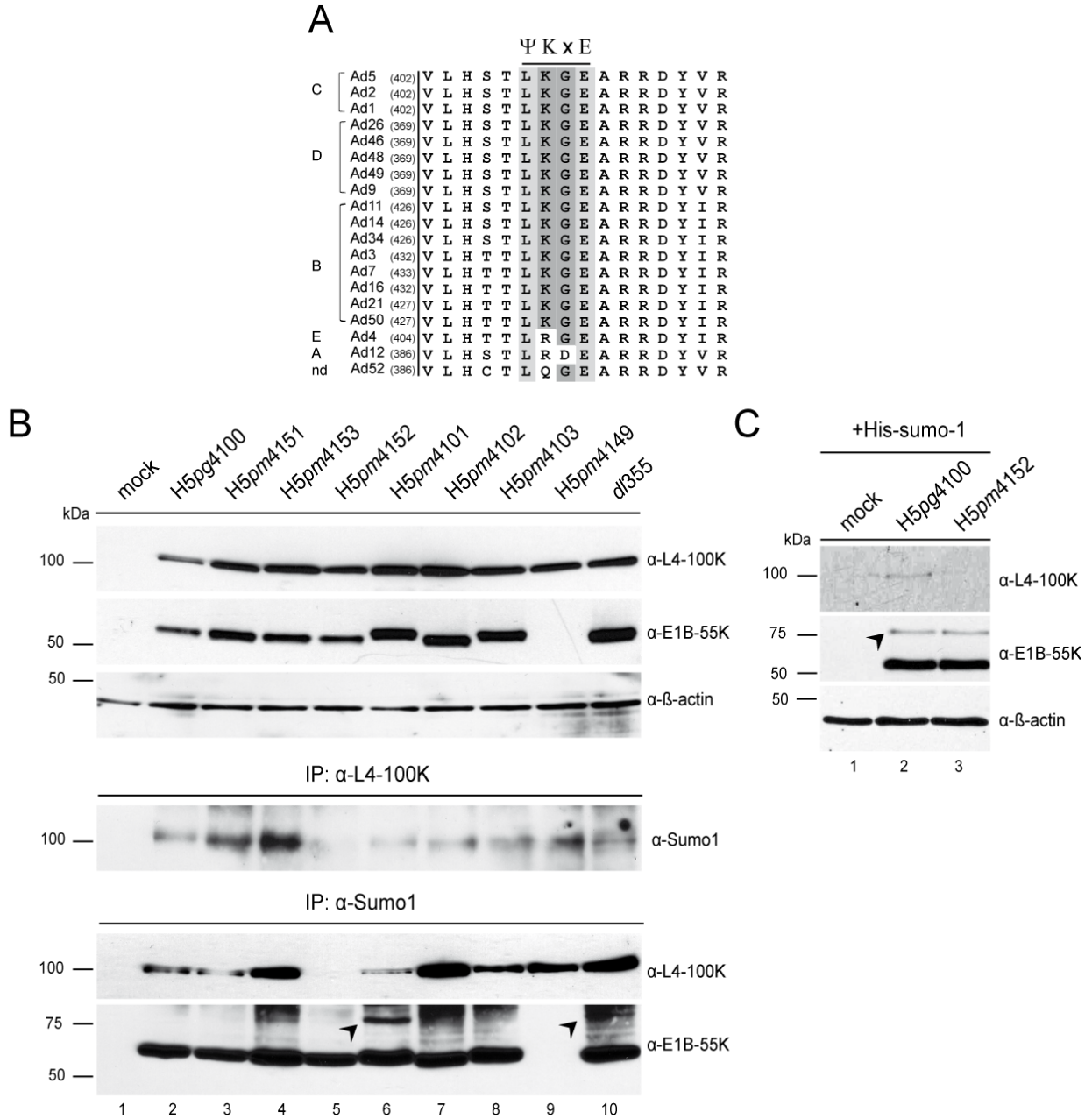


**Figure 22. Putative sumo conjugation motif and its inactivation in L4-100K**

(A) Multiple amino acid sequence alignment of L4-100K polypeptides from different human Ad serotypes classified in 6 subgroups (A-F, nd: not determined). Numbers in brackets refer to amino acid residues. Highly conserved, putative sumoylation motifs in L4-100K sequence are marked. Residues that are identical in all serotypes are shown in light grey boxes and the conserved residues are marked with dark grey boxes. The consensus sumo conjugation motif (SCM) is shown above the sequences. (B) A549 cells were infected with different viruses at a multiplicity of 10 FFU per cell. These cells were

harvested 48 h post infection. Total cell extracts were prepared from mock, transfected, and infected cells, 50 µg aliquots of lysates were separated by SDS-10% PAGE and analyzed by Western blotting using L4-100K rat mab 6B10, and E1B-55K mouse mab 2A6. The same lysates were used for immunoprecipitation (IP) with either L4-100K rat mab 6B10, or anti-sumo mouse mab. The immunocomplexes were separated by SDS-10% PAGE and analyzed by immunoblotting using anti-sumo mouse mab, 6B10 or 2A6. (C) H1299 cells were transfected with pHis-sumo-1 plasmid and 6 h after transfection, infected with H5pg4100 or H5pm4152 at 10 FFU/cell. 30 h p.i., cells were harvested and histidine purification was performed. Purified proteins were separated by SDS-10% PAGE and analyzed by Western blotting using L4-100K rat mab 6B10, and E1B-55K mouse mab 2A6. 10 µl aliquots of lysates were also separated by SDS-10% PAGE and analyzed by Western blotting using anti-β-actin antibody as a loading control. The arrow head indicates the sumoylated E1B-55K bands.

Since the enigma about the size of the putative sumoylated-100K band remained unsolved, another procedure was carried out using a His-tagged-sumo-1 construct to purify sumo-conjugated proteins by histidine purification. For this purpose, H1299 cells were transfected with His-sumo-1 coding plasmid constructs, and concomitantly infected with H5pg4100 and H5pm4152 viruses at 10 FFU/cell. 30 hours post infection, cells were harvested and proteins pulled down by histidine purification. Here, a weak band was only detected from the wt virus infected cell lysate, which was also observed to run at 100 kDa (Fig. 22C, lane 2). When the membrane was analyzed for E1B-55K, expected sumoylated forms were seen above 75 kDa in low quantities from both virus infections. Altogether, these experiments show that L4-100K specifically associates with sumo-1, and substitution of the target lysine with arginine (K408R) abrogates this interaction. However, the unexpected nature of the covalent bonding between 100K and sumo-1 (regarding the size of the complex) requires further exploration. In virus infections, inactivation of the lysine residue in this conserved SCM (K408R) affected neither the stability nor subcellular localization of L4-100K protein (1.2.1), indicating that the tumor cell lines studied compensate for the lack of such a modification in L4-100K.

### 5.4.2 L4-100K is not Sulfated in Lytic Adenovirus Infection

Another putative posttranslational modification site in L4-100K is the ninetieth tyrosine residue, which is highly conserved among different adenovirus serotypes,

and was speculated to be sulfated due to the high similarity of the surrounding residues to the consensus sulfation motif (Fig. 23A). This was compared using “sulfinator” software developed by the SwissProt group at the Swiss Institute of Bioinformatics (Monigatti et al., 2002). Hence, to determine whether L4-100K undergoes a tyrosine sulfation modification during adenovirus infection, and to ascertain the role of this tyrosine on L4-100K functions, this highly conserved tyrosine residue was substituted by an alanine (Y90A), and H5 $pm4153$  mutant was successfully generated using K16 cells (5.1).

Subsequent characterization experiments revealed that the exchange of this residue results in a severe defect in the late phase of infection (5.2.3). Moreover, the L4-100K protein of this mutant virus was observed to form distinct punctuated or filamentous structures in the cytoplasm of 5-20% of all infected cells when analyzed by immunofluorescence microscopy (Fig. 23B, panels a and b, Fig. 11A/B, panel c). However, when H1299 cells were transfected with a pTL-flag-Y90A-100K construct such structures could not be observed (Fig. 23B, panels c and d). Therefore, the possible sulfation of L4-100K during infection was explored in H5 $pg4100$  and H5 $pm4153$  infected A549 cells using [ $^{35}\text{S}$ ]sulfate to track incorporation. As a control, sodium chlorate, which inhibits all tyrosine sulfation reactions, was included in one sample. As shown in Figure 23C, total sulfated proteins from infected and non-infected cells were efficiently detected on the gel unless the inhibitor was included. Since none of these protein bands corresponded to 100 kDa, specific L4-100K bands were identified by direct IP with anti-L4-100K antibody and radiolabeled lysates. This reaction still revealed no sulfated L4-100K band. As a result, we concluded that L4-100K is a non-sulfated protein, and considered the 89-DYLD-92 motif to be an important site of unknown nature.

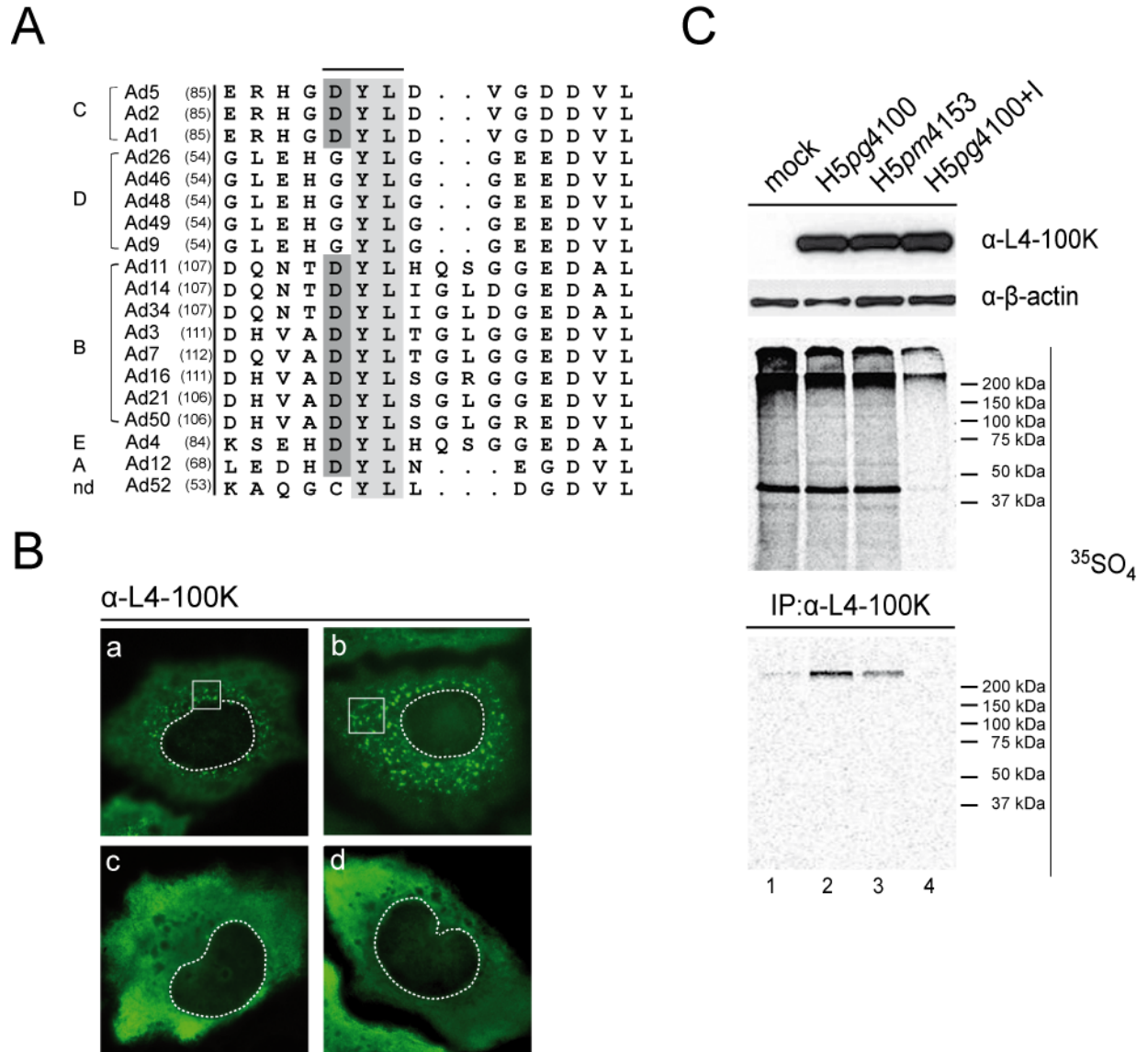


**Figure 23. Putative sulfation motif and its inactivation in L4-100K**

(A) Multiple amino acid sequence alignment of L4-100K polypeptides from different human Ad serotypes classified into 6 subgroups (A-F, nd: not determined). Numbers in brackets refer to amino acid residues. The highly conserved, putative sulfation motif in L4-100K sequences is marked. Residues that are identical in all serotypes are shown in light grey boxes and the conserved residues are marked with dark grey boxes. (B) The tyrosine residue in the motif was substituted by an alanine (Y90A) in H5pm4153, and in pTL-flag-Y90A-100K. H1299 cells were either infected with H5pm4153 (a and b), or transfected with pTL-flag-Y90A-100K (c and d). These cells were fixed with methanol 30 h post infection/transfection, and incubated with L4-100K rat mab 6B10. Signals were detected using FITC-coupled anti-rat antibody. Nuclei are represented within dotted lines based on DAPI staining. (C) A549 cells were either not infected (mock), or infected with H5pg4100 or H5pm4153 at a multiplicity of 100 FFU per cell. Medium of these cells was exchanged with sulfate-free medium 24 h p.i., and the cells were further incubated for 3 h in the presence of 0.5 mCi  $^{35}\text{SO}_4^{2-}$ . In one of the dishes infected with H5pg4100, 10 mM sodium chlorate was added to inhibit sulfation reactions (H5pg4100+I). Total cell extracts were prepared from the samples, 50  $\mu\text{g}$  aliquots of lysates were separated by SDS-10% PAGE and either analyzed by Western blotting using L4-100K rat mab 6B10, and anti- $\beta$ -actin antibody, or by Phosphor-Screen. The same lysates were used for immunoprecipitation (IP) with L4-100K rat mab 6B10. The immunocomplexes were separated by SDS-10% PAGE and analyzed by Phosphor-Screen.

## **5.5 Arginine Methylation of Human Adenovirus Type 5 L4-100K Protein is Required for Efficient Virus Production**

### **5.5.1 Construction of C-terminal L4-100K Mutant Viruses**

Since the cell type-dependent arginine methylation of L4-100K protein during adenovirus infection was identified by our group (Kzhyshkowska et al., 2004), identification of the methylated arginine residues and elucidation of the functional contribution of such a modification to L4-100K functions were included in the aims of this study. Mutant virus H5 $\mu$ m4151, which carries amino acid substitutions in a putative methylation motif (RGG boxes), was generated and propagated as described in 5.2 (Fig. 7). The amino acid exchanges introduced into the RGG boxes of the Ad5 100K polypeptide are summarized in Figure 24B.

Using the same approach, we tried to generate an L4-100K mutant virus carrying arginine to glycine substitutions in the glycine-arginine-rich (GAR) region and a double mutant containing identical amino acid exchanges in both the RGG boxes and the GAR region (Fig. 24B NA, and Fig. 28A). Interestingly, neither mutant virus could be reproducibly grown on K16 cells after transfecting the viral DNA. The reason for these results is unclear but may be due to severe defects in the late functions of L4-100K that K16 cells, which typically express low levels of wt L4-100K protein (Hodges et al., 2001), are unable to complement.

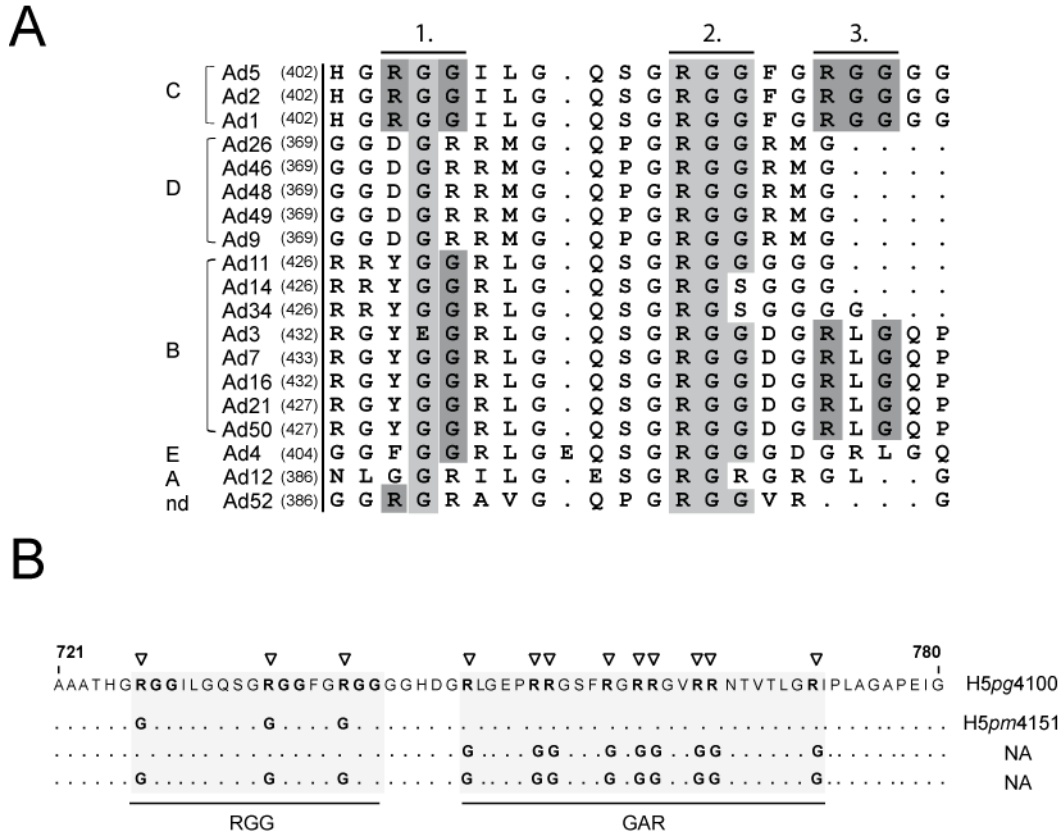


**Figure 24. RGG-boxes of L4-100K and their mutagenesis**

(A) Multiple amino acid sequence alignment of L4-100K polypeptides from different human Ad serotypes classified into 6 subgroups (A-F, nd: not determined). Numbers in brackets refer to amino acid residues. The first, second, and third RGG boxes are marked. Residues that are identical in all serotypes are shown in light grey boxes and the conserved residues are marked with dark grey boxes. (B) The positions of the amino acid changes within the L4-100K mutants are marked by triangles. Numbers refer to amino acid residues in the wt L4-100K protein from H5pg4100. NA: not applicable.

### 5.5.2 Amino Acid Substitutions in the RGG Boxes Reduce Arginine Methylation of L4-100K During Infection

To test whether H5pm4151 produces a stable protein, the steady-state concentration of L4-100K was determined by immunoblot analysis using total-cell lysates from infected A549 cells, as already shown in Section 5.2.1. In parallel, the effect of amino acid exchanges on L4-100K arginine methylation in the absence or presence of the methylation inhibitor AdOx was assessed. Representative samples of these analyses are shown in Figure 25. In the absence of AdOx, H5pm4151 accumulated L4-100K protein to levels comparable to wt H5pg4100 in the course of the infection (Fig. 25A).

A similar result was obtained in the presence of the arginine methylation inhibitor, although expression of the viral protein was delayed under such conditions (Fig. 25A). This delay in viral protein production was also seen when extracts were analyzed for the expression of E2A-72K (DBP), an early Ad protein necessary for viral DNA replication. This confirms that arginine methylation is a critical cellular function required for efficient viral early and late gene expression, as previously observed (Iacovides et al., 2007; Kzhyshkowska et al., 2004). Next, total cell lysates were subjected to immunoprecipitation using polyclonal antibody Asym-24, which reacts with asymmetrically dimethylated arginines (Fig. 25B). Wt and mutant L4-100K proteins were then detected by immunoblotting (Fig. 25A) using the anti-L4-100K mab 6B10. In line with previous work done in our group (Kzhyshkowska et al., 2004) and a recent report (Iacovides et al., 2007), a substantial amount of L4-100K present in wt-infected cells was found to be methylated on arginine residues (Fig. 25A, lanes 3 and 4). In contrast, no L4-100K was detected in the immunoprecipitates from wt-infected cell extracts in the presence of AdOx (Fig. 25A, lanes 9-11), verifying the specificity of the polyclonal antibody Asym-24. Also as anticipated, the amount of methylated L4-100K protein was greatly decreased in H5pm4151-infected cells (Fig. 25A, lanes 5-7), demonstrating that the amino acid substitutions in the RGG boxes substantially reduce, but do not fully eliminate L4-100K arginine methylation. Consistent with this, no methylated form of the mutant protein was immunoprecipitated with Asym-24 in the presence of AdOx (Fig. 25A, lanes 12-14). This result is further supported by the observation that the amino acid exchanges in the RGG boxes greatly reduce binding of this Ad5 protein to cellular PRMT1 (Fig. 25C), which binds its targets through arginine residues clustered within in the context of RGG boxes or GAR regions (Boisvert et al., 2005c; Ostareck-Lederer et al., 2006). Taken together, these data show that Ad5 L4-100K is methylated by PRMT1 at arginine residues mainly in the RGG boxes and hint at a possible partial methylation in the adjacent GAR region.



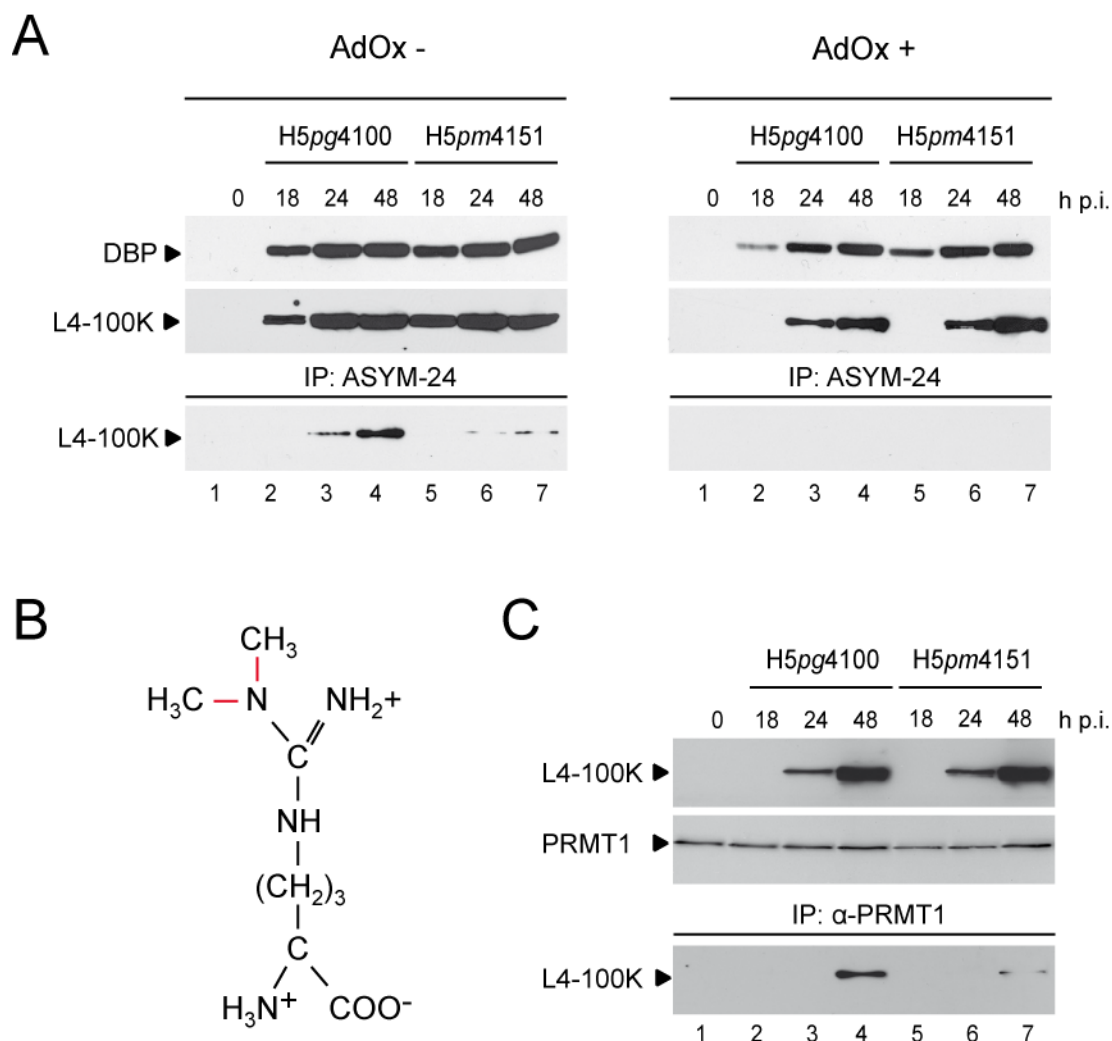


**Figure 25. Protein steady-state levels and 100K methylation in A549 cells infected with H5pg4100 and H5pm4151 viruses**

(A) Cells were infected in the absence (AdOx-) or presence of AdOx (AdOx+) and harvested at the indicated time points after infection (h p.i.). Total cell extracts were prepared from non-infected (0) and infected cells. Twenty-five  $\mu$ g aliquots of lysates were separated by SDS-10% PAGE and analyzed by immunoblotting using L4-100K rat mab 6B10, or B6-8 mouse mab recognizing the E2A-72K (DBP) protein. The same lysates were used for immunoprecipitation (IP) with mab Asym-24 detecting asymmetrically dimethylated arginine residues (depicted in B).. (C) Binding of PRMT1 to L4-100K in infected cells. Whole lysates were prepared as described and used for immunoblotting with mab 6B10 (upper panel) and anti-PRMT1 antibody. The same lysates were used for IP with anti-PRMT1 mab.

### 5.5.3 Arginine Methylation of RGG Motifs in L4-100K is Required for Maximal Virus Growth

To evaluate the contribution of arginine methylation in the RGG boxes of L4-100K to overall virus growth properties, total virus yields were determined in infected A549

cells and primary human hepatocytes (Fig. 26A). Arginine substitutions in L4-100K resulted in a 6- to 10-fold reduction in virus growth depending on the cell type, consistent with the general characterization data (5.2.3). This defect could not be attributed to reductions in early viral protein synthesis or Ad DNA replication, since H5 $pm$ 4151 accumulated E2A-72K (Fig. 9) and viral DNA comparable to wt H5 $pg$ 4100 (Fig. 26B). Rather, the decrease in virus production was directly related to levels of late viral proteins, since H5 $pm$ 4151 showed substantially reduced hexon, penton and particularly fiber protein expression (Fig. 26C). These data show that methylation of arginine residues in the context of RGG boxes contributes to efficient late protein production and maximal virus growth in infected A549 cells and primary human hepatocytes.

The phenotype observed with the mutant virus H5 $pm$ 4151 could be attributed to a number of possible defects in the L4-100K protein, including altered subcellular localization, RNA binding or protein-protein interactions. Therefore, RGG mutant was compared to the wt protein for nucleocytoplasmic shuttling activity and binding to TL-mRNA, eIF4G and hexon during virus infection.

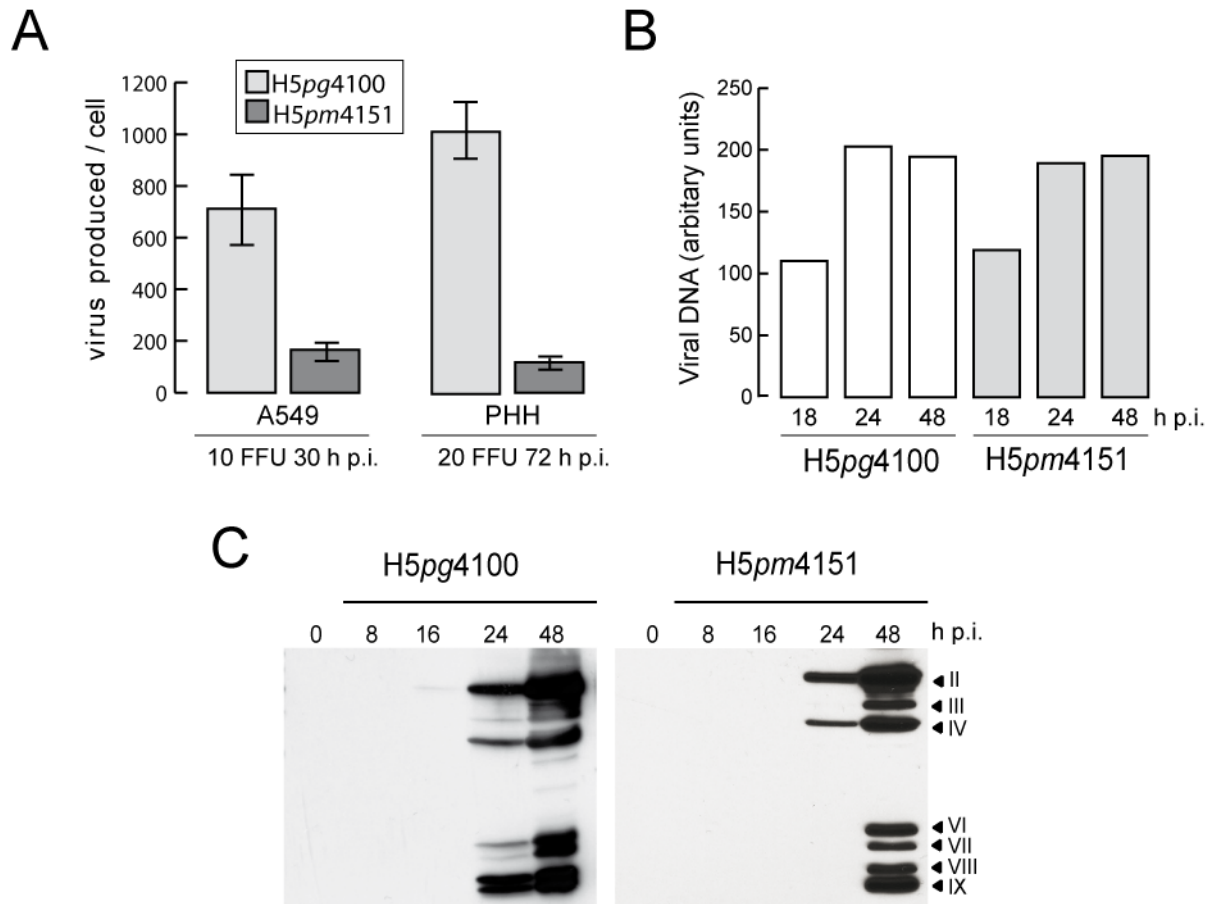


**Figure 26. Effects of amino acid substitutions in L4-100K on virus growth, viral DNA replication, and late protein synthesis**

(A) Virus yield. A549 cells and primary human hepatocytes (PHH) were infected with wt H5pg4100 or H5pm4151 at indicated multiplicities. Viral particles were harvested at indicated time points post infection (h p.i.) and virus yield was determined by quantitative E2A-72K immunofluorescence staining on K16 cells. The results represent the averages from three independent experiments. Error bars indicate the standard error of the mean. (B) Viral DNA accumulation. A549 cells were infected with H5pg4100 and H5pm4151 viruses at a multiplicity of 10 FFU per cell. Total nuclear DNA was isolated at the indicated times after infection (h p. i.) and subjected to semi-quantitative PCR. PCR products were analyzed and quantified using the ChemiDoc system and QuantityOne software (BioRad). The results shown represent the averages from two independent experiments. (C) Viral late protein synthesis. A549 cells were infected with the wt or mutant virus at a multiplicity of 10 FFU per cell. Total cell extracts were prepared at indicated times post infection (h p.i.). Proteins (40  $\mu$ g samples) were separated by SDS-10% PAGE, transferred to nitrocellulose membranes and probed with the anti-Ad5 rabbit polyclonal serum L133. Bands corresponding to viral late proteins hexon (II), penton (III), fiber (IV) and minor capsid proteins (VI, VII, VIII, IX) are indicated on the right.

#### 5.5.4 Effect of Amino Acid Substitutions in the RGG Motifs on the Subcellular Distribution of L4-100K During Infection

Previous work has shown that L4-100K actively shuttles between the nuclear and

cytoplasmic compartments in plasmid transfected cells (Cuesta et al., 2004). Nucleocytoplasmic export of 100K is mediated by a leucine-rich nuclear export signal (NES, Fig. 32) of the HIV-1 Rev-type and can be blocked by either point mutations within the 100K NES or by LMB inhibition (Fig. 28B and 34). Also, fragment deletion analysis has shown that the carboxy-terminal region of 100K (aa 727 – 807) contains a potential nuclear localization signal (NLS) (Cuesta et al., 2004) raising the possibility that nuclear import of 100K is modulated by methylation of arginine residues within the RGG boxes and/or GAR region. Consistent with this observation, a recent study showed that the substitution of arginine and the glycine residues in the third RGG box (RGG3) by alanines in a plasmid construct eliminates import of L4-100K into the nucleus (Iacovides et al., 2007). We therefore determined the subcellular distribution of the wt and mutant 100K in virus infected A549 cells (Fig. 27). In the course of infection, staining for wt L4-100K was mostly seen in the cytoplasm at earlier time points (18 h, Fig. 27A panel a) in the late phase, while most of the protein exhibited a dominant nuclear fluorescence as the infection proceeds (48 h, Fig. 27A panel c). A similar subcellular distribution was observed for the mutant protein in H5pm4151 infected cells. Comparable to the wt product, the 100K mutant was mostly cytoplasmic early after expression and accumulated in the nuclei of infected cells during the late phase (Fig. 27A, panel b and d).

To test the ability of L4-100K to enter the nucleus in a hypomethylated environment, the cells were stained in the presence of the methylation inhibitor AdOx. As before, the wt and mutant L4-100K proteins could be detected in the nuclei of infected cells (Fig. 27B, panels a-b). To further test the nuclear localization of L4-100K, we took advantage of the fact that the majority of cytoplasmic L4-100K is relocalized to the nucleus by mutational inactivation of its NES or in the presence of CRM1 inhibitor Leptomycin B (LMB). Thus, if the amino acid exchanges in the RGG boxes interfere with nuclear import, the mutant protein should not be able to accumulate in the nucleus in LMB-treated cells. As predicted, LMB treatment of H5pg4100-infected cells caused the nuclear accumulation of wt 100K, and notably also of mutant 100K in

## RESULTS

H5pm4151-infected cells (Fig. 27B, panels c and d). As a control, E1B-55K, which was previously reported as a LMB-sensitive shuttling protein (Dobbelstein et al., 1997a; Krätzer et al., 2000), was stained and examined. As can be seen in Figure 27B (panels e and f), this early adenoviral regulatory protein accumulated in the nucleus in dot-like structures upon LMB treatment. Otherwise it was observed as a dominant cytoplasmic protein, so confirming the effect of LMB. Consistent with the immunofluorescence microscopy data, nucleocytoplasmic fractionation of H5pg4100- and H5pm4151-infected cells showed that 100K proteins can be detected in similar amounts from both cytoplasmic and nuclear fractions regardless of the methylation status of the RGG boxes (Fig. 27C).

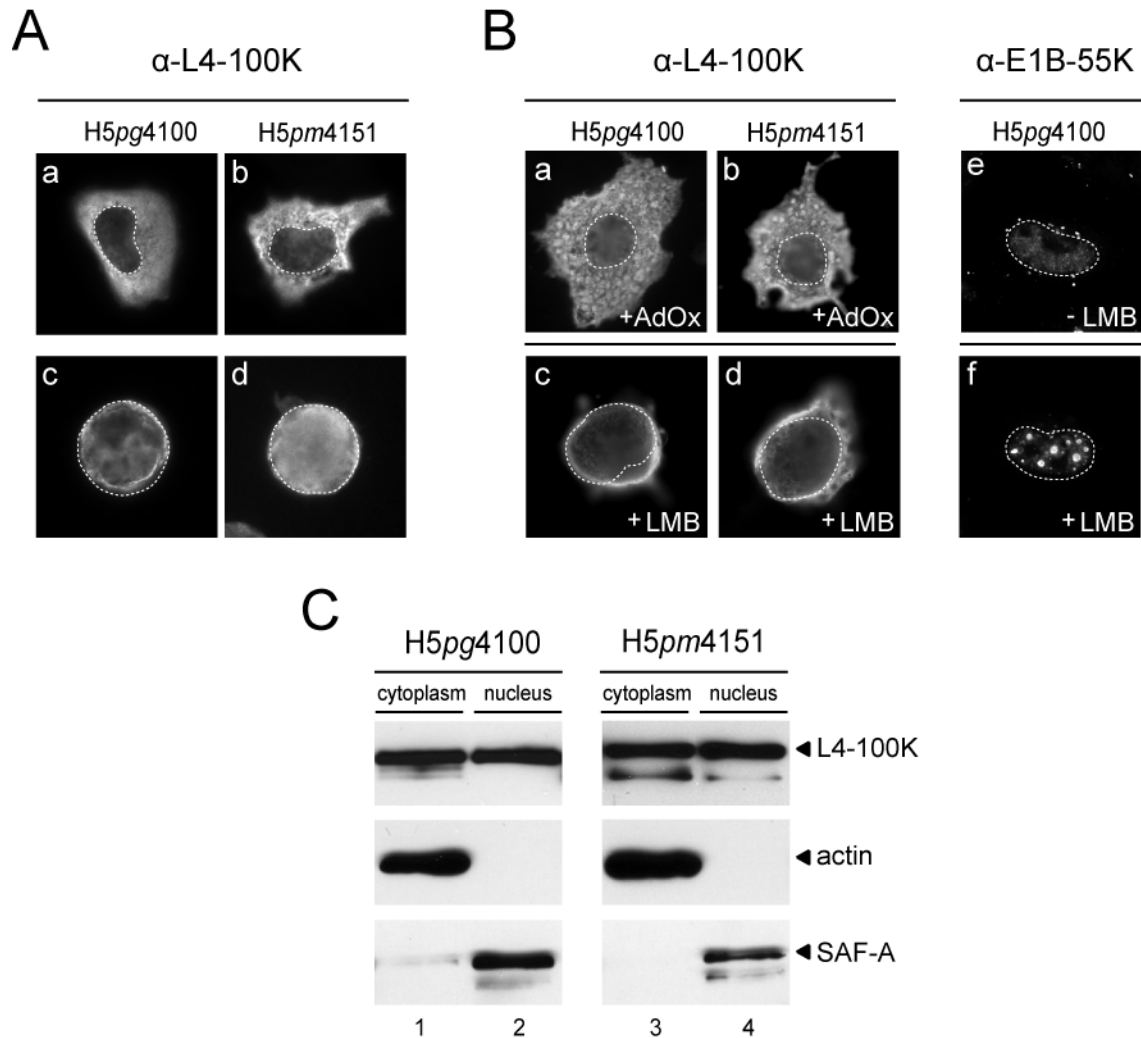


**Figure 27. Subcellular localization of wt and mutant L4-100K during productive infection**

## RESULTS

---

A549 cells were infected with H5pg4100 and H5pm4151 viruses at a multiplicity of 10 FFU per cell. (A) Infected cells were fixed 18 h (panels a and b) and 48 h (panels c and d) after infection and stained with mab 6B10. (B) At 36 h post infection cells were fixed and the subcellular localization of L4-100K was examined by immunofluorescence using mab 6B10. Methylation inhibitor AdOx (100  $\mu$ M) was added 18 h p.i. to the infection medium (panels a and b). Infected cells were kept in the presence of LMB (20 nM) for 3 h before fixation (panels c and d). As a control, cells were stained with mab 2A6 to detect E1B-55K localization in the absence (panel e) or presence of LMB (panel f). In all panels nuclei are indicated by a dotted line. (C) At 36 h post infection cells were collected and fractionated as described. 5  $\mu$ g aliquots of cytoplasmic and 2  $\mu$ g aliquots of nuclear lysates were separated by SDS-10% PAGE and analyzed by Western blotting using L4-100K rat mab 6B10. Anti-actin and anti-SAF-A antibodies were used as cytoplasmic and nuclear markers, respectively.

To further access the role of arginine methylation in 100K nuclear localization, we introduced mutations into plasmid pTL-flag-100K (Fig. 28A) containing flag-tagged, wt 100K cDNA including the tripartite leader (TL). As in the 100K virus mutant H5pm4151, arginine to glycine substitutions were introduced into the RGG boxes. In addition, the leucine residues in the 100K NES were changed to alanines, and the arginines in the RGG3 box, the GAR and RGG plus GAR regions were converted to glycines. H1299 cells were transfected and steady-state localization of wt and mutant proteins was determined by indirect immunofluorescence in the absence or presence of LMB (Fig. 28B). Consistent with a previous report (Cuesta et al., 2004), mutational inactivation of NES resulted in predominant nuclear staining of 100K in the absence or presence of LMB (Fig. 28B panels b and h). Moreover, wt 100K was observed to relocalize from the cytoplasm to the nucleus upon LMB treatment (Fig. 28B panels a and g). An identical result was obtained when cells producing the RGG and RGG3 mutants were treated with LMB (Fig. 28B, panels c, d and i, j). Interestingly, however, no substantial increase in the nuclear fluorescence was seen in LMB-treated cells expressing L4-100K variants carrying amino acid exchanges in the GAR region (Fig. 28B panels e and k) or the RGG plus GAR region (Fig. 6B, panels f and l). The detected steady-state expression levels of wt and the mutant proteins were comparable in transfected H1299 cells (Fig. 28C). Different PRMT1 binding capacities of transfected 100K proteins can also be seen in Figure 28C. Altogether, these results show that neither the arginines in the RGG boxes nor their methylation contribute to 100K nuclear import, rather the arginine residues in the GAR region play a critical role in

---

375 393 721 775

ACKISNVELCN LVSYLGIL AAATHGRGGILGQSGRGGFGRRGGGGHDSRLGEPRRGSFRGRRGVRR NTVTLGRIPL wt

NES RGG GAR pTL-flag-1000

Figure 1 consists of 12 panels (a-l) showing the localization of pTL-tagged proteins. Panels a-f show the localization of pTL-flag-wt, pTL-flag-NES, pTL-flag-RGG, pTL-flag-RGG3, pTL-flag-RGG.GAR, and pTL-flag-GAR, respectively. Panels g-l show the same constructs after treatment with 100 nM leptomycin B (LMB). The images are arranged in two rows of six. The top row (a-f) shows the localization of the pTL-tagged proteins in cells treated with DMSO. The bottom row (g-l) shows the localization of the pTL-tagged proteins in cells treated with 100 nM LMB. The labels for the top row are: a pTL-flag-wt, b pTL-flag-NES, c pTL-flag-RGG, d pTL-flag-RGG3, e pTL-flag-RGG.GAR, f pTL-flag-GAR. The labels for the bottom row are: g +LMB, h +LMB, i +LMB, j +LMB, k +LMB, l +LMB. The images show the localization of the pTL-tagged proteins in cells treated with DMSO (top row) and cells treated with 100 nM LMB (bottom row). The images are arranged in two rows of six. The top row (a-f) shows the localization of the pTL-tagged proteins in cells treated with DMSO. The bottom row (g-l) shows the localization of the pTL-tagged proteins in cells treated with 100 nM LMB. The labels for the top row are: a pTL-flag-wt, b pTL-flag-NES, c pTL-flag-RGG, d pTL-flag-RGG3, e pTL-flag-RGG.GAR, f pTL-flag-GAR. The labels for the bottom row are: g +LMB, h +LMB, i +LMB, j +LMB, k +LMB, l +LMB.

**C**

Mock wt NES RGG RGG3 RGG.GAR GAR

L4-100K ▶

PRMT1 ▶

IP: α-PRMT1

L4-100K ▶

1 2 3 4 5 6 7

(A) Amino acid substitution mutations in L4-100K wt and mutant plasmids. The leucine residues in the 100K NES (pTL-100K-NES) known to be critical for CRM1-mediated nuclear transport (Cuesta et al., 2004) are indicated in bold letters. Numbers refer to amino acids residues in the wt 100K protein from pTL-100K. Amino acid changes in L4 proteins from pTL-100K-RGG, pTL-100K-RGG3, pTL-100K-RGG.GAR and pTL-100K-GAR are indicated below. (B) Subcellular distribution of wt and mutant L4 proteins in the absence or presence of the CRM1 inhibitor LMB. H1299 cells were transfected with the indicated plasmids. 36 h after transfection LMB was added to the medium (+LMB). Three hours later, cells were fixed and steady-state localization of wt and mutant L4-100K was examined by indirect immunofluorescence using mab 6B10. In all panels nuclei are indicated by a dotted line. (C) Steady state expression and PRMT1 binding affinities of transfected wt and mutant plasmids. H1299 cells were harvested 36 h after transfection. Either 50 µg aliquots from total cell lysates were separated by SDS-10% PAGE or 500 µg aliquots were used for PRMT1 IP and analyzed by immunoblotting using mab 6B10 and anti-PRMT1 antibody.

### 5.5.5 Mutations in the RGG Boxes of L4-100K Reduce Interactions with Tripartite Leader RNAs

Next, the binding of wt and mutant 100K to eIF4G was tested by combined immunoprecipitation and immunoblotting experiments using the appropriate antibodies (Fig. 29). Results from these assays demonstrated that amino acid substitutions in the 100K RGG boxes do not affect eIF4G binding, although the same mutations significantly reduced amounts of arginine methylated 100K to non-detectable levels (Fig. 29A). To monitor the mutations' effect on interactions with TL RNAs, wt and mutant proteins were immunoprecipitated and the associated RNAs isolated from the immune complexes were identified by quantitative RT-PCR with specific primers for TL and fiber mRNAs (Fig. 29B). As shown in three different experiments, wt 100K reproducibly associated with TL RNAs 6-fold more efficiently than the mutant 100K RGG protein, and around 5-fold more efficiently with fiber mRNA. Thus, the arginine to glycine substitutions substantially decrease interaction of 100K with TL RNAs, indicating that arginine methylation in the RGG boxes is critical for efficient binding to TL RNAs. Binding of GAPDH, as a cellular mRNA, to 100K could not be quantified since the precipitated RNA levels were much less than that of the late genes (Fig. 29C). This further supports the specific TL-mRNA binding activity of L4-100K.



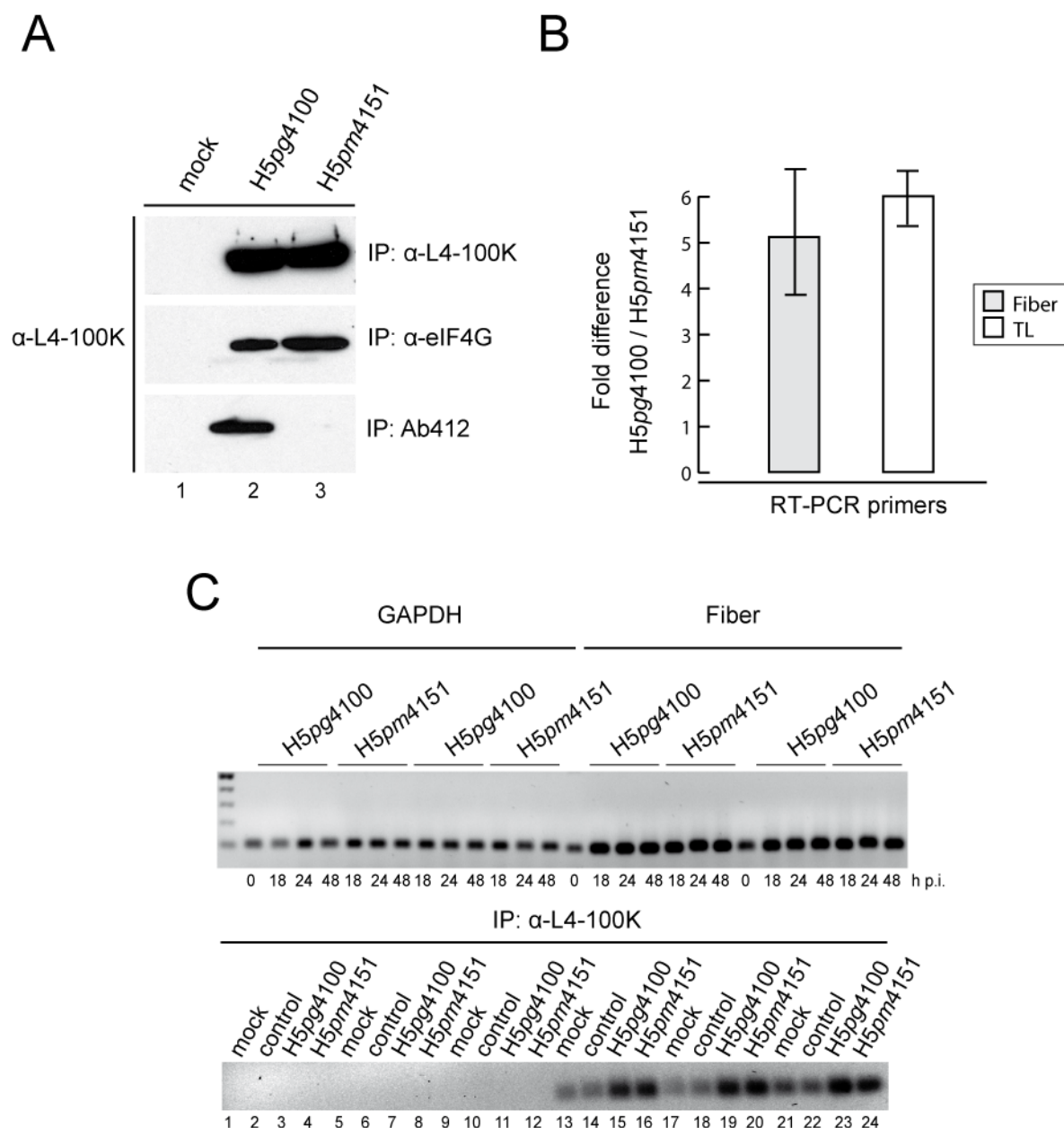


**Figure 29. Binding of wt and mutant L4-100K to eIF4G and viral late mRNAs**

A549 cells were infected with H5pg4100 and H5pm4151 viruses at a multiplicity of 10 FFU per cell. 48 hours after infection total cell lysates were prepared and subjected to immunoprecipitation (IP) with L4-100K antibody, eIF4G antibody or Ab412 (recognizing methylated arginines). The immunocomplexes were separated by SDS-10% PAGE and analyzed by immunoblotting using mab 6B10. (B) RNA was purified from immunoprecipitates, reverse transcribed and subjected to quantitative real-time PCR as described. L5 fiber and tripartite leader (TL) RNA levels are shown relative to the wt values. The results represent the averages from three independent experiments. Error bars indicate the standard error of the mean. (C) cDNA amplifications (duplets) of total GAPDH and fiber mRNAs produced 0, 18, 24, and 48 hours post infection (h p.i.) were loaded on a 1.5 % agarose gel. RNA-IP (48 h p.i.) products (triplets) were also visualized on an agarose gel. Lanes 1-12 were amplified by using GAPDH, and lanes 13-24 were amplified by using fiber primers (40 cycles).

To further understand whether this reduction in TL-mRNA binding activity of mutant

100K interferes with the transport of late viral transcripts, cytoplasmic and nuclear RNAs were isolated from H5pg4100 and H5pm4151 infected A549 cells in a time course, and quantified by RT-PCR using TL-specific primers (Fig. 30). The ratio of cytoplasmic to nuclear late viral RNA levels was calculated in both virus infections. As can be seen in Figure 30A, during adenovirus infection late viral RNAs gradually accumulated in the cytoplasmic fraction. At 48 hours post infection, in the case of H5pg4100, TL-transcripts were found to be 6 times more abundant in the cytoplasm than the nucleus, whereas H5pm4151 displayed a 4.5-fold difference between the two compartments, i.e. it was ~1.3 times less efficient than the wt virus. If the TL-mRNA binding activity of 100K was the only prerequisite for nucleocytoplasmic viral mRNA transport, the defect of H5pm4151 would be expected to be much higher, since the TL-mRNA binding activity of RGG-100K was shown to be ~6 times less than the wt protein. Hence, the incompetence observed in the late protein synthesis and virus yield of H5pm4151 could not be attributed to a nucleocytoplasmic RNA transport defect. Instead, an alteration in the virus specific translation pathway or in protein-protein interactions of methylation-deficient 100K was thought to be the more probable reason for the observed phenotype.

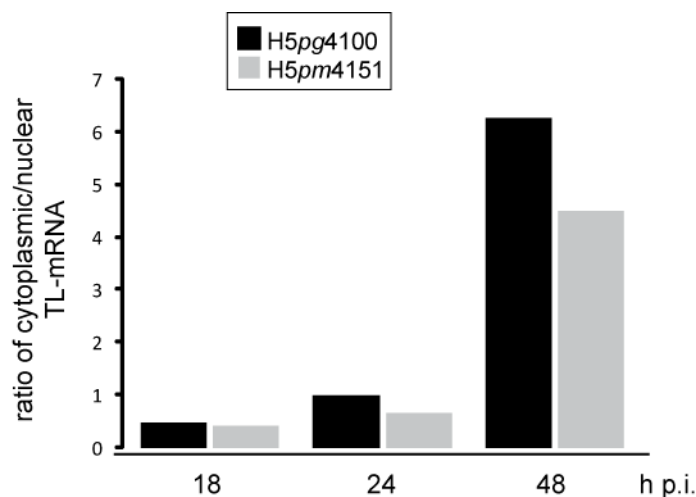


**Figure 30. mRNA transport efficiency of H5pg4100 and H5pm4151**

A549 cells were infected with H5pg4100 and H5pm4151 viruses at a multiplicity of 10 FFU per cell. RNA was purified from cytoplasmic and nuclear compartments 18, 24, and 48 hours post infection (h p.i.), reverse transcribed, and subjected to quantitative real-time PCR as described. The ratio of cytoplasmic to nuclear Tripartite leader (TL) RNA levels are shown in the graph.

---

### 5.5.6 Arginine Methylation of L4-100K may Regulate Hexon Biogenesis

As already mentioned in the previous sections, 100K, in addition to its important role in the cap-independent translation of viral late mRNAs, further contributes to efficient virus growth by facilitating trimerization and nuclear accumulation of hexons through acting as a chaperone for hexon trimerization in the cytoplasm and promoting their nuclear import.

To determine the effect of mutations on 100K binding to hexon, combined immunoprecipitation and immunoblotting assays were performed. As predicted, wt 100K coprecipitated with hexon during the late phase of infection (Fig. 31A, lanes 2, 5 and 8). Unexpectedly, we noticed a positive effect on hexon binding with the 100K RGG mutant. We reproducibly observed a 4 to 6-fold increase in binding of the mutant protein to hexon, in particular at later time points (48 and 72 h) of infection (Fig. 31A, lanes 6 and 9). Significantly, a similar binding pattern was evident when we monitored the interaction of both wt and mutant 100K with hexon in the presence of the arginine methylation inhibitor AdOx (Fig. 8A, lanes 14, 15, 17 and 18) confirming that PRMT1-mediated methylation of arginines in the RGG boxes regulates hexon binding. This was further supported by co-immunoprecipitation experiments using fractionated cell lysates (Fig. 31B). Again, in these assays substantially more 100K RGG mutant protein precipitated with hexon than the wt product in both the cytoplasmic (Fig. 31B, lanes 3, 4, 6 and 7) and nuclear fractions (Fig. 31B, lanes 10, 11, 13 and 14). Also, it appeared that more of the 100K RGG mutant protein was found in a complex with hexon in the nuclear rather than the cytoplasmic fraction (Fig. 31B, compare lanes 7 and 14). One possible explanation for this result is that arginine methylation in the RGG boxes of 100K negatively regulates the interaction with hexon, presumably favoring dissociation of the complex in the nucleus.

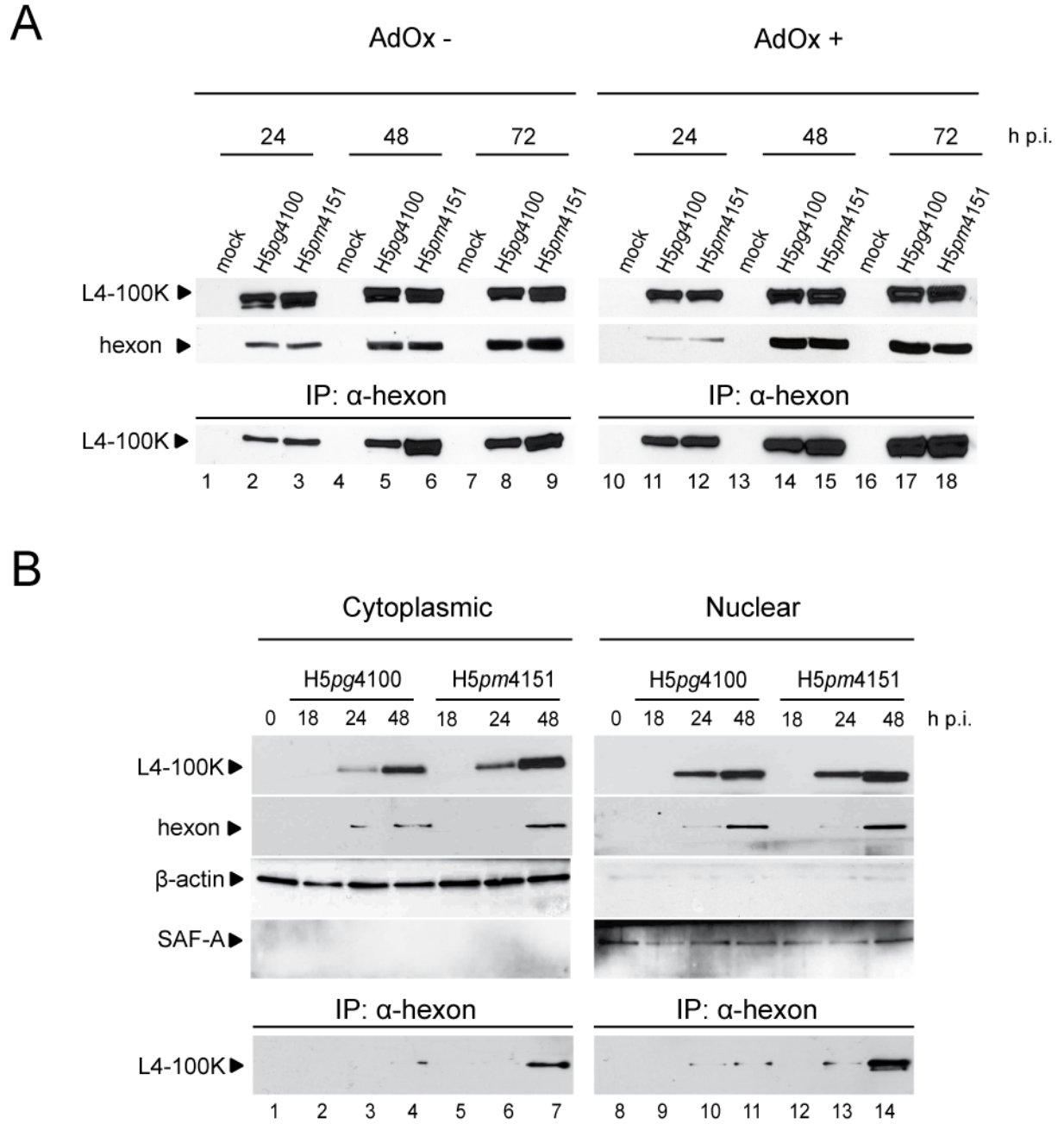


**Figure 31. Arginine methylation in RGG boxes modulates hexon binding to L4-100K**

(A) A549 cells were infected with H5pg4100 and H5pm4151 at a multiplicity of 10 FFU per cell, in the absence or presence of AdOx (AdOx- and AdOx+) and harvested at the indicated time points after infection (h p.i.). Total cell extracts were prepared from non-infected (mock) and infected cells. 50 µg aliquots of lysates were separated by SDS-10% PAGE and analyzed by Western blotting using L4-100K rat mab 6B10 or rabbit mab recognizing the hexon protein. The same lysates were used for immunoprecipitation (IP) with anti-hexon mab. The immunocomplexes were separated by SDS-10% PAGE and analyzed by immunoblotting using mab 6B10. (B) Total cell extracts were prepared and subjected to nucleocytoplasmic fractionation. Aliquots of cell extracts corresponding to cytoplasmic (5 µg) and nuclear (2 µg) fractions were separated by SDS-10% PAGE and analyzed by immunoblotting using 6B10 and anti-hexon mab. The same extracts were subjected to immunoprecipitation (IP) with mab hexon and visualized by SDS-10% PAGE and immunoblotting with mab 6B10.

---

### 5.5.7 Mutations in the RGG Boxes of L4-100K Alters its Proteolytic Cleavage Late in the Infection

During H5pm4151 characterization an abundant faster migrating 100K band was observed late in the infection, which was different from that of the wt protein both in quantity and size (Fig. 27C and Fig. 31). Detailed analysis showed that two additional faster migrating forms (95 and 90 kDa) of wt 100K were forming 48 hours after infection, which were less than 5% of the volume of the 100 kDa band (Fig. 31B, lane 2). In the case of H5pm4151, one dominant shorter form was detected, which was up to 10 times more abundant than its wt counterpart (Fig. 31A, compare lanes 3 and 5, Fig. 31B, lanes 2 and 3). To understand whether these shorter forms are produced by the adenovirus protease, the activity of this enzyme was inhibited during infection to monitor the effect on L4-100K forms. Adenovirus protease (also known as adenain) is a cysteine-type protease that cleaves its substrates from two defined consensus motifs: (M/I/L)XGX-G or (M/I/L)XGG-X (Diouri et al., 1996). *In vitro* assays demonstrated that it is also capable of cleaving other discrete sites resembling these consensus sequences. Adenain has been shown to cleave several adenoviral capsid proteins including pVI and hexon, preterminal protein (pTP), which serves as a primer for DNA replication (Webster et al., 1994), and cellular protein cytokeratin 18 (Chen et al., 1993). Interestingly, it has been shown that the proteolytic activity of this protease is enhanced by the C-terminus of pVI (Cabrita et al., 1997; Diouri et al., 1996). L4-100K was also shown to be cleaved by this enzyme *in vitro* (Ruzindana-Umunyana et al., 2002).

The formation of these shorter forms was efficiently inhibited by the addition of a specific cysteine protease inhibitor (E64) 24 hours post infection (Fig. 31). The same inhibitory effect could not be shown when a serine protease inhibitor was used (3,4-dichloroisocoumarin), suggesting that this cleavage is not caused by a serine protease (e.g. granzymes). These findings hinted at the possible cleavage of 100K by adenovirus protease. Moreover, the amino acid sequence including the second RGG

box (LGQSGR<sup>736</sup>GGFG) resembles the suggested consensus adenain cleavage motifs. The substitution of R<sup>736</sup> to G in the case of H5 $pm$ 4151 might enhance the cleavage by this enzyme. Nonetheless, since there are several cysteine-type proteases in the cell and the individual targeting of a single enzyme is complicated, *in vitro* cleavage assays or RNA interference tools should be employed to confirm that this faster migrating form, which was observed to be more abundant in H5 $pm$ 4151 infection, is due to adenain cleavage.

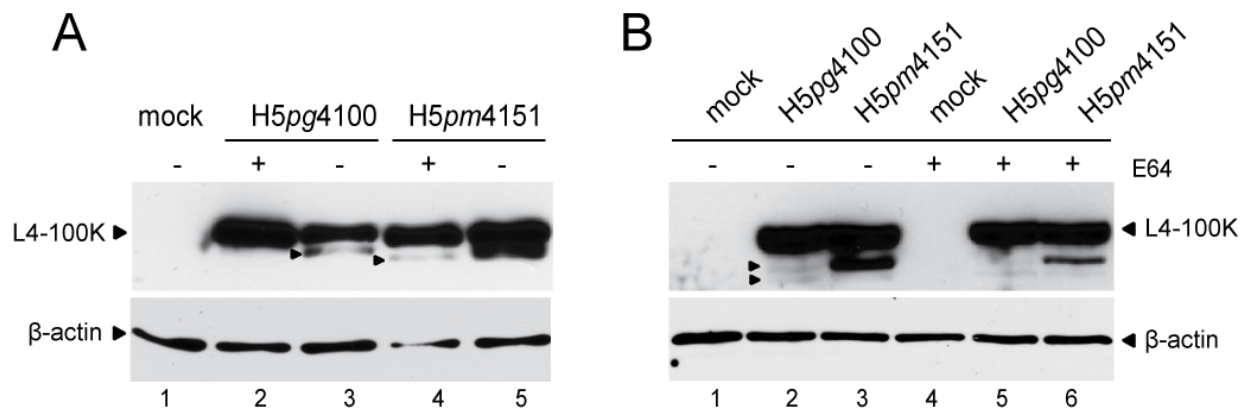


**Figure 31. Proteolytic cleavage of L4-100K**

(A) A549 and (B) H1299 cells were infected with H5pg4100 and H5 $pm$ 4151 at a multiplicity of 10 FFU per cell, and harvested 48 h after infection. E64 (10  $\mu$ M) was added to the infection medium 24 h post infection when indicated (+). Total cell extracts were prepared from non-infected (mock) and infected cells. 50  $\mu$ g aliquots of lysates were separated by SDS-8% PAGE and analyzed by Western blotting using L4-100K rat mab 6B10 or  $\beta$ -actin antibody. Arrows indicate the faster migrating forms of 100K.

## 5.6 Nuclear Export of Adenovirus Type 5 L4-100K is Mediated by CRM1 and is Crucial for Efficient Virus Infection

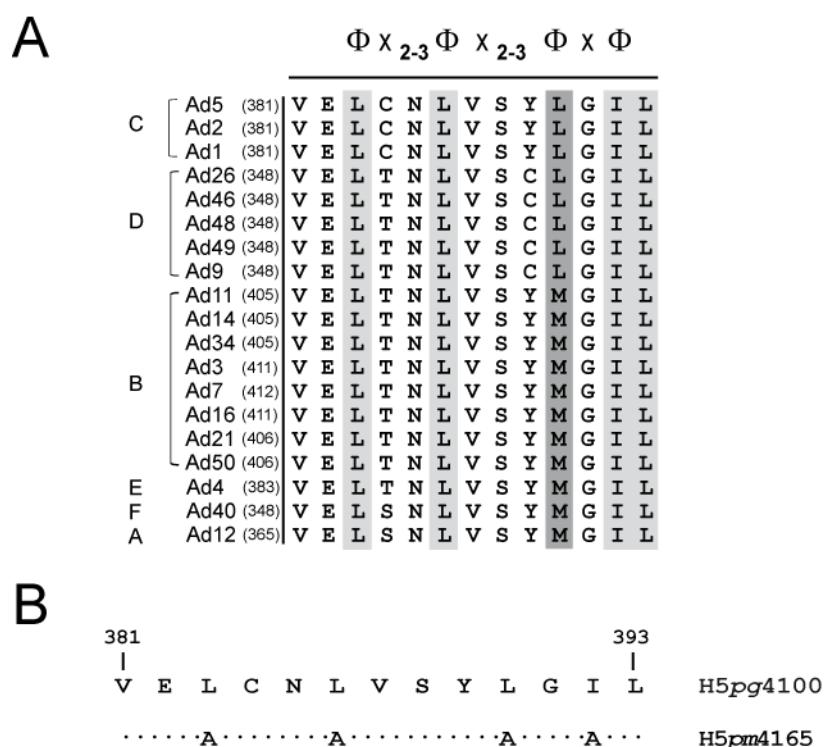
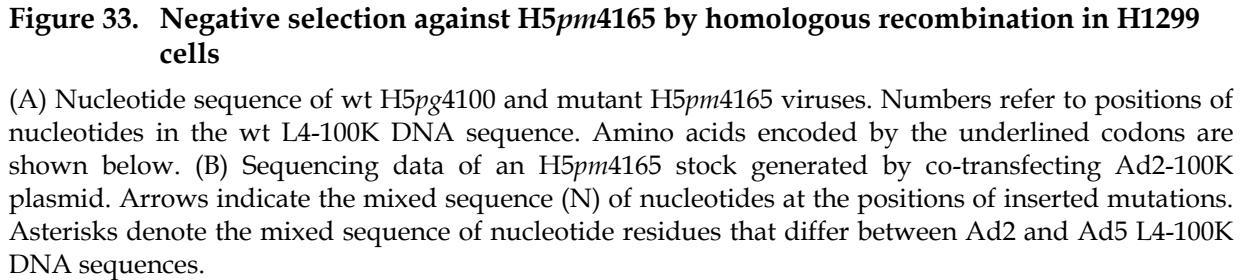


Figure 32A outlines the consensus HIV-Rev-like leucine-rich nuclear export signal (NES) and implicates the high conservation of this motif among different adenovirus serotypes. Previously, substitution of the hydrophobic residues of the motif with alanines was shown to block the nuclear export of L4-100K in transiently transfected

cells (Cuesta et al., 2004). To investigate the role of this motif on adenovirus lytic infection, L4-100K-NES mutant virus was generated by substituting three leucines and one isoleucine (L383/386/390/I392A) in this sequence by alanines (Fig. 32B, 33A). L4-100K-NES bacmid (pH5pm4165) was constructed as previously described (5.1). However, generation of L4-100K mutant virus from the infectious viral DNA transfected into the L4-100K-complementing cell line K16 failed, and no infectious viral particles could be produced, although the same cell line supported the generation of other L4-100K mutants (H5pm4151, H5pm4152, and H5pm4153). This provided a hint about the significance of this motif in the viral life cycle, and pointed out that the low levels of wt-100K expressed by the helper cell line could not compensate for the defect of this mutant virus. Therefore, to supply more wt-100K protein for the generation of this mutant, 2E2 cells were co-transfected with pTL-flag-Ad2-100K plasmid together with the linearized pH5pm4165 bacmid. In this way a low-titer ( $8 \times 10^4$  particles/ $\mu$ l) H5pm4165 virus stock could be produced. To yield a higher titer, H1299 cells that were transfected with pTL-flag-Ad2-100K plasmid were infected with H5pm4165 virus. Surprisingly, several times this generated a chimeric virus with both wt and mutated sequences (Fig. 33), which showed a cytopathic effect after 7-10 days incubation period. In all cases these mixed sequences were not only detected in the mutated positions but also in the residues that differ between Ad2 and Ad5 L4-100K DNA sequences, and spanned 200-250 nucleotides (Fig. 33B). These observations indicated an ongoing homologous recombination process in the cell driven by the strong negative selection pressure against the mutant virus, implicating a severe defect caused by the inserted mutations. Therefore, the low-titer pure L4-100K-NES (H5pm4165) mutant virus was analyzed for L4-100K subcellular localization, early and late phase progression and virus yield properties.





To verify whether the nucleocytoplasmic shuttling of L4-100K is dependent on the CRM1 pathway, first leptomycin B (LMB) was added to the medium of wt or NES-pTL-flag-100K transfected H1299 cells. LMB is a fungal metabolite that targets a conserved cysteine residue (C<sup>528</sup>) within the putative NES-binding region in CRM1 and specifically inhibits its activity (Kudo et al., 1999). The localization of L4-100K was analyzed in the presence and absence of this inhibitor by indirect immunofluorescence staining.

As expected, the blockage of CRM1 by this inhibitor resulted in the nuclear accumulation of wt-100K (Fig. 34A, panel b), which was otherwise observed as a dominant cytoplasmic protein (Fig. 34A panel a). Consistent with a previous report (Cuesta et al., 2004), the mutational inactivation of the NES motif in L4-100K also caused the nuclear retention of this protein in the absence or presence of LMB (Fig. 34A, panels c and d).

The subcellular localization of L4-100K was further examined in H5pg4100 and H5pm4165 infected A549 cells. The localizations of wt and the mutant 100K proteins during adenovirus infection were found to be comparable to that of the plasmid transfected cells. At 36 hours post infection (h p.i.), H5pg4100 virus exhibited a diffuse cytoplasmic and nuclear 100K distribution (Fig. 34B, lane a), whereas H5pm4165 virus displayed a dominant nuclear 100K staining (Fig. 34B, lane b). Nucleocytoplasmic fractionation of the wt and mutant virus infected cells further proved that the majority of L4-100K was captured in the nuclear fraction when the nuclear export signal was inactivated (Fig. 34C). These results confirmed the CRM1-dependent nucleocytoplasmic shuttling of L4-100K during infection.

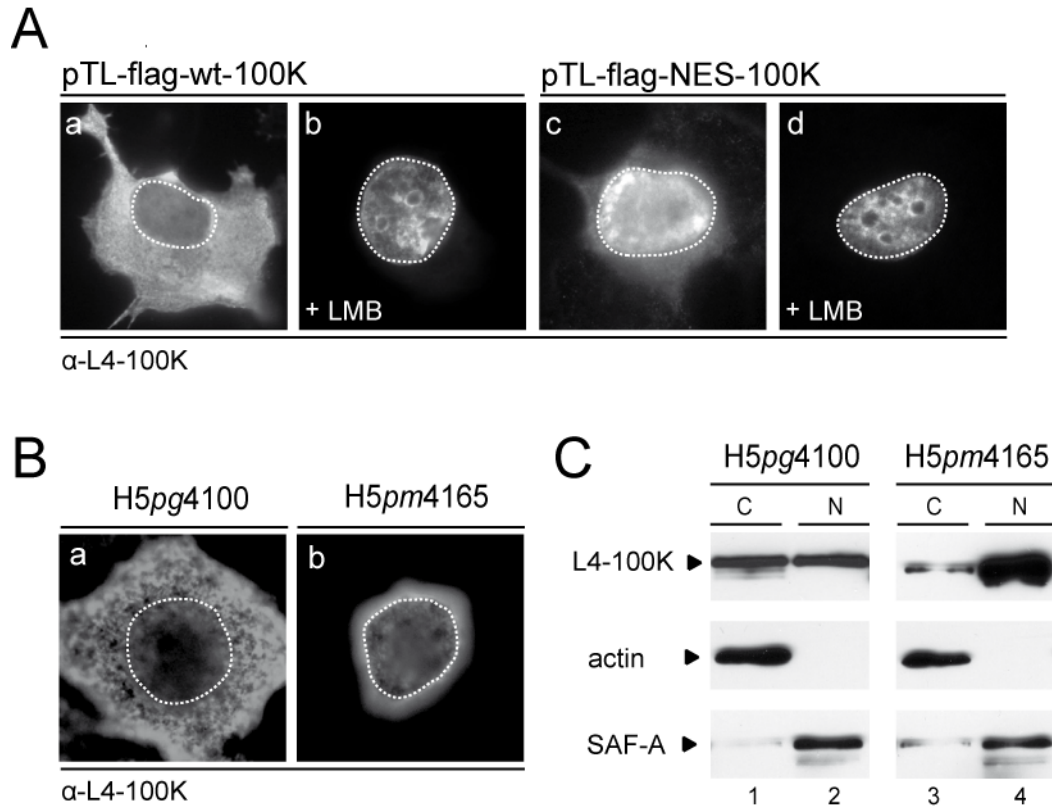


**Figure 34. Subcellular localization of wt and NES L4-100K during transfection and productive infection**

(A) H1299 cells were transfected with the indicated plasmids. 30 h after transfection LMB was added to the medium (+LMB). Three hours later, cells were fixed and steady-state localizations of wt and mutant L4-100K were examined by indirect immunofluorescence staining using rat mab 6B10. (B) A549 cells were infected with H5pg4100 (panel a) and H5pm4165 (panel b) viruses at a multiplicity of 10 FFU per cell. Infected cells were fixed at 36 h post infection (h p.i.) and stained with rat mab 6B10. In all panels nuclei are indicated by a dotted line. (C) At 36 h post infection cells were collected and fractionated as described. 5  $\mu$ g aliquots of cytoplasmic (C) and 2  $\mu$ g aliquots of nuclear (N) lysates were separated by SDS-10% PAGE and analyzed by Western blotting using L4-100K rat mab 6B10, anti-actin as cytoplasmic, and anti-SAF-A antibody as nuclear markers.

### 5.6.3 Effect of L4-100K-NES Mutation on Virus Replication

To assess the role of the L4-100K nuclear export signal on the lytic adenovirus life cycle, first the DNA replication efficiency of the mutant virus H5pm4165 was measured in comparison to the wt virus H5pg4100. As expected, the DNA replication of the mutant virus was not affected by the amino acid substitutions in this late protein and was found to be as efficient as the wt virus (Fig. 35A). Consistently, early protein synthesis was observed to be equal to wt levels (Fig. 35B) showing that the early phase of the infection was not affected by the NES mutations in the L4-100K

gene.

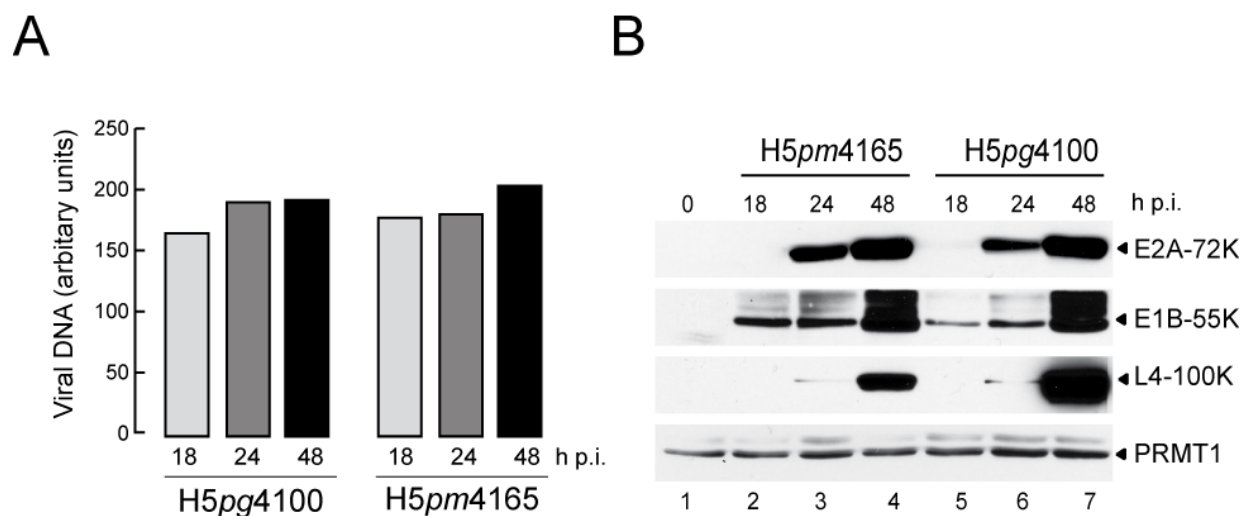


**Figure 35. Effects of amino acid substitutions in L4-100K on viral DNA replication and protein synthesis**

(A) Viral DNA accumulation. A549 cells were infected with H5pg4100 and H5pm4165 viruses at a multiplicity of 10 FFU per cell. Total nuclear DNA was isolated at the indicated times after infection and subjected to quantitative PCR. PCR products were analyzed and quantified using the ChemiDoc system and QuantityOne software (BioRad). The results shown represent the averages from two independent experiments. (B) Viral protein synthesis. A549 cells were infected with the wt or mutant virus at a multiplicity of 10 FFU per cell. Total cell extracts were prepared at indicated times after infection. Proteins (25  $\mu$ g samples) were separated by SDS-10% PAGE, transferred to nitrocellulose membranes and probed with rat mab 6B10 (L4-100K), mouse mab 2A6 (E1B-55K), and anti-PRMT1 as a loading control.

Second, the steady state expression levels of viral proteins were investigated by immunoblotting. The expression of L4-100K in H5pm4165 infection was found to be comparable to the wt virus at the beginning of the late phase (Fig. 35B, lanes 3 and 6), although the accumulation of this mutant protein during the course of the infection was observed to be less than that of H5pg4100 virus (Fig. 35B, lanes 4 and 7). This reduction in L4-100K accumulation was further supported by the significant decrease observed in the structural protein synthesis (Fig. 36A). This defect in late protein production further resulted in a drastic drop in the virus yield of the mutant virus (Fig. 36B). In the low multiplicity of infection time course (1 FFU per cell), 17 -40-fold less virus particles were produced by H5pm4165 in A549 cells in comparison to the wt virus. This ratio was observed to increase further in a higher multiplicity of infection (10 FFU per cell), reaching a 240-fold difference at 72 hours post infection (h p.i.). This

is unlike an early gene mutant virus, which generally compensates for the defect with increased particle numbers per cell especially at later time points (Bridge et al., 1993; Huang and Hearing, 1989).

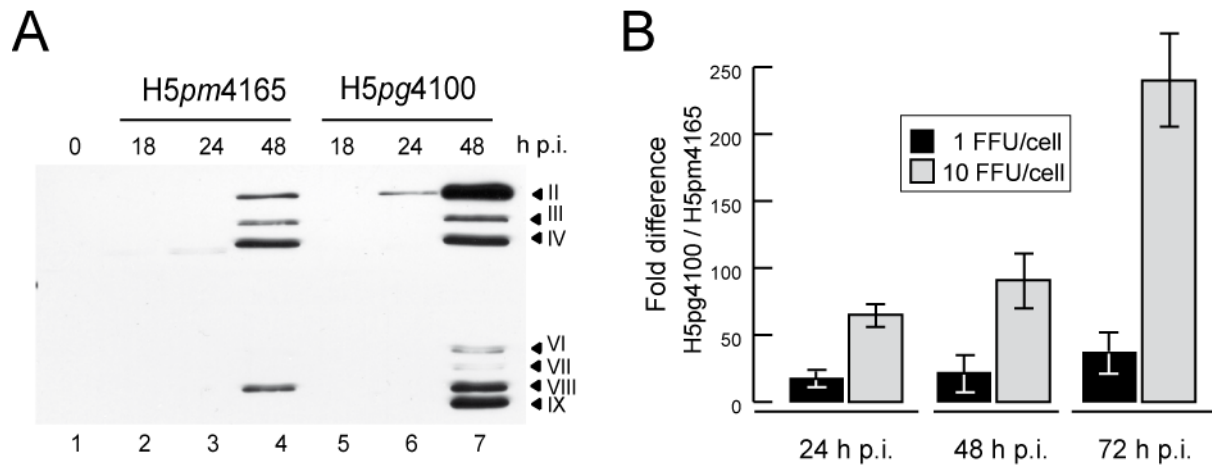


**Figure 36. Effects of amino acid substitutions in L4-100K on late protein synthesis and virus growth**

(A) Late viral protein synthesis. A549 cells were infected with the wt or mutant virus at a multiplicity of 10 FFU per cell. Total cell extracts were prepared at indicated times after infection. Proteins (25  $\mu$ g samples) were separated by SDS-10% PAGE, transferred to nitrocellulose membranes and probed with anti-Ad5 rabbit polyclonal serum L133. Bands corresponding to viral late proteins hexon (II), penton (III) and fiber (IV) are indicated on the right. (B) Virus yield. A549 cells were infected with wt H5pg4100 or H5pm4165 at indicated multiplicities. Viral particles were harvested at indicated time points (h p.i.) and virus yield was determined by quantitative E2A-72K immunofluorescence staining on K16 cells. The results represent the averages from three independent experiments. Error bars indicate the standard error of the mean.

#### 5.6.4 Inhibition of CRM1 by LMB in the Late Phase of Adenovirus Infection Results in Reduced Late Protein Synthesis and Virus Yield

To investigate whether the late phase defect of H5pm4165 arose from inhibiting the CRM1-dependent nuclear export pathway, wt adenovirus infection was studied in the presence of Leptomycin B. First, the viability of A549 and H1299 cells were tested in the presence of this inhibitor. In the experiments, 14 hours treatment of infected or non-infected cells with 20 nM LMB did not cause significant cell damage or death (Fig.

37A). Therefore, LMB was added to the medium of wt virus infected cells 10 hours post infection (h p.i), when DNA replication centers started to form (Fig. 37B, panel a) showing the onset of the late phase. The infected cells were fixed 14 hours post treatment when replication centers grew larger and more numerous, indicating extensive replication and transcription (Fig. 37B, panel b). To ensure that the inhibitor was effective during infection, E1B-55K and L4-100K proteins were localized in the cells. As already published (Dobbelstein et al., 1997a; Krätzer et al., 2000), E1B-55K was observed to translocate into the nuclei of infected cells, forming dot-like structures upon CRM1 inhibition, whereas the non-treated cells showed a dominant structured cytoplasmic staining (Fig. 37B, panels c and d). LMB treatment also caused the nuclear accumulation of L4-100K in the majority (70-90%) of the infected cells (Fig. 37B, panels e and f) at that time point.

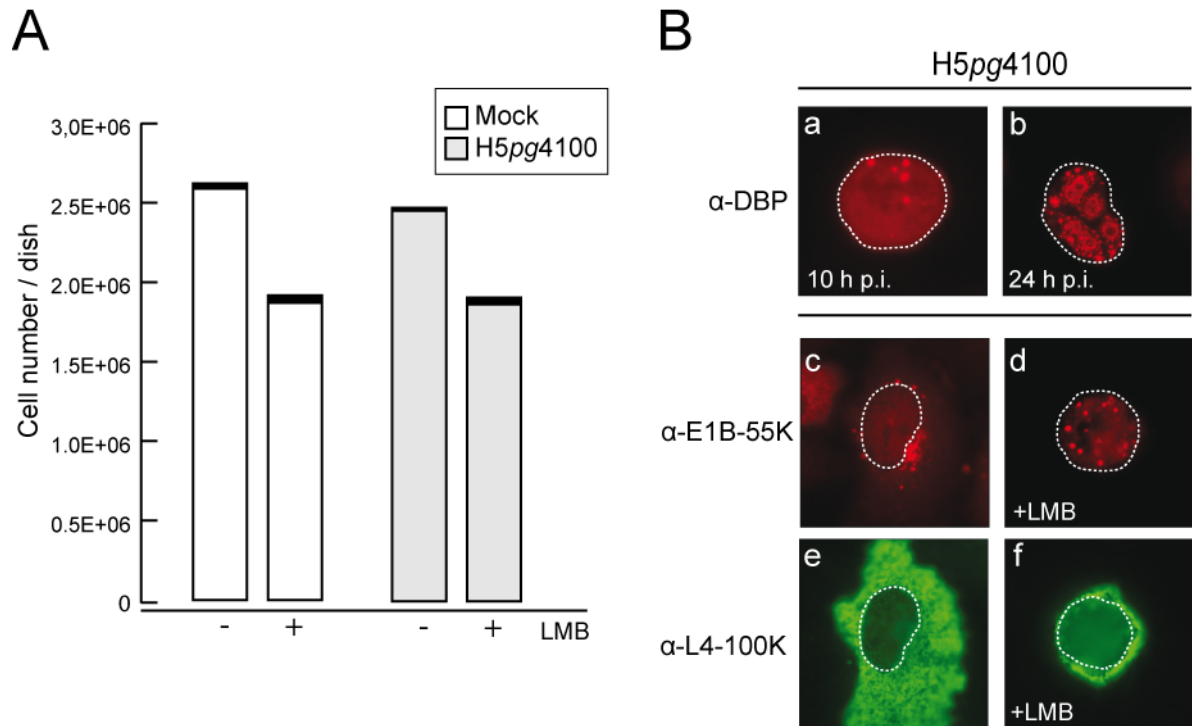


**Figure 37. Effect of LMB on cell growth and localization of adenoviral proteins during infection**

(A) A549 cells were cultured in the absence (-) or presence (+) of 20 nM LMB for 14 hours. At the same time LMB (+) or equal amounts of ethanol (-) were added to the medium of H5pg4100 (10 FFU per cell) or mock infected cells at 10 h post infection (h p.i.). After 14 h of treatment, cells were trypsinized and stained with trypan blue. The number of living or dead cells (black bars) per dish was determined by

## RESULTS

---

counting a fraction of the cell suspension. (B) H5pg4100 infected A549 cells were fixed at 10 h (panel a), and 24 h (panel b) post infection (h p.i.). DNA replication centers were visualized by staining with mouse mab B6-8 against E2A-72K DNA-binding protein (DBP). At 24 h p.i., wt virus infected cells were also stained with either rat mab 6B10 for L4-100K (panels c and d) or mouse mab 2A6 for E1B-55K (panels e and f) localization in the absence (panels c and e) or presence of LMB (panels d and f).. In all panels nuclei are indicated by a dotted line.

Next, the viral protein synthesis and virus yield properties of H5pg4100 infection were analyzed in the presence of LMB compared to that of the non-treated H5pg4100 or H5pm4165 infection. The addition of LMB to adenovirus infected cell medium with the onset of the late phase significantly reduced late protein accumulation efficiency, as can be seen from L4-100K and hexon immunoblots (Fig. 38A, lanes 1 and 2). This negative effect of LMB on the late phase of the infection was further supported by an approximately 15-fold reduction in virus yield (Fig. 38B). Interestingly, in H5pm4165 infection at 24 h p.i., L4-100K expression was not less than the wt virus level (Fig. 38A, lanes 3 and 4). However, hexon protein synthesis was significantly reduced in the mutant virus infection at this time point (Fig. 38A). Moreover, the progeny virion production efficiency of the H5pm4165 mutant was reduced nearly 80 times compared to the H5pg4100 virus, and further affected by the presence of LMB by dropping significantly (Fig. 38B). This implies that other viral factors might be affected by the presence of this inhibitor. These results demonstrate that inhibition of the CRM1 pathway in the late phase of Ad infection, either by LMB or inactivating the NES of L4-100K, reduced adenovirus progeny production in A549 and H1299 cells. Nonetheless, the effect of the L4-100K NES mutation was more profound than the addition of CRM1 inhibitor.

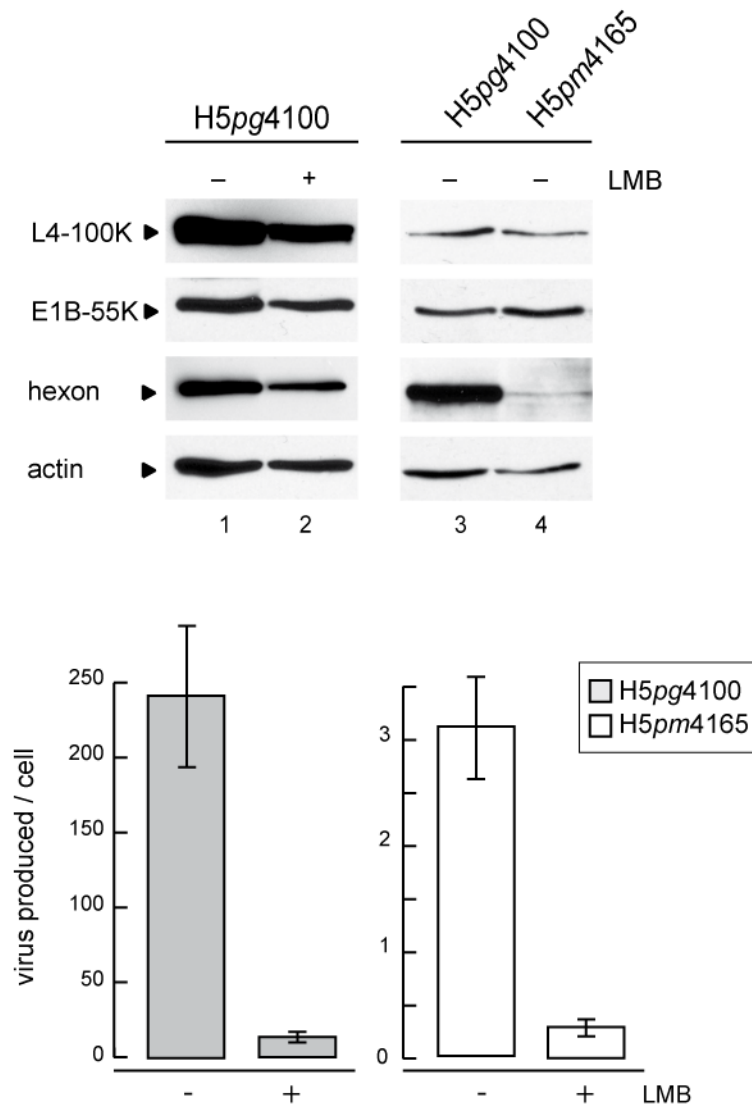


**Figure 38. Effect of LMB on the late phase of adenovirus infection**

A549 cells were infected with H5pg4100 or mutant H5pm4165 viruses at a multiplicity of 10 FFU per cell. LMB was added to the medium 10 h post infection (+) or not (-). (A) Viral early and late protein synthesis. Total cell extracts were prepared at 24 h p.i. and proteins (50 µg samples) were separated by SDS-10% PAGE, transferred to nitrocellulose membranes and probed with the mab 6B10, mab 2A6, anti-hexon and anti-actin antibodies. (B) Virus yields of H5pg4100 and H5pm4165 infections in the absence or presence of LMB. Viral particles were harvested at 24 h post infection (h p.i.) and virus yield was determined by quantitative E2A-72K immunofluorescence staining on K16 cells. The results represent the mean value of two independent experiments.



### 5.6.5 Inactivation of NES in L4-100K does not Block its Binding to Hexon, E1B-55K and PRMT1 but Reduces eIF4G Interaction

To investigate the underlying reasons for the severe defect observed in H5 $pg4165$  late protein synthesis and progeny virion production, the interaction of L4-100K-NES protein with its interaction partners was examined using a combined transfection and infection procedure. Co-immunoprecipitation assays were performed using wt or NES-pTL-flag-100K transfected H1299 cells that were simultaneously infected with H5 $pg4100$  to establish an infection environment supporting efficient late protein synthesis. Steady-state expression levels of wt and NES-pTL-flag-100K plasmids were tested using anti-flag antibody (Fig. 39). The equimolar presence of viral (hexon, E1B-55K) and cellular (eIF4G, PRMT1) proteins was confirmed using appropriate antibodies (Fig. 39) in the immunoblots. Transfected L4-100K was discriminated from the viral 100K and immunoprecipitated using anti-flag antibody.

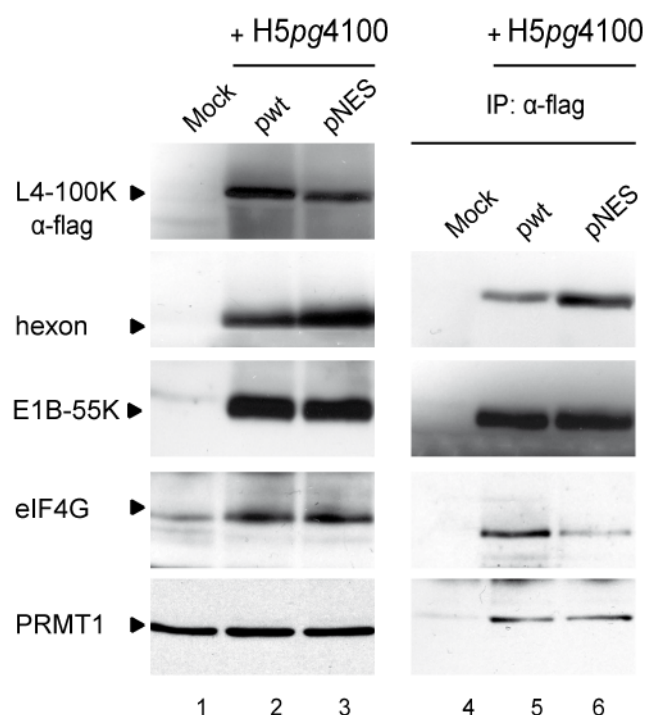


**Figure 39. Analysis of L4-100K-NES mutation on its binding to interaction partners**

H1299 cells were transfected with wt (pwt) or NES pTL-flag-100K (pNES) plasmids and 6 h after transfection infected with H5 $pg4100$  virus (10 FFU/cell). Total cell extracts were prepared from non-infected (mock) and transfected-infected cells 30 h after infection. 25  $\mu$ g aliquots of lysates were separated by SDS-10% PAGE and analyzed by immunoblotting using anti-flag, anti-hexon, E1B-55K

## RESULTS

---

mouse mab 2A6, anti-eIF4G and anti-PRMT1 antibodies. The same lysates were used for immunoprecipitation (IP) with anti-flag mab. The immunocomplexes were separated by SDS-10% PAGE and analyzed by immunoblotting using anti-hexon, E1B-55K mouse mab 2A6, anti-eIF4G and anti-PRMT1 antibodies.

Hexon and E1B-55K proteins were found to be co-immunoprecipitated by NES-100K as efficiently as the wt protein. As expected, PRMT1 binding was also not affected by the mutations since the PRMT1-interaction motif on L4-100K was found to be at the C-terminus (RGG boxes) and the interaction between these two proteins is thought to occur shortly after the expression of 100K when the protein is still cytoplasmic. On the other hand, the binding of the translation initiation factor eIF4G was observed to be slightly less than the wt protein. The nuclear retention of L4-100K could be a reason for this reduced precipitation, since the translation factor is cytoplasmic and nuclear export of 100K might be required for this interaction. As a conclusion, these data further indicate that mutating the NES of L4-100K neither affects the protein folding or stability, nor abolishes the binding of known interaction partners, but severely reduces virus growth efficiency due to aberrant L4-100K nucleocytoplasmic shuttling, which could trigger further functional inefficiencies.

## 6 Discussion

---

### 6.1 L4-100K Plays Major Roles During the Late Phase of Adenovirus Infection

The late phase of adenovirus infection can be characterized by excess viral mRNA export to the cytoplasm, vast amounts of structural protein synthesis, and efficient nuclear import of these capsid components accompanied by blocking host cell mRNA export and protein expression pathways (Beltz and Flint, 1979; Mathews and Shenk, 1991; Zhang and Schneider, 1993). To orchestrate these extreme synthesis, transport, encapsidation, and *host-shut-off* processes, viral regulatory proteins cooperate with each other and modify cellular machineries in favor of progeny virus particles. One of the few regulatory proteins of the adenovirus late phase is a large, multifunctional phosphoprotein; L4-100K that has been well conserved during evolution. This non-structural late protein not only plays a vital role in hexon biogenesis (Cepko and Sharp, 1982; Hong et al., 2005; Kauffman and Ginsberg, 1976; Oosterom-Dragon and Ginsberg, 1981), but also coordinates the virus specific translation (Cuesta et al., 2000; Riley and Flint, 1993; Xi et al., 2004) and contributes to the inhibition of untimely host cell apoptosis (Andrade et al., 2001; Andrade et al., 2003). Interestingly, it was suggested that this late protein contributes to the tumor selective potential of oncolytic *dl1520* ( $\Delta$ E1B-55K) (O'Shea et al., 2004), a virus that shows different replication capacities depending on the tumor type. To accomplish all these tasks, L4-100K continuously shuttles between the cytoplasm and nucleus, interacts with several viral and cellular factors and also undergoes different posttranslational modifications. In the last decade ever increasing reports shedding light on some of the multifaceted functions of this protein encouraged us to investigate the properties of L4-100K in more detail. In this study, functional analyses of L4-100K concentrated on its shuttling, protein-protein/protein-RNA interaction, and posttranslational modification properties by generating appropriate virus mutants.

### 6.1.1 L4-100K Interacts with eIF4G, hexon, PRMT1, and E1B-55K During Infection

Research over the last decade has clearly demonstrated the indispensable role of L4-100K in the translation of tripartite-leader-containing late viral mRNAs (TL-mRNAs). Previous reports described the interaction of L4-100K with the TL containing transcripts (Riley and Flint, 1993), and the enhancing role of these non-coding RNA structures on the transport and translation of viral mRNA (Dolph et al., 1990; Dolph et al., 1988; Hayes et al., 1990b; Huang and Flint, 1998b). In the following years, elaborate experiments by Schneider and coworkers recognized the association of L4-100K with the scaffolding component (eIF4G) of the eukaryotic translation initiation complex eIF4F, and identified a 66-residue region (amino acids 280 to 345) in L4-100K as being responsible for this interaction (Cuesta et al., 2004; Xi et al., 2004). Moreover, they discovered that the association of L4-100K with eIF4G competitively inhibits the Mnk1-eIF4G interaction, which in turn inhibits phosphorylation of the cap binding component (eIF4E) of the complex (Cuesta et al., 2000; Cuesta et al., 2004; Huang and Schneider, 1991; Zhang and Schneider, 1993). This blocks linear cap-dependent translation leading to translational shut-off on cellular transcripts (Cuesta et al., 2000; Zhang et al., 1994; Zhang and Schneider, 1993). They also showed that the tyrosine phosphorylation of L4-100K (Y365 and Y682) determines the specific TL-mRNA interaction of this protein, which subsequently drives ribosome shunting on these transcripts (Xi et al., 2005). In summary, these experiments clarified the role of L4-100K in the virus-specific ribosome shunting translation mechanism, the TL-mRNA and eIF4G binding sites, as well as the phosphorylated tyrosine residues in L4-100K.

To gain a further understanding of the overall functions of L4-100K, we aimed to analyze the possible modification sites, interaction domains, and nucleocytoplasmic shuttling properties of this protein. For this purpose, we screened the conserved regions in L4-100K showing similarities to known interaction or modification motifs, and chose to inactivate the most prominent ones. Corresponding adenovirus mutants

were generated and analyzed in the context of viral early and late phase progression, virus yield, L4-100K subcellular localization, and protein-protein/RNA interactions. Moreover, the associations between known L4-100K interaction partners such as hexon and PRMT1 were examined to reveal their binding sites in the L4-100K protein sequence.

As we know from publications spanning thirty years, the most significant role of L4-100K is to trimerize hexon monomers, the major components of the adenovirus capsid (Cepko and Sharp, 1983; Hong et al., 2005; Oosterom-Dragon and Ginsberg, 1981). Several publications demonstrated that L4-100K is further involved in the nuclear import of these trimers (Hong et al., 2005; Kauffman and Ginsberg, 1976). In the nucleus, acting as a scaffolding platform, 100K promotes the encapsidation of newly synthesized progeny genomes (Cepko and Sharp, 1982). Although the function of 100K in these processes was successfully proved by either using virus mutants or *in vitro* assays, how 100K accomplishes hexon binding, trimerization, and their capsid assembly remained an open question. Therefore in this study, GST-fused-100K deletion constructs were used to identify the hexon binding site in L4-100K. According to the GST pull-down experiments, the 100K region containing amino acids 215 to 420 (mid-N-terminus) strongly associates with hexons. Interestingly, the same region contains the SCM, NES and one of the phosphorylated tyrosine residues. At this point, it is tempting to speculate that competition (cross-talk) between hexon and CRM1 for binding to the same site (NES) in L4-100K ensures the nuclear export of only hexon-dissociated L4-100K under physiological conditions (6.3). Such a regulation was reported for p53, tetramerization of which occludes its NES to prevent the nuclear export of the DNA-binding form (Stommel et al., 1999).

In addition, the C-terminal fragment of L4-100K was also observed to pull down hexon, although in lower quantities than the mid-N-terminal fragment. This last fragment contains the other phosphorylated tyrosine residue and the arginine-glycine-glycine repeats, which were found to be methylated. To reveal whether the

inactivation of SCM, NES, or RGG boxes interferes with L4-100K's hexon binding activity, co-immunoprecipitation assays were performed using appropriate virus mutants. Surprisingly, neither inactivation of SCM, nor NES altered L4-100K-hexon interaction, but surprisingly substitutions in the RGG boxes resulted in a significant increase in this interaction, which indicates that arginine methylation may regulate the association of L4-100K with hexon. This will be discussed in more detail in Section 6.2. The GST constructs were also used to assay the binding of PRMT1. Although not as clearly seen as in the case of hexon, this interaction occurred via the C-terminal fragment, confirming that the RGG repeats are the target site for methylation mediated by this enzyme. Since L4-100K was shown to form dimers (Xi et al., 2005), the same approach was followed to map the dimerization domain of L4-100K, which was found to be located in the amino terminus of the protein (amino acids 1 to 220).

In this study, the early regulatory protein E1B-55K was identified as a novel interaction partner of L4-100K in adenovirus infection. The association of these regulatory proteins in the late phase of infection is plausible, since the functions of L4-100K and E1B-55K overlap in the viral mRNA transport and translation pathways. In combined immunoprecipitation and immunoblotting experiments, E1B-55K was efficiently precipitated by L4-100K during adenovirus infection. This binding was retained in all virus mutants examined in this study. Therefore, mapping the interaction regions in both proteins required using GST fusions of full length or fragmented 100K and E1B-55K constructs. Results of GST pull-down experiments showed that E1B-55K interacts with two 100K fragments, amino acids 1 - 220, and 215 - 420, with the same efficiency. The overlapping sequence including amino acids 215 to 220 was found to be completely conserved among different Ad serotypes and should be further analyzed by inserting point mutations and *in vitro* binding assays to be able to identify the specific E1B-55K-interacting residues of L4-100K.

Reciprocal pull-down experiments revealed that both the amino and carboxy terminals of E1B-55K protein can interact with L4-100K, and the interaction was

significantly enhanced when both fragments were included. The N-termini of E1B-products display a highly disordered structure including a well-conserved Usp7 (ubiquitin specific protease 7) binding motif (personal communications), whereas the C-terminal parts contain a transcriptional repression domain. The N-terminal 79 residues and the C-terminal 76 residues of this protein comprise another E1B splice variant, 156R with unknown lytic functions (Anderson et al., 1984; Virtanen and Pettersson, 1985). Analysis of a possible association between L4-100K and E1B-156R during lytic adenovirus infection should further contribute to our understanding of both E1B-156R and L4-100K functions in the adenovirus replication cycle.

#### **6.1.2 The Association of L4-100K with E1B-55K may Contribute to Virus-Specific mRNA Transport and Translation Mechanisms**

Adenoviral late mRNAs are transported from the nucleus to the cytoplasm by the E1B-55K/E4orf6 ubiquitin ligase complex (Blanchette et al., 2008; Woo and Berk, 2007). One major gap in the adenovirus-specific mRNA transport issue is the lack of either a specific TL-mRNA binding activity in any of the identified E1B-55K/E4orf6 complex components, or a specific transport receptor. Therefore, discrimination between viral and cellular transcripts was believed to be accomplished through efficient compartmentalization in the nucleus (Leppard, 1998; Leppard and Shenk, 1989). Nevertheless, a specific RNA binding protein must be employed to enable the E1B-55K/E4orf6 complex to couple the late transcripts to an export receptor as well as to the virus-specific translation machinery. At this point, L4-100K, after being translated, may contribute to the viral mRNA transport activity of the E1B-55K/E4orf6 complex by selectively binding to TL-mRNAs and introducing them to the complex. However, both the immunoprecipitation and GST pull-down experiments confirmed that L4-100K binds E1B-55K, independently of E4orf6, and no interaction could be detected between L4-100K and E4orf6. This indicates that formation of an E1B-55K/E4orf6/L4-100K trimeric complex does not occur, or the

association of E1B-55K and L4-100K serves a distinct function apart from the ubiquitin ligase complex. Since the cytoplasmic translocation of the late viral transcripts was shown to require the ubiquitin ligase activity of the E1B-55K/E4orf6 complex, L4-100K and E1B-55K interaction was speculated not to be involved in the mRNA transport process. In the light of a previous observation suggesting that E1B-55K might directly be involved in the eIF4E dephosphorylation process (Zhang et al., 1994), a possible interaction between E1B-55K, L4-100K and eIF4G was explored in regard to virus specific translation pathway. Indeed, co-immunoprecipitation experiments showed that E1B-55K associates with eIF4G both in virus infected A549 and Ad transformed HEK-293 cells. Interestingly, the previously identified interaction of L4-100K and eIF4G was observed to be highly dependent on E1B-55K levels. During wt adenovirus infection L4-100K was efficiently precipitated by eIF4G. However, the binding of plasmid encoded 100K to eIF4G could only be shown successfully in HEK-293 cells, which stably express high levels of E1B-55K. These data not only suggest that E1B-55K plays a mediatory role in L4-100K and eIF4G interaction, but also provides an explanation for such a dephosphorylation defect observed in *dl388* (E1B-55K mutant) infection (Zhang et al., 1994). The E1B product of this mutant virus contains the N-terminal 262, and C-terminal 60 residues which should be sufficient to interact with L4-100K (5.3.2), but lacks a 174-residue fragment from the middle region which was reported to contain a putative ribonucleoprotein (RNP) (Horridge and Leppard, 1998b) and a zinc finger motif (Gonzalez and Flint, 2002). As the strong interaction of E1B-55K and eIF4G was determined, this central region could be considered to include a binding site for eIF4G. If the eIF4G interacting activity is missing in the E1B-55K protein of *dl388*, this could prevent or complicate 100K and eIF4G association. Since L4-100K is the factor directly stimulating the eIF4E dephosphorylation via preventing the Mnk1 binding to eIF4G (Cuesta et al., 2000; Cuesta et al., 2004), inefficient 100K-eIF4G association would lead to “leaky” phosphorylation of eIF4E by Mnk1. Although this model explains the L4-100K and E1B-55K collaboration in the viral translation and *host-shut-off* mechanisms, it does not answer all of the questions such as: How is the translation of particular cellular



mRNAs that are strictly required for the virus growth (e.g. transcription, translation, or transport factors) ensured without the cap-dependent translation machinery? By which mechanism, are the early transcripts lacking a TL structure (e.g. E1B-55K and E4orf6) translated in the late phase of the infection? Has E1B-55K general RNA binding activity *in vivo* as previously shown *in vitro* (Horridge and Leppard, 1998b), and does this RNP-region mediate eIF4G binding? These questions require further investigations on E1B-55K protein to verify the suggested hypothesis about the L4-100K/E1B-55K/eIF4G network.

If the role of L4-100K is more pronounced in the late viral mRNA translation and *host-shut-off* mechanisms, then another RNA binding protein should interact with the E1B-55K/E4orf6 complex as a transport adaptor. A possible candidate for such a task was thought to be one of the interaction partners of E1B-55K protein; E1B-AP which is a member of the heterogeneous nuclear ribonucleoprotein (hnRNP) family (Gabler et al., 1998). According to a previously suggested model, adenovirus achieves selective viral mRNA transport by recruiting certain transcription and transport factors in specific viral microenvironments in the nucleus such as replication/transcription centers. This not only ensures the transport of the viral transcripts, but will also deprive the cellular ones of these factors (Ornelles and Shenk, 1991). Consistent with this hypothesis, immunofluorescence analysis of infected and non-infected cells showed that E1B-AP is redistributed to the periphery of viral replication centers during infection. Indeed, such an accumulation of splicing factors and hnRNPs at replication centers had previously been observed during adenovirus infection (Jiménez-García and Spector, 1993). Since overexpression of E1B-AP5 stimulates both viral and cellular mRNA transport during infection (Gabler et al., 1998) this strengthens its possible role as a transport adaptor for late viral transcripts, but still does not explain how TL-mRNAs are preferentially exported. Co-immunoprecipitation experiments demonstrated that E1B-AP5 indirectly precipitates with L4-100K, most probably via E1B-55K, since *dl1520* ( $\Delta$ E1B-55K) infection exhibited no such interaction. These data hint at a complex network of regulatory viral and cellular proteins that are involved in

adenoviral mRNA transport and translation mechanisms, and also indicate that L4-100K may also contribute to the selective transport of these TL-mRNAs by the help of its TL-recognizing activity. If E1B-AP5 collaborates with the E1B-55K/E4orf6 complex to export viral transcripts, the TAP pathway might be used for this purpose since E1B-AP5 interacts with this receptor (Bachi et al., 2000). Since TAP is the predominant mRNA export receptor in the cell, investigating its role in adenovirus infection will provide further insight into this issue. Furthermore, the role of E1B-AP5 in adenovirus infection is not restricted to mRNA transport, but also includes binding and inhibiting p53's transcriptional activity (Barral et al., 2005), as well as regulating the ATR signaling pathway activated during infection by being involved in the phosphorylation of RPA32 (Blackford et al., 2008).

### **6.1.3 Posttranslational Modifications Regulate L4-100K's Multiple Functions**

When considering the several diverse functions of L4-100K, the requirement for regulatory mechanisms to efficiently accomplish these tasks becomes highly important. The first posttranslational modification identified in L4-100K was the phosphorylation of serine and tyrosine residues (Gambke and Deppert, 1981b). The tyrosine phosphorylation of L4-100K was later shown to play a significant role in its TL-mRNA interaction activity, which stimulates ribosome shunting on adenoviral late transcripts (Xi et al., 2005). When we screened the amino acid sequence of L4-100K for conserved motifs that might be candidates for other posttranslational modifications, the similarity of the amino acid arrangement between residues 407 and 410 to the consensus sumo conjugation motif (SCM) was striking. Sumoylation can modulate several aspects of a protein's functions, influencing its subcellular localization, interaction with its partners, stability and enzymatic activity (Boggio and Chiocca, 2006; Melchior, 2000). Several viral and cellular proteins have been found to be modified by sumoylation (Boggio and Chiocca, 2006). The covalent attachment of

sumo-1 to a specific lysine residue of a protein is a four-step process mediated by several enzymes. The rapidly reversible nature of this modification precludes investigators from efficiently detecting the *in vivo* interaction between the target protein and sumo-1. In L4-100K, this motif, in addition to being highly conserved, locates 16 residues away from the nuclear export signal (NES) of L4-100K. Such an SCM identified in E1B-55K not only affected this oncoprotein's transforming activity (Endter et al., 2001), but also regulated its nucleocytoplasmic shuttling by affecting the neighboring nuclear export signal of this protein (Kindsmuller et al., 2007).

To be able to identify such a modification in L4-100K, the active lysine of the predicted SCM was substituted by an arginine in both a viral and plasmid context. The resultant mutant virus was tested for several properties. Interestingly, the SCM mutation had no significant effect on virus growth or on L4-100K nucleocytoplasmic shuttling activity. Further investigations into the sumoylation potential of L4-100K revealed a direct/indirect binding between wt-100K and sumo-1, which was abolished when the target lysine was inactivated in H5pm4152 virus. Surprisingly, the putative sumo-conjugated L4-100K protein was not detected as being larger than 100 kDa as it should be, since conjugation of this modifier increases a protein's molecular mass from between 20 to 40 kDa. This raises the possibility that another sumoylated protein strongly interacting with L4-100K also runs on SDS-PAGE at a size of 100 kDa when sumoylated. However, the fact that the inactivation of L4-100K-SCM abrogates this interaction undermines this possibility and suggests that probably one of the faster migrating forms (5.5.7) of L4-100K is sumoylated. Hence, the sumoylation of L4-100K will be clarified only after confirming the direct conjugation of sumo-1 to L4-100K by an *in vitro* sumoylation assay. If such an assay proves the sumoylation of L4-100K, then it would be interesting to analyze whether a cleavage product of L4-100K becomes a target for this modification, as well as the reason for it.

Another possible modification site in L4-100K worth investigating was the N-terminal tyrosine residue in a well-conserved amino acid sequence (Y<sup>90</sup>). The fact that this

residue had not been identified as one of the phosphorylated tyrosine residues (Xi et al., 2005) precluded us from considering it as a target for phosphorylation. Hence, we opted for tyrosine sulfation (also known as sulfonation) due to the high similarity of this conserved amino acid pattern to the established sulfation motifs (Monigatti et al., 2002). Such a modification would introduce a new aspect into L4-100K's functional repertoire regarding virus-host cross-talk. Although not as well known as phosphorylation, sulfation of tyrosine residues has been found in many proteins in mammalian cells. Secreted or transmembrane proteins represent the majority of sulfated proteins (Moore, 2003). There are two classes of sulfotransferases (STs) that catalyze the transfer of a sulfuryl group from the universal sulfate donor, adenosine 3'-phosphate 5'-phosphosulfate (PAPS), to the hydroxyl group of a peptidyltyrosine residue: cytosolic STs and membrane associated STs (Chapman et al., 2004). Membrane-associated STs have been implicated in several highly important biological processes, including viral entry into cells, leukocyte adhesion, and anticoagulation. More generally, enzymatic transformations of cell-surface proteoglycans by STs appear to trigger vital molecular-recognition and signal-transduction events. This suggests that STs govern extracellular signaling events and are thus analogous to kinases, which control signaling cascades inside the cell. Such a tyrosine modification was shown to play a critical role in the internalization of HIV, since a major HIV co-receptor was identified as being sulfated (Farzan et al., 1999).

To reveal whether L4-100K is a target for STs, the putative sulfated residue was exchanged with an alanine (Y90A), and mutant virus H5pm4153 was generated. Pulse-chase experiments were performed using <sup>35</sup>S labeled sulfate molecules during H5pg4100 and H5pm4153 infections. If the radiolabeled molecules were only detected in the L4-100K immunoprecipitates from H5pg4100 infected cells, then this would prove that Y<sup>90</sup> is sulfated. However, such a signal could not be detected with L4-100K either in H5pg4100 or in H5pm4153 infections. Thus there was no proof for L4-100K being a target of sulfotransferases. Since the same tyrosine residue is not a phosphorylation target either, this amino acid substitution seemed to affect an

unknown function or interaction of L4-100K, or even its self-association since the dimerization domain was mapped to the N-terminus of this protein.

Interestingly, the Y90A substitution did indeed impair some of the late functions of L4-100K during adenovirus infection. Late protein synthesis efficiency and virus yields of the H5*pm*4153 mutant virus were found to be severely reduced, although the early phase of infection remained unaffected. Moreover, the mutant L4-100K protein displayed distinct cytoplasmic signals when the infected cells were analyzed by indirect immunofluorescence microscopy. Atypically, L4-100K formed numerous dot and/or rod shaped structures in the cytoplasm of 5-20% of all H5*pm*4153 infected cells. Notably, such cytoplasmic aggregates were not observed in the cytoplasm of H1299 cells transiently transfected with pTL-flag-Y90A-100K, indicating the role of another viral protein, or the infection environment in forming such structures. However, nucleocytoplasmic fractionation of the infected cells demonstrated that the Y to A substitution at position 90 does not alter L4-100K shuttling between the cytoplasm and the nucleus, neither did it interfere with hexon, eIF4G, E1B-55K, or PRMT1 binding activity of L4-100K. Only a change in the binding pattern of hexon could be observed during the course of H5*pm*4153 infection, which showed a gradual increase followed by a decrease late in the infection. Nevertheless, this tyrosine residue is apparently highly significant for L4-100K functions since a single amino acid exchange resulted in a drastic drop in the progeny production efficiency of the virus.

## **6.2 Arginine methylation of L4-100K is Critical for Efficient Lytic Infection**

Cell type dependent posttranslational modification of wt 100K mediated by PRMT1 during the course of an infection was previously reported by our group (Kzhyshkowska et al., 2004), highlighting for first time the methylation of an

adenoviral protein. However, the effects of this modification on virus reproduction were unknown. Therefore, this work investigated the consequences of L4-100K methylation throughout the infection cycle particularly focusing on late-phase functions and interactions. The results confirmed that methylated 100K is required during adenovirus infection to ensure sufficient late protein synthesis and virus yield.

L4-100K protein contains three RGG boxes followed by glycine-arginine-rich (GAR) sequences in its C-terminus. This remarkable pattern of arginine-glycine-glycine repeats resembles a methylation motif (Bedford and Richard, 2005; Kzhyshkowska et al., 2004), inspiring us to monitor the effects of such a modification in the viral context. To investigate whether these RGG boxes are the target domain for methylation, we designed and generated a virus mutant encoding a 100K protein with arginine to glycine exchanges in all of the RGG boxes. Indeed, the mutant virus proved defective in 100K methylation compared to the wt virus, pointing to the RGG boxes as the major methylation target, although the protein was slightly methylated at later time points hinting at other methylated arginine residues. Since methylation of arginines in a RGG cluster was shown to alter a protein's conformation (Dery et al., 2008), affect its destination (Bedford and Richard, 2005; Boisvert et al., 2005b; Nichols et al., 2000), protein interactions, and DNA (Boisvert et al., 2005c) or RNA (Mears and Rice, 1996; Riley and Flint, 1993) binding, the properties of this mutant were analyzed in more detail.

First the subcellular distribution of the mutant protein was investigated. Surprisingly, no obvious difference in the localization or appearance of mutant 100K was observed compared to wt protein, either in A549 or other tested cell lines such as H1299 and primary hepatocytes. Furthermore, addition of a general methylation inhibitor (AdOx) did not affect the nucleocytoplasmic shuttling of L4-100K, although the efficiency of lytic infection decreased. These results contradicted a recent report claiming that methylation of the arginine in the third RGG box is required for nuclear import of L4-100K (Iacovides et al., 2007). These different observations may be a result

of different assay set-ups. The authors converted the RGG boxes into AAA sequences in plasmid constructs and transfected cells that were infected with wt virus. However, this study used a virus mutant with only arginine to glycine exchanges in three RGG boxes. Since alanine also contains a methyl group, we planned to substitute arginines with either lysines or glycines. In the viral context, to avoid affecting the L4-33K and L4-22K coding sequence (Fig. 4A) we opted for glycines rather than lysines. None of the virus mutants or plasmid constructs (including the 3RGG mutant) showed any defect in nuclear import, indicating that neither the arginines in the RGG boxes nor their methylation are involved in this process.

The possible residual methylation of the arginines in the downstream GAR region was further investigated to assess their impact on nuclear localization. Examples of several methylated arginine residues have been reported in a RG cluster, some of which are partially methylated (Liu and Dreyfuss, 1995; Ostareck-Lederer et al., 2006; Smith et al., 1999). To analyze this effect, we intended to construct a mutant virus that expresses L4-100K with no possible methylated arginine residues, including GAR motifs in the downstream sequence, as well as a GAR-only mutant. However, these constructs could not be grown as viruses in the helper cell line used here. This indicated how incompetent these mutants are compared to the RGG-box mutant, which was successfully produced. Therefore, RGG.GAR and GAR mutants were generated using a pTL-flag100K plasmid and indeed transfection studies revealed methylation differences compared to wt and the RGG mutant. Co-immunoprecipitation assays with ASYM-24 resulted in no precipitated RGG.GAR.100K protein, and while slight methylation of RGG.100K was observed, it was much less than the wt protein. These results confirmed the partial methylation of arginine residues not in the RGG box domain but in the downstream GAR region. Interestingly, these GAR and RGG.GAR mutants were exclusively located in the cytoplasm and apparently unable to enter the nucleus. Since the nuclear localization signal (NLS) of L4-100K is located in the carboxy terminus (Cuesta et al., 2004), these data suggest that the GAR domain, not the RGG boxes are responsible for nuclear

import.

Next, the RNA and protein interactions of the mutant virus were analyzed. Contributing to selective translation of Ad late mRNAs, 100K can bind both cellular and viral mRNAs, in addition to the eIF4G scaffold protein of the translation initiation complex (Cuesta et al., 2000; Cuesta et al., 2004; Xi et al., 2004; Xi et al., 2005). One of the most important characteristics of RNA binding proteins (such as hnRNPs) is arginine methylation in GAR RNA binding domains (Kzhyshkowska et al., 2001). Several examples demonstrated that arginine methylation acts as a direct signal for RNA interaction, either in a positive or negative way (Bedford and Richard, 2005; Liu and Dreyfuss, 1995; Mears and Rice, 1996). In our experiments we detected up to 6-fold reduction in TL-mRNA binding activity of methylation-defective L4-100K, which was surprising in the light of a previous report demonstrating phosphorylation as the factor deciding this protein's TL-mRNA binding specificity (Xi et al., 2005). The TL-mRNA binding reduction we observed may hint at a possible interplay between two posttranslational modifications, since one of the two phosphorylated tyrosine residues (Y365 and Y682) is in close proximity to the first RGG box (R727). This may be modulated by methylation of this arginine since there is evidence of masking effects between adjacent posttranslational modifications (Bedford and Richard, 2005).

Another very important function of L4-100K involves interacting with hexon monomers to assist their maturation into trimers (Hong et al., 2005; Oosterom-Dragon and Ginsberg, 1981). Although it was shown that hexon protein was precipitated in large amounts with L4-100K specific antibodies (Oosterom-Dragon and Ginsberg, 1980; Riley and Flint, 1993) the hexon interacting domain of 100K was not identified until this study. Therefore, it was explored whether the methylation of RGG boxes could be a signal for this vital interaction. Unexpectedly, we observed improved binding of hexon to the methylation-deficient 100K, although late protein synthesis efficiency was lower than the wt virus. This increase was unique to the hexon interaction since eIF4G binding was not affected by the substitution mutations.



If 100K is sufficient for hexon trimerization and contributes to transporting trimeric hexons into the nucleus, the 100K interaction with hexon molecules should be transient so that 100K can translocate back to the cytoplasm for its other tasks. Dissociation of the complex was thought to occur only if the trimers are efficiently integrated into the capsid (Hong et al., 2005; Oosterom-Dragon and Ginsberg, 1981). In efficient adenovirus infection these maturation and integration steps should proceed rapidly. The tested H5 $\mu$ m4151 mutant might show increased 100K binding to hexon due to prolonged interactions caused by an interfering factor or the loss of some control mechanism. Such a delay in hexon maturation and capsid assembly could account in part for the reduced virus yield observed in these studies. There is also evidence in the literature showing that arginine methylation can be a negative regulator of protein-protein interactions (Bedford and Richard, 2005; Ostareck-Lederer et al., 2006). Thus blocking the methylation of 100K may alter the tuning of 100K-hexon interactions, leading to inefficient hexon trimerization, transport, or capsid assembly, which could further affect other 100K tasks such as TL-mRNA binding. This hypothesis raises a number of questions, including whether this cascade of events requires reversible arginine methylation. Previously, only deiminases were known to convert methylarginine to citrulline by demethylation (Bedford, 2007). Recently, another enzyme called JMJD6 was identified as a histone arginine demethylase located in the nucleus (Chang et al., 2007). To date, it remains unknown whether this arginine demethylase has other substrates, but it is tempting to speculate that this mechanism is also involved in the regulation of 100K-hexon interactions.

Several studies have demonstrated and discussed the role of 100K in the nuclear import of hexons (Cepko and Sharp, 1982; Cepko and Sharp, 1983; Hong et al., 2005). In addition, pVI protein has also been implicated in this process (Kauffman and Ginsberg, 1976; Wodrich et al., 2003). However, some of these data are contradictory, particularly about the transport of hexon trimers favoring either 100K or pVI. It will be of great interest to study the triple interaction of 100K, hexon and pVI and the effect of 100K arginine methylation on this process.

In summary, arginine methylation of 100K in triple RGG boxes was not found to regulate the subcellular localization of 100K protein or selective translation of viral late mRNAs via eIF4G binding. However, it did contribute to efficient adenoviral late protein synthesis by modulating protein-protein/RNA interactions or regulating intracellular trafficking, possibly regulating TL-mRNA binding, hexon biogenesis and virus assembly, topics that should be further investigated.

### **6.3 The Nuclear Export of L4-100K is Mediated by CRM1 During Lytic Infection**

Over the last decade protein and mRNA export receptors utilized by adenoviruses have been explored and eagerly anticipated. However, the nuclear export pathways used by Ads, especially in the late phase of infection are still not as well understood as those in HIV or HSV infection. The late phase of an Ad infection involves extensive mRNA transcription and transport, translation and assembly of the structural proteins, which are mostly orchestrated by E1B-55K, E4orf6 and the late viral regulator L4-100K (Adam and Dreyfuss, 1987; Babiss et al., 1985; Blanchette et al., 2008; Cepko and Sharp, 1982; Dobner and Kzhyskowska, 2001; Hayes et al., 1990a; Leppard and Shenk, 1989). Nucleocytoplasmic shuttling properties of the early viral proteins were extensively studied by *in vitro* and *in vivo* assays (Dobbelstein, 2000; Dobbelstein et al., 1997b; Dosch et al., 2001; Kindsmuller et al., 2007; Kratzer et al., 2000; Weigel and Dobbelstein, 2000). In this study the nuclear export signal and receptor involved in L4-100K nucleocytoplasmic transport was investigated using a mutant virus. The mutational inactivation of a previously suggested (Cuesta et al., 2004) nuclear export signal (NES) in the L4-100K sequence in the viral context confirmed that this leucine-rich motif is also crucial for 100K shuttling in the case of an infection. Moreover, the chemical inhibition of CRM1 by LMB resulted in the nuclear accumulation of 100K in either plasmid transfected or virus infected cells, demonstrating CRM1 as the major export receptor for this late viral protein.

Although several reports affirmed that CRM1, particularly in the late phase of infection is not essential for the adenoviral life cycle (Carter et al., 2003; Flint et al., 2005; Rabino et al., 2000b; Weigel and Dobbelstein, 2000), this study pointed to a great demand for this receptor during infection in the context of 100K export. First of all, mutational inactivation of the L4-100K NES dramatically diminished virus production efficiency, and homologous recombination in the helper cell lines caused reversion to wt virus several times in the propagation process. This reversion not only points a severe defect caused by the inserted mutations but also implicates that the mutations in the 100K gene, not another failure in the genome, is the cause of such an incompetency since only the wt-100K complementation can revert the phenotype. The wt reversion was managed to be overcome by one-step, small-scale virus production which yielded a low-titer of pure L4-100K-NES virus stock (H5pm4165). Second, characterization of H5pm4165 revealed an approximately 200-fold drop in progeny virus production in tested human tumor cell lines, indicating that this signal is essential for efficient completion of the lytic cycle. This result was further supported by the observation that wt virus, in the presence of LMB during the late phase of infection, yielded 15 times less progeny virions. Altogether, these data confirmed that adenovirus utilizes a CRM1-dependent nuclear export pathway late in the infection, although the defect in the wt plus LMB situation was milder than mutational inactivation of the 100K nuclear export signal. A possible explanation for this 'milder defect' could be that although we determined the onset of DNA replication by DBP immune staining, the late phase could have started before LMB addition, and some 100K was still able to use active CRM1. However, in the case of the 100K-NES mutant virus infection, since all 100K expressed from the start carries inactive NES, this might limit the infection capacity. Hindering the L4-100K and CRM1 interaction could result in a chain reaction leading to abrogation of subsequent 100K functions. Another explanation could be that in the case of adenovirus infection LMB was not capable of inhibiting every CRM1 molecule as efficiently as in a non-infection situation. This should be further tested using reporter constructs to monitor the activity of this metabolite during infection.

Moreover, both these possibilities are not mutually exclusive. It should also be noted that the dose, the application time and even the batch of the inhibitor, as well as the infected cell type, may affect the result of these assays. Hence one should be careful in evaluating the consequences of LMB inhibition. The discrepancies between several publications concerning the role of CRM1 in the Ad life cycle may result from the use of different inhibitor substances, in different cell lines, infected at varying multiplicities. Therefore, mutational inactivation of the target protein's NES or downregulation of specific adaptors in the export pathway by siRNA technology may provide more straightforward data about the role of CRM1 in Ad infection.

Together with the finding that the immediate early protein E1A also translocates to the cytoplasm via CRM1 in the late phase of the infection, which was shown to be critical for virus growth (Jiang et al., 2006), and burst size reduction with wt virus in the presence of a CRM1 competitor (Weigel and Dobbelstein, 2000), the results of this study confirm a critical role for CRM1 in adenovirus production.

It is known that the nuclear export of early Ad proteins such as E1A, E1B-55K and E4orf6 requires CRM1 interactions for shuttling in virus infection (Dobbelstein et al., 1997b; Jiang et al., 2006; Kratzer et al., 2000; Weigel and Dobbelstein, 2000). However, the inactivation of NESs in E1B-55K and E4orf6, which together form a ubiquitin ligase complex (Blanchette et al., 2004; Querido et al., 2001), or the inhibition of CRM1 by chemical and peptide inhibitors apparently have no significant effect on the infection progress in tested human tumor cell lines in terms of mRNA export (Flint et al., 2005), or protein synthesis efficiency (Carter et al., 2003; Rabino et al., 2000b). However, our group previously demonstrated that an E1B-55K-NES mutant can translocate to the cytoplasm via a CRM1-independent pathway upon inactivation of its neighboring Sumo conjugation motif (Kindsmuller et al., 2007). Therefore, this early protein could be considered to use more than one export pathway to promote the shuttling of the complex in the absence of CRM1. This may explain why the authors above observed no deficiency in mRNA transport when they blocked the

CRM1 pathway. This further points to CRM1-independent transport of adenoviral mRNAs or an altered CRM1 pathway as suggested by Shindoh and colleagues (Higashino et al., 2005).

In contrast to these two early proteins, we observed a severe defect in the 100K-NES virus mutant, demonstrating that 100K is dependent on CRM1 for its cytoplasmic translocation and further tasks. This motif may be required for selective translation of viral late mRNAs where 100K confers selective binding to TL-mRNAs (Xi et al., 2005) in conjunction with the translation initiation factor eIF4G (Xi et al., 2004). This latter interaction results in the inhibition of a cap-dependent translation mechanism leading to host shut-off, while viral mRNAs are translated via ribosome shunting (Cuesta et al., 2004; Xi et al., 2004; Xi et al., 2005; Zhang et al., 1994; Zhang and Schneider, 1993). The decrease observed in late protein expression (and in eIF4G binding) despite efficient early phase progression may be explained by this hypothesis. However, the drastic reduction in progeny virus production hints that a further encapsidation defect arose from the substitution mutations. This defect may involve hexon trimerization and transport as well as capsid assembly. Since this study demonstrated that the leucine-rich NES motif is not essential for 100K - hexon binding, the 100K - CRM1 interaction might be important for regulating efficient hexon maturation and transport. For instance, hexon - 100K binding may mask the NES of 100K preventing export of the complex to the cytoplasm, suggesting that efficient capsid integration of hexon trimers is a prerequisite for exposing 100K NES and allowing CRM1 interaction. Our data support the model that 100K not only trimerizes hexon monomers but also promotes their nuclear localization (Cepko and Sharp, 1982; Morin and Boulanger, 1986). The role of pVI in this process and the nuclear export receptor mediating the shuttling of this structural protein should be studied further, since pVI was also shown to be involved in hexon transport and bears two leucine-rich nuclear export motifs (Wodrich et al., 2003). Moreover, since addition of LMB in the late phase further decreased the virus yield of 100K-NES mutant, CRM1 may indeed be required for shuttling another late protein, which may well be pVI.

In conclusion, these results demonstrate that CRM1 is the major nuclear export receptor for L4-100K in both plasmid-transfected and virus-infected cells. According to this study, efficient virus replication in different human cell lines was found to depend on a functional 100K-NES and active CRM1. In contrast to some of the previous reports, these data support the model that CRM1 and CRM1-dependent nuclear export are critical to promote adenoviral late gene expression and maximum virus growth. It would be interesting to investigate the effect of the 100K NES mutation on TL-mRNA translation and hexon maturation pathways, as well as identifying the nuclear export receptor responsible for viral mRNA transport and pVI shuttling in the future.

## 7 References

---

- Adachi, Y., and Yanagida, M. (1989). Higher order chromosome structure is affected by cold-sensitive mutations in a *Schizosaccharomyces pombe* gene *crm1+* which encodes a 115-kD protein preferentially localized in the nucleus and its periphery. *J Cell Biol* 108, 1195-1207.
- Adam, S. A., and Dreyfuss, G. (1987). Adenovirus proteins associated with mRNA and hnRNA in infected HeLa cells. *J Virol* 61, 3276-3283.
- Adam, S. A., Nakagawa, T., Swanson, M. S., Woodruff, T. K., and Dreyfuss, G. (1986). mRNA polyadenylate-binding protein: gene isolation and sequencing and identification of a ribonucleoprotein consensus sequence. *Mol Cell Biol* 6, 2932-2943.
- Anderson, C. W., Schmitt, R. C., Smart, J. E., and Lewis, J. B. (1984). Early region 1B of adenovirus 2 encodes two coterminal proteins of 495 and 155 amino acid residues. *J Virol* 50, 387-396.
- Andrade, F., Bull, H. G., Thornberry, N. A., Ketner, G. W., Casciola-Rosen, L. A., and Rosen, A. (2001). Adenovirus L4-100K assembly protein is a granzyme B substrate that potently inhibits granzyme B-mediated cell death. *Immunity* 14, 751-761.
- Andrade, F., Casciola-Rosen, L. A., and Rosen, A. (2003). A novel domain in adenovirus L4-100K is required for stable binding and efficient inhibition of human granzyme B: possible interaction with a species-specific exosite. *Mol Cell Biol* 23, 6315-6326.
- Andrade, F., Fellows, E., Jenne, D. E., Rosen, A., and Young, C. S. (2007). Granzyme H destroys the function of critical adenoviral proteins required for viral DNA replication and granzyme B inhibition. *Embo J* 26, 2148-2157.
- Ankerst, J., and Jonsson, N. (1989). Adenovirus type 9-induced tumorigenesis in the rat mammary gland related to sex hormonal state. *J Natl Cancer Inst* 81, 294-298.
- Araya, N., Hiraga, H., Kako, K., Arao, Y., Kato, S., and Fukamizu, A. (2005). Transcriptional down-regulation through nuclear exclusion of EWS methylated by PRMT1. *Biochem Biophys Res Commun* 329, 653-660.
- Babich, A., Feldman, L. T., Nevins, J. R., Darnell, J. E., and Weinberger, C. (1983). Effect of adenovirus on metabolism of specific host mRNAs: transport control and specific translation discrimination. *Mol Cell Biol* 3, 1212-1221.
- Babiss, L. E., and Ginsberg, H. S. (1984). Adenovirus type 5 early region 1b gene product is required for efficient shutoff of host protein synthesis. *J Virol* 50, 202-212.
- Babiss, L. E., Ginsberg, H. S., and Darnell, J. J. (1985). Adenovirus E1B proteins are required for accumulation of late viral mRNA and for effects on cellular mRNA translation and transport. *Mol Cell Biol* 5, 2552-2558.
- Bachi, A., Braun, I. C., Rodrigues, J. P., Panté, N., Ribbeck, K., von Kobbe, C., Kutay, U., Wilm, M., Görlich, D., Carmo-Fonseca, M., and Izaurralde, E. (2000). The C-terminal domain of TAP interacts with the nuclear pore complex and promotes export of specific CTE-bearing RNA substrates. *RNA* 6, 136-158.

- Baker, A., Rohleder, K. J., Hanakahi, L. A., and Ketner, G. (2007). Adenovirus E4 34k and E1b 55k oncoproteins target host DNA ligase IV for proteasomal degradation. *J Virol* 81, 7034-7040.
- Barker, D. D., and Berk, A. J. (1987). Adenovirus proteins from both E1B reading frames are required for transformation of rodent cells by viral infection and DNA transfection. *Virology* 156, 107-121.
- Barral, P. M., Rusch, A., Turnell, A. S., Gallimore, P. H., Byrd, P. J., Dobner, T., and Grand, R. J. (2005). The interaction of the hnRNP family member E1B-AP5 with p53. *FEBS Lett* 579, 2752-2758.
- Bedford, M. T. (2007). Arginine methylation at a glance. *J Cell Sci* 120, 4243-4246.
- Bedford, M. T., and Richard, S. (2005). Arginine methylation an emerging regulator of protein function. *Mol Cell* 18, 263-272.
- Beltz, G. A., and Flint, S. J. (1979). Inhibition of HeLa cell protein synthesis during adenovirus infection: restriction of cellular messenger RNA sequences to the nucleus. *J Mol Biol* 131, 353-373.
- Benkö, M., Elo, P., Ursu, K., Ahne, W., LaPatra, S. E., Thomson, D., and Harrach, B. (2002). First molecular evidence for the existence of distinct fish and snake adenoviruses. *J Virol* 76, 10056-10059.
- Bergelson, J. M., Cunningham, J. A., Droguett, G., Kurt-Jones, E. A., Krithivas, A., Hong, J. S., Horwitz, M. S., Crowell, R. L., and Finberg, R. W. (1997). Isolation of a common receptor for coxsackie B viruses and adenoviruses 2 and 5. *Science* 275, 1320-1323.
- Berk, A. J. (2007). *Adenoviridae: The viruses and their replication*, 5 edn (New York, N. Y., Raven Press).
- Bernards, R., Vaessen, M. J., van der Eb, A. J., and Sussenbach, J. S. (1983). Construction and characterization of an adenovirus type 5/adenovirus type 12 recombinant virus. *Virology* 131, 30-38.
- Blackford, A. N., Bruton, R. K., Dirlik, O., Stewart, G. S., Taylor, A. M., Dobner, T., Grand, R. J., and Turnell, A. S. (2008). A role for E1B-AP5 in ATR signaling pathways during adenovirus infection. *J Virol* 82, 7640-7652.
- Blanchette, P., Cheng, C. Y., Yan, Q., Ketner, G., Ornelles, D. A., Dobner, T., Conaway, R. C., Conaway, J. W., and Branton, P. E. (2004). Both BC-box motifs of adenovirus protein E4orf6 are required to efficiently assemble an E3 ligase complex that degrades p53. *Mol Cell Biol* 24, 9619-9629.
- Blanchette, P., Kindsmuller, K., Groitl, P., Dallaire, F., Speiseder, T., Branton, P. E., and Dobner, T. (2008). Control of mRNA export by adenovirus E4orf6 and E1B55K proteins during productive infection requires E4orf6 ubiquitin ligase activity. *J Virol* 82, 2642-2651.
- Boggio, R., and Chiocca, S. (2006). Viruses and sumoylation: recent highlights. *Curr Opin Microbiol* 9, 430-436.
- Boisvert, F. M., Dery, U., Masson, J. Y., and Richard, S. (2005a). Arginine methylation of MRE11 by PRMT1 is required for DNA damage checkpoint control. *Genes Dev* 19, 671-676.
- Boisvert, F. M., Hendzel, M. J., Masson, J. Y., and Richard, S. (2005b). Methylation of MRE11 regulates its nuclear compartmentalization. *Cell Cycle* 4, 981-989.
- Boisvert, F. M., Rhie, A., Richard, S., and Doherty, A. J. (2005c). The GAR motif of 53BP1 is arginine methylated by PRMT1 and is necessary for 53BP1 DNA binding activity. *Cell Cycle* 4, 1834-1841.



- Boulanger, M. C., Liang, C., Russell, R. S., Lin, R., Bedford, M. T., Wainberg, M. A., and Richard, S. (2005). Methylation of Tat by PRMT6 regulates human immunodeficiency virus type 1 gene expression. *J Virol* 79, 124-131.
- Bradford, M. M. (1976). A rapid and sensitive method for the quantitation of microgram quantities of protein utilizing the principle of protein-dye binding. *Anal Biochem* 72, 248-254.
- Bridge, E., and Ketner, G. (1989). Redundant control of adenovirus late gene expression by early region 4. *J Virol* 63, 631-638.
- Bridge, E., and Ketner, G. (1990). Interaction of adenoviral E4 and E1b products in late gene expression. *Virology* 174, 345-353.
- Bridge, E., Medghalchi, S., Ubol, S., Leesong, M., and Ketner, G. (1993). Adenovirus early region 4 and viral DNA synthesis. *Virology* 193, 794-801.
- Bullock, W. O., Fernandez, J.M., und Short, J.M. (1987). XL1-Blue: A high efficiency plasmid transforming recA Escherichia coli strain with b-galactosidase selection. In *Biotechniques*, pp. 376-379.
- Burgert, H. G., Ruzsics, Z., Obermeier, S., Hilgendorf, A., Windheim, M., and Elsing, A. (2002). Subversion of host defense mechanisms by adenoviruses. *Curr Top Microbiol Immunol* 269, 273-318.
- Byrd, M. P., Zamora, M., and Lloyd, R. E. (2005). Translation of eukaryotic translation initiation factor 4G1 (eIF4G1) proceeds from multiple mRNAs containing a novel cap-dependent internal ribosome entry site (IRES) that is active during poliovirus infection. *J Biol Chem* 280, 18610-18622.
- Cabrita, G., Iqbal, M., Reddy, H., and Kemp, G. (1997). Activation of the adenovirus protease requires sequence elements from both ends of the activating peptide. *J Biol Chem* 272, 5635-5639.
- Carter, C. C., Izadpanah, R., and Bridge, E. (2003). Evaluating the role of CRM1-mediated export for adenovirus gene expression. *Virology* 315, 224-233.
- Catalucci, D., Sporeno, E., Cirillo, A., Ciliberto, G., Nicosia, A., and Colloca, S. (2005). An adenovirus type 5 (Ad5) amplicon-based packaging cell line for production of high-capacity helper-independent deltaE1-E2-E3-E4 Ad5 vectors. *J Virol* 79, 6400-6409.
- Cepko, C. L., and Sharp, P. A. (1982). Assembly of adenovirus major capsid protein is mediated by a nonvirion protein. *Cell* 31, 407-415.
- Cepko, C. L., and Sharp, P. A. (1983). Analysis of Ad5 hexon and 100K ts mutants using conformation-specific monoclonal antibodies. *Virology* 129, 137-154.
- Chang, B., Chen, Y., Zhao, Y., and Bruick, R. K. (2007). JMJD6 is a histone arginine demethylase. *Science* 318, 444-447.
- Chapman, E., Best, M. D., Hanson, S. R., and Wong, C. H. (2004). Sulfotransferases: structure, mechanism, biological activity, inhibition, and synthetic utility. *Angew Chem Int Ed Engl* 43, 3526-3548.
- Chauvin, C., Suh, M., Remy, C., and Benabid, A. L. (1990). Failure to detect viral genomic sequences of three viruses (herpes simplex, simian virus 40 and adenovirus) in human and rat brain tumors. *Ital J Neurol Sci* 11, 347-357.
- Chen, D., Ma, H., Hong, H., Koh, S. S., Huang, S. M., Schurter, B. T., Aswad, D. W., and Stallcup, M. R. (1999). Regulation of transcription by a protein methyltransferase. *Science* 284, 2174-2177.

- Chen, P. H., Ornelles, D. A., and Shenk, T. (1993). The adenovirus L3 23-kilodalton proteinase cleaves the amino-terminal head domain from cytokeratin 18 and disrupts the cytokeratin network of HeLa cells. *J Virol* 67, 3507-3514.
- Cook, J. L., and Lewis, A. M., Jr. (1987). Immunological surveillance against DNA-virus-transformed cells: correlations between natural killer cell cytolytic competence and tumor susceptibility of athymic rodents. *J Virol* 61, 2155-2161.
- Cuesta, R., Xi, Q., and Schneider, R. J. (2000). Adenovirus-specific translation by displacement of kinase Mnk1 from cap-initiation complex eIF4F. *EMBO J* 19, 3465-3474.
- Cuesta, R., Xi, Q., and Schneider, R. J. (2004). Structural basis for competitive inhibition of eIF4G-Mnk1 interaction by the adenovirus 100-kilodalton protein. *J Virol* 78, 7707-7716.
- Cutt, J. R., Shenk, T., and Hearing, P. (1987). Analysis of adenovirus early region 4-encoded polypeptides synthesized in productively infected cells. *J Virol* 61, 543-552.
- Davison, A. J., Benko, M., and Harrach, B. (2003). Genetic content and evolution of adenoviruses. *J Gen Virol* 84, 2895-2908.
- Dery, U., Coulombe, Y., Rodrigue, A., Stasiak, A., Richard, S., and Masson, J. Y. (2008). A glycine-arginine domain in control of the human MRE11 DNA repair protein. *Mol Cell Biol* 28, 3058-3069.
- Dingle, J. H., and Langmuir, A. D. (1968). Epidemiology of acute, respiratory disease in military recruits. *Am Rev Respir Dis* 97, Suppl:1-65.
- Diouri, M., Keyvani-Amineh, H., Geoghegan, K. F., and Weber, J. M. (1996). Cleavage efficiency by adenovirus protease is site-dependent. *J Biol Chem* 271, 32511-32514.
- Dobbelstein, M. (2000). The nuclear export signal within the adenovirus E4orf6 protein contributes to several steps in the viral life cycle. *J Virol* 74, 12000.
- Dobbelstein, M., Roth, J., Kimberly, W. T., Levine, A. J., and Shenk, T. (1997a). Nuclear export of the E1B 55-kDa and E4 34-kDa adenoviral oncoproteins mediated by a rev-like signal sequence. *EMBO J* 16, 4276-4284.
- Dobbelstein, M., Roth, J., Kimberly, W. T., Levine, A. J., and Shenk, T. (1997b). Nuclear export of the E1B 55-kDa and E4 34-kDa adenoviral oncoproteins mediated by a rev-like signal sequence. *Embo J* 16, 4276-4284.
- Dobner, T., Horikoshi, N., Rubenwolf, S., and Shenk, T. (1996). Blockage by adenovirus E4orf6 of transcriptional activation by the p53 tumor suppressor. *Science* 272, 1470-1473.
- Dobner, T., and Kzhyshkowska, J. (2001). Nuclear export of adenovirus RNA. *Curr Top Microbiol Immunol* 259, 25-54.
- Dolph, P. J., Huang, J. T., and Schneider, R. J. (1990). Translation by the adenovirus tripartite leader: elements which determine independence from cap-binding protein complex. *J Virol* 64, 2669-2677.
- Dolph, P. J., Racaniello, V., Villamarin, A., Palladino, F., and Schneider, R. J. (1988). The adenovirus tripartite leader may eliminate the requirement for cap-binding protein complex during translation initiation. *J Virol* 62, 2059-2066.

- Dosch, T., Horn, F., Schneider, G., Kratzer, F., Dobner, T., Hauber, J., and Stauber, R. H. (2001). The adenovirus type 5 E1B-55K oncoprotein actively shuttles in virus-infected cells, whereas transport of E4orf6 is mediated by a CRM1-independent mechanism. *J Virol* 75, 5677-5683.
- Dulbecco, R., and Freeman, G. (1959). Plaque production by the polyoma virus. *Virology* 8, 396-397.
- Endter, C., and Dobner, T. (2004). Cell transformation by human adenoviruses. *Curr Top Microbiol Immunol* 273, 163-214.
- Endter, C., Kzhyshkowska, J., Stauber, R., and Dobner, T. (2001). SUMO-1 modification required for transformation by adenovirus type 5 early region 1B 55-kDa oncoprotein. *Proc Natl Acad Sci U S A* 98, 11312-11317.
- Engelsma, D., Bernad, R., Calafat, J., and Fornerod, M. (2004). Supraphysiological nuclear export signals bind CRM1 independently of RanGTP and arrest at Nup358. *Embo J* 23, 3643-3652.
- Englmeier, L., Fornerod, M., Bischoff, F. R., Petosa, C., Mattaj, I. W., and Kutay, U. (2001). RanBP3 influences interactions between CRM1 and its nuclear protein export substrates. *EMBO Rep* 2, 926-932.
- Eystathioy, T., Chan, E. K., Tenenbaum, S. A., Keene, J. D., Griffith, K., and Fritzler, M. J. (2002). A phosphorylated cytoplasmic autoantigen, GW182, associates with a unique population of human mRNAs within novel cytoplasmic speckles. *Mol Biol Cell* 13, 1338-1351.
- Fackelmayer, F. O. (2005). Protein arginine methyltransferases: guardians of the Arg? *Trends Biochem Sci* 30, 666-671.
- Fallaux, F. J., Kranenburg, O., Cramer, S. J., Houweling, A., Van Ormondt, H., Hoebe, R. C., and Van Der Eb, A. J. (1996). Characterization of 911: a new helper cell line for the titration and propagation of early region 1-deleted adenoviral vectors. *Hum Gene Ther* 7, 215-222.
- Farley, D. C., Brown, J. L., and Leppard, K. N. (2004). Activation of the early-late switch in adenovirus type 5 major late transcription unit expression by L4 gene products. *J Virol* 78, 1782-1791.
- Farzan, M., Mirzabekov, T., Kolchinsky, P., Wyatt, R., Cayabyab, M., Gerard, N. P., Gerard, C., Sodroski, J., and Choe, H. (1999). Tyrosine sulfation of the amino terminus of CCR5 facilitates HIV-1 entry. *Cell* 96, 667-676.
- Fischer, U., Huber, J., Boelens, W. C., Mattaj, I. W., and Luhrmann, R. (1995). The HIV-1 Rev activation domain is a nuclear export signal that accesses an export pathway used by specific cellular RNAs. *Cell* 82, 475-483.
- Flint, S. J., and Gonzalez, R. A. (2003). Regulation of mRNA production by the adenoviral E1B 55-kDa and E4 Orf6 proteins. *Curr Top Microbiol Immunol* 272, 287-330.
- Flint, S. J., Huang, W., Goodhouse, J., and Kyin, S. (2005). A peptide inhibitor of exportin1 blocks shuttling of the adenoviral E1B 55 kDa protein but not export of viral late mRNAs. *Virology* 337, 7-17.
- Fornerod, M., Ohno, M., Yoshida, M., and Mattaj, I. W. (1997). CRM1 is an export receptor for leucine-rich nuclear export signals. *Cell* 90, 1051-1060.
- Futterer, J., Kiss-Laszlo, Z., and Hohn, T. (1993). Nonlinear ribosome migration on cauliflower mosaic virus 35S RNA. *Cell* 73, 789-802.

- Gabler, S., Schütt, H., Groitl, P., Wolf, H., Shenk, T., and Dobner, T. (1998). E1B 55-kilodalton-associated protein: a cellular protein with RNA-binding activity implicated in nucleocytoplasmic transport of adenovirus and cellular mRNAs. *J Virol* 72, 7960-7971.
- Gambke, C., and Deppert, W. (1981a). Late nonstructural 100,000- and 33,000-dalton proteins of adenovirus type 2. I. Subcellular localization during the course of infection. *J Virol* 40, 585-593.
- Gambke, C., and Deppert, W. (1981b). Late nonstructural 100,000- and 33,000-dalton proteins of adenovirus type 2. II. Immunological and protein chemical analysis. *J Virol* 40, 594-598.
- Gey, G. O., Coffman, W. D., and Kubicek, M. T. (1952). Tissue culture studies of the proliferative capacity of cervical carcinoma and normal epithelium. *Cancer Res* 12L, 264.
- Giard, R. J., Aaronson, S. A., Todaro, G. J., Arnstein, P., Kersey, J. H., Dosik, H., and Parks, W. P. (1973). *In vitro* cultivation of human tumors: establishment of cell lines derived from a series of solid tumors. *J Natl Cancer Inst* 51, 1417-1423.
- Ginsberg, H. S., Gold, E., Jordan, W. S., Jr., Katz, S., Badger, G. F., and Dingle, J. H. (1955). Relation of the new respiratory agents to acute respiratory diseases. *Am J Public Health* 45, 915-922.
- Gonzalez, R. A., and Flint, S. J. (2002). Effects of mutations in the adenoviral E1B 55-kilodalton protein coding sequence on viral late mRNA metabolism. *J Virol* 76, 4507-4519.
- Görlich, D., and Kutay, U. (1999). Transport between the cell nucleus and the cytoplasm. *Annu Rev Cell Dev Biol* 15, 607-660.
- Graham, F. L. (1984). Transformation by and oncogenicity of human adenoviruses. In *The adenoviruses*, H. S. Ginsberg, ed. (New York, Plenum Press), pp. 339-398.
- Graham, F. L., Rowe, D. T., McKinnon, R., Bacchetti, S., Ruben, M., and Branton, P. E. (1984). Transformation by human adenoviruses. *J Cell Physiol Suppl* 3, 151-163.
- Graham, F. L., Smiley, J., Russel, W. C., and Nairn, R. (1977). Characteristics of a human cell line transformed by DNA from human adenovirus type 5. *J Gen Virol* 36, 59-72.
- Graham, F. L., and van der Eb, A. J. (1973). A new technique for the assay of infectivity of human adenovirus 5 DNA. *Virology* 52, 456-467.
- Groitl, P., and Dobner, T. (2007). Construction of adenovirus type 5 early region 1 and 4 virus mutants. *Methods Mol Med* 130, 29-39.
- Guillouzo, A., Corlu, A., Aninat, C., Glaise, D., Morel, F., and Guguen-Guillouzo, C. (2007). The human hepatoma HepaRG cells: a highly differentiated model for studies of liver metabolism and toxicity of xenobiotics. *Chem Biol Interact* 168, 66-73.
- Gustafsson, B., Huang, W., Bogdanovic, G., Gauffin, F., Nordgren, A., Talekar, G., Ornelles, D. A., and Gooding, L. R. (2007). Adenovirus DNA is detected at increased frequency in Guthrie cards from children who develop acute lymphoblastic leukaemia. *Br J Cancer* 97, 992-994.
- Halbert, D. N., Cutt, J. R., and Shenk, T. (1985). Adenovirus early region 4 encodes functions required for efficient DNA replication, late gene expression, and host cell shutoff. *J Virol* 56, 250-257.
- Hanahan, D. (1983). Studies on transformation of *Escherichia coli* with plasmids. *J Mol Biol* 166, 557-580.

- Harada, J. N., and Berk, A. J. (1999). p53-independent and -dependent requirements for E1B-55k in adenovirus type 5 replication. *J Virol* 73, 5333-5344.
- Hartl, B., Zeller, T., Blanchette, P., Kremmer, E., and Dobner, T. (2008). Adenovirus type 5 early region 1B 55-kDa oncoprotein can promote cell transformation by a mechanism independent from blocking p53-activated transcription. *Oncogene* 27, 3673-3684.
- Hayes, B. W., Telling, G. C., Myat, M. M., Williams, J. F., and Flint, S. J. (1990a). The adenovirus L4 100-kilodalton protein is necessary for efficient translation of viral late mRNA species. *J Virol* 64, 2732-2742.
- Hayes, B. W., Telling, G. C., Myat, M. M., Williams, J. F., and Flint, S. J. (1990b). The adenovirus L4 100-kilodalton protein is necessary for efficient translation of viral late mRNA species. *J Virol* 64, 2732-2742.
- Herrmann, F., Bossert, M., Schwander, A., Akgun, E., and Fackelmayer, F. O. (2004). Arginine methylation of scaffold attachment factor A by heterogeneous nuclear ribonucleoprotein particle-associated PRMT1. *J Biol Chem* 279, 48774-48779.
- Herrmann, F., Lee, J., Bedford, M. T., and Fackelmayer, F. O. (2005). Dynamics of human protein arginine methyltransferase 1 (PRMT1) in vivo. *J Biol Chem* 280, 38005-38010.
- Higashino, F., Aoyagi, M., Takahashi, A., Ishino, M., Taoka, M., Isobe, T., Kobayashi, M., Totsuka, Y., Kohgo, T., and Shindoh, M. (2005). Adenovirus E4orf6 targets pp32/LANP to control the fate of ARE-containing mRNAs by perturbing the CRM1-dependent mechanism. *J Cell Biol* 170, 15-20.
- Hilleman, M. R., and Werner, J. H. (1954). Recovery of new agents from patients with acute respiratory illness. *Proc Soc Exp Biol Med* 85, 183-188.
- Hodges, B. L., Evans, H. K., Everett, R. S., Ding, E. Y., Serra, D., and Amalfitano, A. (2001). Adenovirus vectors with the 100K gene deleted and their potential for multiple gene therapy applications. *J Virol* 75, 5913-5920.
- Hong, S. S., Szolajska, E., Schoehn, G., Franqueville, L., Myhre, S., Lindholm, L., Ruigrok, R. W., Boulanger, P., and Chroboczek, J. (2005). The 100K-chaperone protein from adenovirus serotype 2 (Subgroup C) assists in trimerization and nuclear localization of hexons from subgroups C and B adenoviruses. *J Mol Biol* 352, 125-138.
- Horridge, J. J., and Leppard, K. N. (1998a). RNA-binding activity of the E1B 55-kilodalton protein from human adenovirus type 5. *J Virol* 72, 9374-9379.
- Horridge, J. J., and Leppard, K. N. (1998b). RNA-binding activity of the E1B 55-kilodalton protein from human adenovirus type 5. *J Virol* 72, 9374-9379.
- Horwitz, M. S. (1996). Adenoviruses. In *Virology*, B. N. Fields, D. M. Knipe, and P. M. Howley, eds. (New York, Lippincott-Raven), pp. 2149-2171.
- Huang, J. T., and Schneider, R. J. (1991). Adenovirus inhibition of cellular protein synthesis involves inactivation of cap-binding protein. *Cell* 65, 271-280.
- Huang, M. M., and Hearing, P. (1989). Adenovirus early region 4 encodes two gene products with redundant effects in lytic infection. *J Virol* 63, 2605-2615.
- Huang, W., and Flint, S. J. (1998a). The tripartite leader sequence of subgroup C adenovirus major late mRNAs can increase the efficiency of mRNA export. *J Virol* 72, 225-235.

- Huang, W., and Flint, S. J. (1998b). The tripartite leader sequence of subgroup C adenovirus major late mRNAs can increase the efficiency of mRNA export. *J Virol* 72, 225-235.
- Hutten, S., and Kehlenbach, R. H. (2007). CRM1-mediated nuclear export: to the pore and beyond. *Trends Cell Biol* 17, 193-201.
- Hutton, F. G., Turnell, A. S., Gallimore, P. H., and Grand, R. J. (2000). Consequences of disruption of the interaction between p53 and the larger adenovirus early region 1B protein in adenovirus E1 transformed human cells. *Oncogene* 19, 452-462.
- Iacovides, D. C., O'Shea, C. C., Osés-Prieto, J., Burlingame, A., and McCormick, F. (2007). Critical role for arginine methylation in adenovirus-infected cells. *J Virol* 81, 13209-13217.
- Izaurrealde, E., and Mattaj, I. W. (1995). RNA export. *Cell* 81, 153-159.
- Javier, R. T., Raska, K., Jr., Macdonald, G. J., and Shenk, T. (1991). Human adenovirus type 9-induced rat mammary tumors. *J Virol* 65, 3192-3202.
- Jawetz, E. (1959). The story of shipyard eye. *Br Med J*, 873-876.
- Jiang, H., Olson, M. V., Medrano, D. R., Lee, O. H., Xu, J., Piao, Y., Alonso, M. M., Gomez-Manzano, C., Hung, M. C., Yung, W. K., and Fueyo, J. (2006). A novel CRM1-dependent nuclear export signal in adenoviral E1A protein regulated by phosphorylation. *Faseb J* 20, 2603-2605.
- Jiménez-García, L. F., and Spector, D. L. (1993). In vivo evidence that transcription and splicing are coordinated by a recruiting mechanism. *Cell* 73, 47-59.
- Jones, N., and Shenk, T. (1979). Isolation of adenovirus type 5 host range deletion mutants defective for transformation of rat embryo cells. *Cell* 17, 683-689.
- Kamura, T., Burian, D., Yan, Q., Schmidt, S. L., Lane, W. S., Querido, E., Branton, P. E., Shilatifard, A., Conaway, R. C., and Conaway, J. W. (2001). Muf1, a novel Elongin BC-interacting leucine-rich repeat protein that can assemble with Cul5 and Rbx1 to reconstitute a ubiquitin ligase. *J Biol Chem* 276, 29748-29753.
- Kao, C. C., Yew, P. R., and Berk, A. J. (1990). Domains required for in vitro association between the cellular p53 and the adenovirus 2 E1B 55K proteins. *Virology* 179, 806-814.
- Kauffman, R. S., and Ginsberg, H. S. (1976). Characterization of a temperature-sensitive, hexon transport mutant of type 5 adenovirus. *J Virol* 19, 643-658.
- Kindsmüller, K. (2002) Molekularbiologische Charakterisierung von Mutanten des Adenovirus Typ 5 E1B-55kDa-Proteins, Diplomarbeit, Universität Regensburg.
- Kindsmüller, K., Groitl, P., Hartl, B., Blanchette, P., Hauber, J., and Dobner, T. (2007). Intranuclear targeting and nuclear export of the adenovirus E1B-55K protein are regulated by SUMO1 conjugation. *Proc Natl Acad Sci U S A* 104, 6684-6689.
- Kosulin, K., Haberler, C., Hainfellner, J. A., Amann, G., Lang, S., and Lion, T. (2007). Investigation of adenovirus occurrence in pediatric tumor entities. *J Virol* 81, 7629-7635.
- Kratzer, F., Rosorius, O., Heger, P., Hirschmann, N., Dobner, T., Hauber, J., and Stauber, R. H. (2000). The adenovirus type 5 E1B-55K oncoprotein is a highly active shuttle protein and shuttling is independent of E4orf6, p53 and Mdm2. *Oncogene* 19, 850-857.

- Krätzer, F., Rosorius, O., Heger, P., Hirschmann, N., Dobner, T., Hauber, J., and Stauber, R. H. (2000). The adenovirus type 5 E1B-55k oncoprotein is a highly active shuttle protein and shuttling is independent of E4orf6, p53 and Mdm2. *Oncogene* 19, 850-857.
- Kudo, N., Matsumori, N., Taoka, H., Fujiwara, D., Schreiner, E. P., Wolff, B., Yoshida, M., and Horinouchi, S. (1999). Leptomycin B inactivates CRM1/exportin 1 by covalent modification at a cysteine residue in the central conserved region. *Proc Natl Acad Sci U S A* 96, 9112-9117.
- Kutay, U., and Guttinger, S. (2005). Leucine-rich nuclear-export signals: born to be weak. *Trends Cell Biol* 15, 121-124.
- Kzhyshkowska, J., Kremmer, E., Hofmann, M., Wolf, H., and Dobner, T. (2004). Protein arginine methylation during lytic adenovirus infection. *Biochem J* 383, 259-265.
- Kzhyshkowska, J., Schütt, H., Liss, M., Stauber, R., Wolf, H., and Dobner, T. (2000). The adenovirus type 5 early 1B 55-kDa-associated protein E1B-AP5 is methylated in vitro and in vivo. In Vorbereitung.
- Kzhyshkowska, J., Schütt, H., Liss, M., Kremmer, E., Stauber, R., Wolf, H., and Dobner, T. (2001). Heterogeneous nuclear ribonucleoprotein E1B-AP5 is methylated in its Arg-Gly-Gly (RGG) box and interacts with human arginine methyltransferase HRMT1L1. *Biochem J* 358, 305-314.
- Laemmli, U. K. (1970). Cleavage of structural proteins during the assembly of the head of bacteriophage T4. *Nature* 227, 680-685.
- Lamphear, B. J., and Panniers, R. (1991). Heat shock impairs the interaction of cap-binding protein complex with 5' mRNA cap. *J Biol Chem* 266, 2789-2794.
- Leppard, K. N. (1998). Regulated RNA processing and RNA transport during adenovirus infection. *Semin Virol* 8, 301-307.
- Leppard, K. N., and Shenk, T. (1989). The adenovirus E1B 55 kd protein influences mRNA transport via an intranuclear effect on RNA metabolism. *EMBO J* 8, 2329-2336.
- Li, Y. J., Stallcup, M. R., and Lai, M. M. (2004). Hepatitis delta virus antigen is methylated at arginine residues, and methylation regulates subcellular localization and RNA replication. *J Virol* 78, 13325-13334.
- Lichtenstein, D. L., Doronin, K., Toth, K., Kuppuswamy, M., Wold, W. S., and Tollefson, A. E. (2004a). Adenovirus E3-6.7K protein is required in conjunction with the E3-RID protein complex for the internalization and degradation of TRAIL receptor 2. *J Virol* 78, 12297-12307.
- Lichtenstein, D. L., Toth, K., Doronin, K., Tollefson, A. E., and Wold, W. S. (2004b). Functions and mechanisms of action of the adenovirus E3 proteins. *Int Rev Immunol* 23, 75-111.
- Lindsay, M. E., Holaska, J. M., Welch, K., Paschal, B. M., and Macara, I. G. (2001). Ran-binding protein 3 is a cofactor for Crm1-mediated nuclear protein export. *J Cell Biol* 153, 1391-1402.
- Liu, Q., and Dreyfuss, G. (1995). In vivo and in vitro arginine methylation of RNA-binding proteins. *Mol Cell Biol* 15, 2800-2808.
- Lukong, K. E., and Richard, S. (2004). Arginine methylation signals mRNA export. *Nat Struct Mol Biol* 11, 914-915.
- Mackey, J. K., Green, M., Wold, W. S. M., and Ridgen, P. (1979). Analysis of human cancer DNA for DNA sequences of human adenovirus type 4. *J Natl Cancer Inst* 62, 23-26.

- Mackey, J. K., Rigden, P. M., and Green, M. (1976). Do highly oncogenic group A human adenoviruses cause human cancer? Analysis of human tumors for adenovirus 12 transforming DNA sequences. *Proc Natl Acad Sci USA* 73, 4657-4661.
- Marton, M. J., Baim, S. B., Ornelles, D. A., and Shenk, T. (1990). The adenovirus E4 17-kilodalton protein complexes with the cellular transcription factor E2F, altering its DNA-binding properties and stimulating E1A-independent accumulation of E2 mRNA. *J Virol* 64, 2345-2359.
- Mathews, M. B., and Shenk, T. (1991). Adenovirus virus-associated RNA and translation control. *J Virol* 65, 5657-5662.
- Mathias, P., Wickham, T., Moore, M., and Nemerow, G. (1994). Multiple adenovirus serotypes use alpha v integrins for infection. *J Virol* 68, 6811-6814.
- Mears, W. E., and Rice, S. A. (1996). The RGG box motif of the herpes simplex virus ICP27 protein mediates an RNA-binding activity and determines in vivo methylation. *J Virol* 70, 7445-7453.
- Melchior, F. (2000). SUMO - nonclassical ubiquitin. *Annu Rev Cell Biol* 16, 591-626.
- Mitsudomi, T., Steinberg, S. M., Nau, M. M., Carbone, D., D'Amico, D., Bodner, H. K., Oie, H. K., Linnoila, R. I., Mulshine, J. L., Minna, J. D., and Gazdar, A. F. (1992). p53 gene mutations in non-small-lung cell cancer cell lines and their correlation with the presence of ras mutations and clinical features. *Oncogene* 7, 171-180.
- Modrow, S., and Falke, D. (1997). *Molekulare Virologie* (Heidelberg, Spektrum Akademischer Verlag GmbH).
- Monigatti, F., Gasteiger, E., Bairoch, A., and Jung, E. (2002). The Sulfinator: predicting tyrosine sulfation sites in protein sequences. *Bioinformatics* 18, 769-770.
- Moore, K. L. (2003). The biology and enzymology of protein tyrosine O-sulfation. *J Biol Chem* 278, 24243-24246.
- Morin, N., and Boulanger, P. (1986). Hexon trimerization occurring in an assembly-defective, 100K temperature-sensitive mutant of adenovirus 2. *Virology* 152, 11-31.
- Muller, S., Berger, M., Lehembre, F., Seeler, J. S., Haupt, Y., and Dejean, A. (2000). c-Jun and p53 activity is modulated by SUMO-1 modification. *J Biol Chem* 275, 13321-13329.
- Nevels, M., Täuber, B., Kremmer, E., Spruss, T., Wolf, H., and Dobner, T. (1999). Transforming potential of the adenovirus type 5 E4orf3 protein. *J Virol* 73, 1591-1600.
- Nevins, J. R., and Vogt, P. K. (1996). Cell transformation by viruses. In *Virology* D. M. K. B. N. Fields, and P. M. Howley, ed. (New York, Lippincott-Raven), pp. 301-343.
- Nichols, R. C., Wang, X. W., Tang, J., Hamilton, B. J., High, F. A., Herschman, H. R., and Rigby, W. F. (2000). The RGG domain in hnRNP A2 affects subcellular localization. *Exp Cell Res* 256, 522-532.
- O'Shea, C. C., Johnson, L., Bagus, B., Choi, S., Nicholas, C., Shen, A., Boyle, L., Pandey, K., Soria, C., Kunich, J., *et al.* (2004). Late viral RNA export, rather than p53 inactivation, determines ONYX-015 tumor selectivity. *Cancer Cell* 6, 611-623.
- Oosterom-Dragon, E. A., and Ginsberg, H. S. (1980). Purification and preliminary immunological characterization of the type 5 adenovirus, nonstructural 100,000-dalton protein. *J Virol* 33, 1203-1207.



- Oosterom-Dragon, E. A., and Ginsberg, H. S. (1981). Characterization of two temperature-sensitive mutants of type 5 adenovirus with mutations in the 100,000-dalton protein gene. *J Virol* 40, 491-500.
- Oosterom Dragon, E. A., and Ginsberg, H. S. (1981). Characterization of two temperature-sensitive mutants of type 5 adenovirus with mutations in the 100,000-dalton protein gene. *J Virol* 40, 491-500.
- Ornelles, D. A., and Shenk, T. (1991). Localization of the adenovirus early region 1B 55-kilodalton protein during lytic infection: association with nuclear viral inclusions requires the early region 4 34-kilodalton protein. *J Virol* 65, 424-429.
- Ostapchuk, P., Anderson, M. E., Chandrasekhar, S., and Hearing, P. (2006). The L4 22-kilodalton protein plays a role in packaging of the adenovirus genome. *J Virol* 80, 6973-6981.
- Ostareck-Lederer, A., Ostareck, D. H., Rucknagel, K. P., Schierhorn, A., Moritz, B., Huttelmaier, S., Flach, N., Handoko, L., and Wahle, E. (2006). Asymmetric arginine dimethylation of heterogeneous nuclear ribonucleoprotein K by protein-arginine methyltransferase 1 inhibits its interaction with c-Src. *J Biol Chem* 281, 11115-11125.
- Palacios, S., Perez, L. H., Welsch, S., Schleich, S., Chmielarska, K., Melchior, F., and Locker, J. K. (2005). Quantitative SUMO-1 modification of a vaccinia virus protein is required for its specific localization and prevents its self-association. *Mol Biol Cell* 16, 2822-2835.
- Pilder, S., Moore, M., Logan, J., and Shenk, T. (1986). The adenovirus E1B-55K transforming polypeptide modulates transport or cytoplasmic stabilization of viral and host cell mRNAs. *Mol Cell Biol* 6, 470-476.
- Querido, E., Blanchette, P., Yan, Q., Kamura, T., Morrison, M., Boivin, D., Kaelin, W. G., Conaway, R. C., Conaway, J. W., and Branton, P. E. (2001). Degradation of p53 by adenovirus E4orf6 and E1B55K proteins occurs via a novel mechanism involving a Cullin-containing complex. *Genes Dev* 15, 3104-3117.
- Querido, E., Chu-Pham-Dang, H., and Branton, P. E. (2000). Identification and elimination of an aberrant splice product from cDNAs encoding the human adenovirus type 5 E4orf6 protein. *Virology* 275, 263-266.
- Rabino, C., Aspegren, A., Corbin-Lickfett, K., and Bridge, E. (2000a). Adenovirus late gene expression does not require a rev-like nuclear RNA export pathway. *J Virol* 74, 6684-6688.
- Rabino, C., Aspegren, A., Corbin-Lickfett, K., and Bridge, E. (2000b). Adenovirus late gene expression does not require a Rev-like nuclear RNA export pathway. *J Virol* 74, 6684-6688.
- Raska, K., Jr., and Gallimore, P. H. (1982). An inverse relation of the oncogenic potential of adenovirus-transformed cells and their sensitivity to killing by syngeneic natural killer cells. *Virology* 123, 8-18.
- Reich, N. C., Sarnow, P., Duprey, E., and Levine, A. J. (1983). Monoclonal antibodies which recognize native and denatured forms of the adenovirus DNA-binding protein. *Virology* 128, 480-484.
- Riley, D., and Flint, S. J. (1993). RNA-binding properties of a translational activator, the adenovirus L4 100-kilodalton protein. *J Virol* 67, 3586-3595.
- Rowe, W. P., Huebner, R. J., Gilmore, L. K., Parrot, R. H., and Ward, T. G. (1953). Isolation of a cytopathogenic agent from human adenoids undergoing spontaneous degeneration in tissue culture. *Proc Soc Exp Biol Med* 84, 570-573.

- Ruzindana-Umunyana, A., Imbeault, L., and Weber, J. M. (2002). Substrate specificity of adenovirus protease. *Virus Res* 89, 41-52.
- Ryabova, L. A., and Hohn, T. (2000). Ribosome shunting in the cauliflower mosaic virus 35S RNA leader is a special case of reinitiation of translation functioning in plant and animal systems. *Genes Dev* 14, 817-829.
- Salvesen, G. S., and Dixit, V. M. (1997). Caspases: intracellular signaling by proteolysis. *Cell* 91, 443-446.
- Sambrook, J., Fritsch, E. F. and Maniatis, T. (1989). *Molecular cloning: A laboratory manual*, Vol 2 (Cold Spring Harbor, Cold Spring Harbor Laboratory Press).
- Sarin, A., Williams, M. S., Alexander-Miller, M. A., Berzofsky, J. A., Zacharchuk, C. M., and Henkart, P. A. (1997). Target cell lysis by CTL granule exocytosis is independent of ICE/Ced-3 family proteases. *Immunity* 6, 209-215.
- Sarnow, P., Ho, Y. S., Williams, J., and Levine, A. J. (1982a). Adenovirus E1b-58kd tumor antigen and SV40 large tumor antigen are physically associated with the same 54 kd cellular protein in transformed cells. *Cell* 28, 387-394.
- Sarnow, P., Sullivan, C. A., and Levine, A. J. (1982b). A monoclonal antibody detecting the adenovirus type 5-E1b-58Kd tumor antigen: characterization of the E1b-58Kd tumor antigen in adenovirus-infected and -transformed cells. *Virology* 120, 510-517.
- Sharma, R. C., and Schimke, R. T. (1996). Preparation of electrocompetent *E. coli* using salt-free growth medium. *Biotechniques* 20, 42-44.
- Shen, Y., Kitzes, G., Nye, J. A., Fattaey, A., and Hermiston, T. (2001). Analyses of single-amino-acid substitution mutants of adenovirus type 5 E1B-55K protein. *J Virol* 75, 4297-4307.
- Shenk, T. (2001). Adenoviridae: the viruses and their replication. In *Virology*, a. P. M. H. D. M. Knipe, ed. (New York, Lippincott-Raven), pp. 2265-2300.
- Smith, J. J., Rucknagel, K. P., Schierhorn, A., Tang, J., Nemeth, A., Linder, M., Herschman, H. R., and Wahle, E. (1999). Unusual sites of arginine methylation in Poly(A)-binding protein II and in vitro methylation by protein arginine methyltransferases PRMT1 and PRMT3. *J Biol Chem* 274, 13229-13234.
- Spaeny-Dekking, E. H., Hanna, W. L., Wolbink, A. M., Wever, P. C., Kummer, A. J., Swaak, A. J., Middeldorp, J. M., Huisman, H. G., Froelich, C. J., and Hack, C. E. (1998). Extracellular granzymes A and B in humans: detection of native species during CTL responses in vitro and in vivo. *J Immunol* 160, 3610-3616.
- Stommel, J. M., Marchenko, N. D., Jimenez, S. G., Moll, U. M., Hope, T. J., and Wahl, G. M. (1999). A leucine-rich nuclear export signal in the p53 tetramerization domain: regulation of subcellular localization and p53 activity by NES masking. *EMBO J* 18, 1660-1672.
- Stracker, T. H., Carson, C. T., and Weitzman, M. D. (2002). Adenovirus oncoproteins inactivate the Mre11-Rad50-NBS1 DNA repair complex. *Nature* 418, 348-352.
- Strahl, B. D., Briggs, S. D., Brame, C. J., Caldwell, J. A., Koh, S. S., Ma, H., Cook, R. G., Shabanowitz, J., Hunt, D. F., Stallcup, M. R., and Allis, C. D. (2001). Methylation of histone H4 at arginine 3 occurs in vivo and is mediated by the nuclear receptor coactivator PRMT1. *Curr Biol* 11, 996-1000.

- Tang, J., Frankel, A., Cook, R. J., Kim, S., Paik, W. K., Williams, K. R., Clarke, S., and Herschman, H. R. (2000). PRMT1 is the predominant type I protein arginine methyltransferase in mammalian cells. *J Biol Chem* 275, 7723-7730.
- Tauber, B., and Dobner, T. (2001a). Adenovirus early E4 genes in viral oncogenesis. *Oncogene* 20, 7847-7854.
- Tauber, B., and Dobner, T. (2001b). Molecular regulation and biological function of adenovirus early genes: the E4 ORFs. *Gene* 278, 1-23.
- Thomas, D. L., Schaack, J., Vogel, H., and Javier, R. T. (2001). Several E4 region functions influence mammary tumorigenesis by human adenovirus type 9. *J Virol* 75, 557-568.
- Trentin, J. J., Yabe, Y., and Taylor, G. (1962). The quest for human cancer viruses: a new approach to an old problem reveals cancer induction in hamster hy human adenoviruses. *Science* 137, 835-849.
- Virtanen, A., and Pettersson, U. (1985). Organization of early region 1B of human adenovirus type 2: identification of four differentially spliced mRNAs. *J Virol* 54, 383-391.
- Webster, A., Leith, I. R., and Hay, R. T. (1994). Activation of adenovirus-coded protease and processing of preterminal protein. *J Virol* 68, 7292-7300.
- Weigel, S., and Dobbstein, M. (2000). The nuclear export signal within the E4orf6 protein of adenovirus type 5 supports virus replication and cytoplasmic accumulation of viral mRNA. *J Virol* 74, 764-772.
- Wen, W., Meinkoth, J. L., Tsien, R. Y., and Taylor, S. S. (1995). Identification of a signal for rapid export of proteins from the nucleus. *Cell* 82, 463-473.
- Wickham, T. J., Filardo, E. J., Cheres, D. A., and Nemerow, G. R. (1994). Integrin alpha v beta 5 selectively promotes adenovirus mediated cell membrane permeabilization. *J Cell Biol* 127, 257-264.
- Wickham, T. J., Mathias, P., Cheres, D. A., and Nemerow, G. R. (1993). Integrins alpha v beta 3 and alpha v beta 5 promote adenovirus internalization but not virus attachment. *Cell* 73, 309-319.
- Williams, J., Karger, B. D., Ho, Y. S., Castiglia, C. L., Mann, T., and Flint, S. J. (1986). The adenovirus E1B 495R protein plays a role in regulating the transport and stability of the viral late messages. *Cancer Cells* 4, 275-284.
- Williams, J., Williams, M., Liu, C., and Telling, G. (1995). Assessing the role of E1A in the differential oncogenicity of group A and group C human adenoviruses. *Curr Top Microbiol Immunol* 199 ( Pt 3), 149-175.
- Wodrich, H., Guan, T., Cingolani, G., Von Seggern, D., Nemerow, G., and Gerace, L. (2003). Switch from capsid protein import to adenovirus assembly by cleavage of nuclear transport signals. *Embo J* 22, 6245-6255.
- Wold, W. S., Mackey, J. K., Rigden, P., and Green, M. (1979). Analysis of human cancer DNA's for DNA sequence of human adenovirus serotypes 3, 7, 11, 14, 16, and 21 in group B1. *Cancer Res* 39, 3479-3484.
- Woo, J. L., and Berk, A. J. (2007). Adenovirus ubiquitin-protein ligase stimulates viral late mRNA nuclear export. *J Virol* 81, 575-587.
- Xi, Q., Cuesta, R., and Schneider, R. J. (2004). Tethering of eIF4G to adenoviral mRNAs by viral 100k protein drives ribosome shunting. *Genes Dev* 18, 1997-2009.

- Xi, Q., Cuesta, R., and Schneider, R. J. (2005). Regulation of translation by ribosome shunting through phosphotyrosine-dependent coupling of adenovirus protein 100k to viral mRNAs. *J Virol* 79, 5676-5683.
- Xirodimas, D., Saville, M. K., Edling, C., Lane, D. P., and Lain, S. (2001). Different effects of p14ARF on the levels of ubiquitinated p53 and Mdm2 in vivo. *Oncogene* 20, 4972-4983.
- Yew, P. R., and Berk, A. J. (1992). Inhibition of p53 transactivation required for transformation by adenovirus early 1B protein. *Nature* 357, 82-85.
- Yew, P. R., Kao, C. C., and Berk, A. J. (1990). Dissection of functional domains in the adenovirus 2 early 1B 55K polypeptide by suppressor-linker insertional mutagenesis. *Virology* 179, 795-805.
- Yolken, R. H., Lawrence, F., Leister, F., Takiff, H. E., and Strauss, S. E. (1982). Gastroenteritis associated with enteric type adenovirus in hospitalized infants. *J Pediatr* 101, 21-26.
- Zeller, T. (2004) In-vitro- und In-vivo-Untersuchungen funktioneller Bereiche des Adenovirus Typ 5 E1B-55kDa-Proteins., Dissertation, Universität Regensburg.
- Zhang, Y., Feigenbaum, D., and Schneider, R. J. (1994). A late adenovirus factor induces eIF-4E dephosphorylation and inhibition of cell protein synthesis. *J Virol* 68, 7040-7050.
- Zhang, Y., and Schneider, R. T. (1993). Adenovirus inhibition of cellular protein synthesis and the specific translation of late viral mRNAs. *Semin Virol* 4, 229-236.
- Zhao, Y., Kwon, S. W., Anselmo, A., Kaur, K., and White, M. A. (2004). Broad spectrum identification of cellular small ubiquitin-related modifier (SUMO) substrate proteins. *J Biol Chem* 279, 20999-21002.
- Zheng, N., Schulman, B. A., Song, L., Miller, J. J., Jeffrey, P. D., Wang, P., Chu, C., Koepp, D. M., Elledge, S. J., Pagano, M., *et al.* (2002). Structure of the Cul1-Rbx1-Skp1-F boxSkp2 SCF ubiquitin ligase complex. *Nature* 416, 703-709.

## 8 Publications

---

### I. Publications in Scientific Journals

Blackford, A.N., Burton, R.K., Dirlik, O., Stewart, G.S., Taylor, A.M., Dobner, T., Grand, R.J., Turnell, A.S., (2008). A role for E1B-AP5 in ATR signalling pathway during adenovirus infection. *J Virol.*, 82, 7640-7652.

Koyuncu, O. and Dobner, T., (2009). Arginine methylation of human adenovirus type 5 L4-100K protein is required for efficient virus production, *J Virol.*, Epub ahead of print.

Koyuncu, O. and Dobner, T., (2009). Nuclear export of adenovirus type 5 L4-100K is mediated by CRM1 and is crucial for efficient virus infection, *J Virol.*, manuscript in preparation.

### II. Oral Presentations at Scientific Meetings

Dirlik-Koyuncu, O. and Dobner, T.: Arginine methylation of Ad5 L4-100K protein is required for efficient virus replication. *Adenovirus Tagung, Ulm/Germany, 01.-02. March 2007.*

Dirlik-Koyuncu, O. and Dobner, T.: Arginine methylation of Ad5 L4-100K protein is required for efficient virus replication. *ICGEB DNA Tumor Virus Meeting, Trieste/Italy, 17.-22. July 2007.*

Dirlik-Koyuncu, O. and Dobner, T.: CRM1-mediated nucleocytoplasmic shuttling of adenovirus type 5 L4-100K protein is required for efficient virus growth. *Molecular Biology of DNA Tumor Viruses Conference, Madison/USA, 22.-27. July 2008.*

Koyuncu, O. and Dobner, T.: CRM1-mediated nucleocytoplasmic shuttling of adenovirus type 5 L4-100K protein is required for efficient virus growth. *Second Adenovirus Workshop, Hamburg/Germany, 11.-13. February 2009.*

### III. Poster Presentations at Scientific Meetings

Groitzl, P., Dirlik, O., Zeller, T., Kindsmüller, K. and Dobner, T.: Efficient generation of E1 and E4 adenovirus type 5 mutants. *Annual Meeting of German Society of Virology, Erlangen/Germany, April 2002.*

# Acknowledgements

---

My first thanks go to my supervisor *Prof. Dr. Thomas Dobner* for giving me a position in his group, introducing the amazing and beautiful adenovirus to me, being my inspiration in science, and encouraging me to fulfill this project. Ich danke ihn auch für die leckere Gans, und für die sehr lustige „freezers“ spiele (*Gabi Dobner*, danke ich sehr für die nette Gastfreundschaft).

Thanks to *Prof. Dr. Hans Wolf* for giving me the opportunity to work at the Institut für Medizinische Mikrobiologie und Hygiene der Universität Regensburg. I also would like to thank *Prof. Dr. Hauber*, and *Prof. Dr. Deppert* from Heinrich-Pette-Institut, and *Prof. Dr. Lüthen* from Department Biologie der Universität Hamburg for evaluating my thesis.

*Peter Groitl*, thanks for inviting us to Germany and also for the technical support during my project. I'll never forget the good-old-Regensburg-days...

Thanks to my co-workers and lab colleagues who spent some time with me either in Regensburg, or Hamburg; we enjoyed together doing research, had fun afterwards, shared adventures, and of course collected bittersweet memories; especially *Timo Sieber*, my ex-bench-mate, thanks a lot for reading my paper and thesis manuscripts, and also for being such a nice person.

Many thanks also to *Avril Arthur-Goettig* for reading and correcting my paper and thesis.

Of course, without their love, support, and patience nothing would be possible for me to accomplish, thanks to my family; my father, brother, my mother- & father-in-law. It was very hard to stay away that long from you, but I'm sure we will make it up. *Hepinizi çok seviyorum ve tesekkür ediyorum.*

Last but not least, my deepest thanks go to *Emre Koyuncu* for bringing love, joy, happiness, and light to my life, and also for sharing my ideals and view of life. I feel like we can do everything together. Thanks for always standing by me...